

MAREES TERRESTRES
BULLETIN D'INFORMATIONS

N ° 83

15 AVRIL 1980

Association Internationale de Geodesie
Commission Permanente des Marees Terrestres

Editeur Prof. Paul MELCHIOR
Observatoire royal de Belgique
Avenue Circulaire 3
1180 Bruxelles

15

16

TABLE DES MATIERES N°83

F. DE MEYER	A study of various harmonic analysis methods for earth tides observations	5187
C. DENIS et A. IBRAHIM	MØDPØL - Programme numérique permettant de représenter des modèles terrestres, planétaires et stellaires de manière cohérente	5236
NGUYEN NGOC THUY	Specific Tidal Phenomena of the East Sea (South China Sea) and the problem of calculation of tidal characteristics	5294
P. VARGA	Stresses in the Earth caused by Earth tides and loading influences	5312

A study of various harmonic analysis

methods for earth tides observations .

De Meyer Frans

Abstract.

The harmonic analysis methods of Venedikov and Chojnicki together with several new approaches are examined in the paper; their relative merits can be weighed against each other from the results in Tables 1 - 8. It is shown how the reconstructed tides, obtained through an earlier developed model, can be turned to account to detect conspicuous data intervals in the observations. Taking the autocorrelations of the observed residuals into consideration, more realistic estimates of the standard errors of the tidal constants are acquired, i.e. the structure of the residual spectrum is explicitly incorporated into the computations. The Markov estimation method is also considered and is proven to yield slightly better results than the classical least squares analysis. A new procedure of drift elimination, not founded on the principle of numerical filtering, is tested and looks very promising in the sense that a modification of Chojnicki's idea results in coherent tidal parameters with standard errors smaller than those hitherto obtained. Investigation of the residual spectrum after least squares adjustment discloses the existence of some non-linear waves which find their origin in shallow water loading and which, therefore, must be included in the harmonic analysis.

1. Introduction.

In earth tide studies the comparison of the observed amplitudes and phases with the theoretical constants provides the parameters related to the earth's rheology. Since the motive forces of the luni-solar attraction are known beforehand, the tide - generating potential can be decomposed into a number of constituents of accurately determined frequencies and the problem reduces in practice to the fitting of a linear trigonometric model to the observations. The methods of Venedikov (1966), Usandivaras-Ducarme (1969) and Chojnicki (1972) for the harmonic analysis of earth tide data are devised mainly to treat long series and are based on the principles of numerical filtering and least squares. The tidal parameters obtained by these approaches are in good agreement but there is much controversy about the reliability of the standard errors of the estimated constants.

Though the signal is extremely well defined in the observations, the statistical properties of the noise process are in general poorly understood and controlled. The method of least squares give dependable mean square errors providing that the error series is uncorrelated, i.e. when the noise is uniform at all frequencies of the spectrum. Even in the case of input white noise the filtering introduces a severe correlation in the output noise and transforms the white noise into coloured noise. When we think in terms of "noise" we generally have in mind reading or accidental errors. But the

situation is more complicated for the earth tides : slow variations, of any origin, in the instrumental conditions produce a so called "drift" of the instrumental zero; external effects acting upon or inside the Earth's crust may superpose themselves on the drift, such as changes in the underground water level, atmospheric pressure, or other unknown local disturbances. For the harmonic analysis it is very difficult to separate such irregular phenomena from the tidal waves. Noise is also generated in the tidal wave bands as a result of temperature variations acting on the instruments and which combine their effect into a S_1 meteorological wave, and as a result also of atmospheric pressure fluctuations, which produce a S_2 meteorological component. In this context the concept of "noise" stands for a combination of a more or less smoothly changing time function, disturbances at the frequencies of the theoretical model and small random perturbations.

The statistical structure of the residual series ought to be incorporated into the calculations in order to obtain more reliable estimates of the standard errors of the unknowns. It will be shown how the autocorrelation function of the observed residuals can be used for this purpose. Moreover the residual spectrum after tidal analysis betrays the existence in the observations of a number of non-linear waves, due to shallow water loading, which are generally not included into the model. This corroborates the point of view of Barker (1978).

Up to now the generalized least squares method, which gives the best linear unbiased estimates of the regression coefficients, did not seem to be applicable in practice for long series because of computational difficulties. Using the observed residuals of the least squares analysis it will be possible to approximate the unknown drift by an autoregressive model of low order and to transform it to nearly white noise. In this way the use of the Markov estimation becomes possible.

2. The classical method of least squares.

We consider the problem of estimating the value of the dependent variable y on the basis of information on the fixed variates x_1, \dots, x_n ; in this context it will be assumed always that the x_j are determinate functions which can be computed without error. Let us assume that y can be approximated by a linear model of the form

$$y = \sum_{j=1}^n b_j x_j + \epsilon = \sum_{j=1}^n \hat{b}_j x_j + \hat{\epsilon} \quad (1)$$

where the unknown regression coefficients b_1, \dots, b_n are to be determined from $m \geq n + 1$ simultaneous observations x_{tj} on the x_j and observations y_t on y , with $1 \leq t \leq m$ and $1 \leq j \leq n$. At the time instant t we have

$$y_t = \sum_{j=1}^n x_{tj} b_j + \epsilon_t = \sum_{j=1}^n x_{tj} \hat{b}_j + \hat{\epsilon}_t \quad (2)$$

To simplify the notations the means of all variables are considered to be zero; in practice this implies that the arithmetical means of the variates should be subtracted from the individual values. The first relationship in Eq. (1) represents the true model in terms of the parameters b_j and the true, although unknown, error ϵ , while the second is in terms of the estimates \hat{b}_j of the parameters and the residual $\hat{\epsilon}$.

Using the matrix notation Eq. (2) is expressed in the form

$$Y = XB + E = X\hat{B} + \hat{E} \quad (3)$$

where $Y = (y_1, \dots, y_m)'$, $B = (b_1, \dots, b_n)'$, $E = (\epsilon_1, \dots, \epsilon_m)'$ and where X denotes the $m \times n$ matrix with elements x_{tj} (the transpose of any vector or matrix M is indicated by M'). If the normal matrix $A = X'X$ is nonsingular the least squares estimate \hat{B} of B is given by

$$\hat{B} = (X'X)^{-1} X'Y \quad (4)$$

with covariance matrix

$$\mathbb{E}[(\hat{B} - B)(\hat{B} - B)'] = (X'X)^{-1} X' V X (X'X)^{-1} \quad (5)$$

(Grenander and Rosenblatt, 1966, p.234), where \mathbb{E} stands for the mathematical expectation value and V is the $m \times m$ covariance matrix of the realization $(\epsilon_1, \dots, \epsilon_m)$ of the random process ϵ , with elements $v_{ij} = \mathbb{E}[\epsilon_i \epsilon_j]$.

Should ϵ be purely white noise, uncorrelated with the regressors x_1, \dots, x_n , and with variance $\sigma_\epsilon^2 = \mathbb{E}[\epsilon^2]$, then the covariance matrix V becomes diagonal, $V = \sigma_\epsilon^2 I$, since $v_{ij} = \sigma_\epsilon^2 \delta_{ij}$, with I the identity matrix and δ_{ij} the Kronecker delta. The covariance matrix for the least squares estimation for uncorrelated residuals consequently reduces to the classical expression

$$\mathbb{E}[(\hat{B} - B)(\hat{B} - B)'] = \sigma_\epsilon^2 (X'X)^{-1} \quad (6)$$

In general, however, the theoretical residuals ϵ_t are more or less correlated; this does not prevent us from estimating the model parameters b_j with the least squares method and, hence, from obtaining an unbiased estimate $\hat{\sigma}_\epsilon^2 = \hat{E}'\hat{E}/(m-n)$ of the variance of the noise process ϵ , but the expression (6) for the covariance matrix of the regression coefficients can no longer be trusted to provide realistic error limits in the case of autocorrelated residuals. If the correlation in the ϵ_t is strong the errors on the \hat{b}_j can be largely underestimated by Eq. (6).

Though generally the matrix $V = \mathbb{E}[EE']$ itself is not known a priori, use can be made of Eq. (5) by substituting the covariance matrix \hat{V} of the observed residuals

$$\hat{\epsilon}_t = y_t - \sum_{j=1}^n x_{tj} \hat{b}_j \quad (7)$$

for the covariance matrix V of the theoretical residuals. The covariance matrix of the regression parameters is then estimated by

$$\mathbb{E}[(\hat{B} - B)(\hat{B} - B)'] = (X'X)^{-1} C(X'X)^{-1} \quad (8)$$

where C is the $n \times n$ matrix $C = X' \hat{V} X$. For a stationary random process $\hat{\epsilon}$ with zero mean and autocorrelations

$$\hat{\rho}_k = \mathbb{E}[\hat{\epsilon}_t \hat{\epsilon}_{t+k}] / \hat{\sigma}_\epsilon^2, \quad k = 0, 1, 2, \dots \quad (9)$$

the matrix \hat{V} takes a Toeplitz structure with elements

$$\hat{v}_{ij} = \hat{\sigma}_\epsilon^2 \hat{\rho}_{|i-j|}, \quad 1 \leq i, j \leq n \quad (10)$$

Since the autocorrelations $\hat{\rho}_k$ can be computed from the series of observed residuals $\hat{\epsilon}_t$, the elements c_{ij} of the matrix C are given by the expression

$$\begin{aligned} c_{ij} &= \hat{\sigma}_\epsilon^2 \sum_{r=1}^n \sum_{s=1}^n x_{ri} x_{sj} \hat{\rho}_{|s-r|} \\ &= \hat{\sigma}_\epsilon^2 \left\{ \chi_{ij}(0) + \sum_{k=1}^m \hat{\rho}_k [\chi_{ij}(k) + \chi_{ji}(k)] \right\} \end{aligned} \quad (11)$$

where

$$\chi_{ij}(k) = \sum_{t=1}^{m-k} x_{ti} x_{t+k,j} \quad (12)$$

are the cross-covariances between x_i and x_j .

3. The generalized method of least squares.

If the covariance matrix V of the noise process ϵ is known it follows from the Gauss - Markov theorem that each element of the Markov estimate

$$\tilde{B} = (X' V^{-1} X)^{-1} X' V^{-1} Y \quad (13)$$

is the best linear unbiased estimate (B.L.U.E.) of the corresponding component of B , in the sense that its covariance matrix

$$\mathcal{E}[(\tilde{B} - B)(\tilde{B} - B)'] = (X' V^{-1} X)^{-1} \quad (14)$$

has the property that the matrix $\mathcal{E}[(\hat{B} - B)(\hat{B} - B)' - (\tilde{B} - B)(\tilde{B} - B)']$ is positive semidefinite for any other unbiased estimate \hat{B} of B , which means that \tilde{B} is a minimum variance linear unbiased estimate of B . For the theory of efficient estimation we refer to the works of Hannan (1960, Chapter 5), Grenander and Rosenblatt (1966, Chapter 7) and Anderson (1971, Chapter 10).

At first sight the use of the Markov estimation meets with insuperable difficulties. Indeed, the covariance matrix V of the true residuals ϵ_t is not known beforehand in most cases and even if V is replaced by the covariance matrix \hat{V} of the observed residuals $\hat{\epsilon}_t$, obtained by a previously executed least squares analysis, we still have the problem of inverting the $m \times m$ matrix \hat{V} before it can be used in Eqs (13) and (14). For a large number of observations (m of the order of 10^4) the Markov estimation seems to be inapplicable, even if ^{it} can reasonably be assumed that \hat{V} has a Toeplitz structure with only m independent elements $\hat{\rho}_0, \hat{\rho}_1, \dots, \hat{\rho}_{m-1}$.

This problem, however, can be solved explicitly if the noise process is of the autoregressive (AR) type; in this case the process ϵ_t satisfies the finite difference equation

$$\sum_{k=0}^p \alpha_k \epsilon_{t-k} = \nu_t \quad (15)$$

with constant coefficients $\alpha_0, \alpha_1, \dots, \alpha_p$, such that the sequence v_t consists of independently and identically distributed random variables (white noise). The elements v^{ij} of V^{-1} are then explicitly determined by the AR parameters α_j

$$v^{ij} = \sum_{k=0}^{p|i-j|} \alpha_k \alpha_{k+|i-j|}, \quad 0 \leq |i-j| \leq p \quad (16)$$

$$= 0, \quad p < |i-j|$$

(Anderson, 1971, p. 576), which means that V^{-1} is again of the Toeplitz type and completely determined by the autocorrelations of the AR operator $(\alpha_0, \alpha_1, \dots, \alpha_p)$. It then follows that V^{-1} can be uniquely decomposed as

$$V^{-1} = \Delta' \Delta \quad (17)$$

with Δ the subdiagonal matrix

$$\Delta = \begin{bmatrix} \alpha_{11} & 0 & 0 & \dots & 0 & 0 & 0 & \dots & 0 & 0 \\ \alpha_{21} & \alpha_{22} & 0 & \dots & 0 & 0 & 0 & \dots & 0 & 0 \\ \alpha_{31} & \alpha_{32} & \alpha_{33} & \dots & 0 & 0 & 0 & \dots & 0 & 0 \\ \vdots & \vdots & \vdots & \ddots & \vdots & \vdots & \vdots & & \vdots & \vdots \\ \alpha_{p1} & \alpha_{p2} & \alpha_{p3} & \dots & \alpha_{pp} & 0 & 0 & \dots & 0 & 0 \\ \alpha_p & \alpha_{p-1} & \alpha_{p-2} & \dots & \alpha_1 & \alpha_0 & 0 & \dots & 0 & 0 \\ 0 & \alpha_p & \alpha_{p-1} & \dots & \alpha_2 & \alpha_1 & \alpha_0 & \dots & 0 & 0 \\ \vdots & \vdots & \vdots & \ddots & \vdots & \vdots & \vdots & & \vdots & \vdots \\ 0 & 0 & 0 & \dots & 0 & 0 & 0 & \dots & \alpha_0 & 0 \\ 0 & 0 & 0 & \dots & 0 & 0 & 0 & \dots & \alpha_1 & \alpha_0 \end{bmatrix} \quad (18)$$

where the numbers α_{ij} are chosen so that the expression (17) is dependable (Grenander and Rosenblatt, 1966, p. 238).

Suppose now that a least squares analysis yields the estimates $\hat{b}_1, \dots, \hat{b}_n$ of the regression coefficients and that the observed residuals $\hat{\epsilon}_1, \dots, \hat{\epsilon}_m$ can be reasonably well approximated by an autoregressive model of low order p of the form

$$\sum_{k=0}^p \hat{\alpha}_k \hat{\epsilon}_{t-k} = \hat{v}_t \quad (19)$$

with \hat{v}_t quasi white noise. From Eq. (3) it follows that the linear model can be transformed into another linear model

$$\tilde{Y} = \tilde{X}B + \tilde{E} \quad (20)$$

with

$$\tilde{Y} = \Delta Y, \quad \tilde{X} = \Delta X, \quad \tilde{E} = \Delta E \quad (21)$$

Using Eq. (17) it is easy to see that the covariance matrix \tilde{V} of the transformed noise \tilde{E} equals the identity matrix, i.e. $\tilde{V} = \mathbb{E}[\tilde{E} \tilde{E}'] = \Delta V \Delta' = I$. Therefore the Markov estimate (13) can be written

$$\tilde{B} = (\tilde{X}' \tilde{X})^{-1} \tilde{X}' \tilde{Y} \quad (22)$$

with covariance matrix

$$\mathbb{E}[(\tilde{B} - B)(\tilde{B} - B)'] = (\tilde{X}' \tilde{X})^{-1} \quad (23)$$

so that the Markov estimation amounts to an ordinary least squares analysis with uncorrelated residuals on the transformed linear model (20).

In view of the special structure of the matrix Δ we only have to estimate the AR parameters $(\hat{\alpha}_0, \dots, \hat{\alpha}_p)$ from the sequence of observed residuals, to perform the discrete convolutions

$$\tilde{y}_t = \sum_{k=0}^p \hat{\alpha}_k y_{t-k}, \quad \tilde{x}_{tj} = \sum_{k=0}^p \hat{\alpha}_k x_{t-k,j} \quad (24)$$

and to proceed to the estimation of the b_j from the transformed model

$$\tilde{y}_t = \sum_{j=1}^n \tilde{x}_{tj} \tilde{b}_j + \tilde{v}_t \quad (25)$$

Since the \tilde{v}_t are nearly uncorrelated the method of least squares, applied to the model (25), will give reliable estimates (23) of the standard errors of the regression parameters \tilde{b}_j .

4. Application to the trigonometric model of the earth tides.

Let us represent the hourly ordinate readings of an earth tide record by

$$y_t = s_t + d_t + \epsilon_t \quad (26)$$

where

$$s_t = \sum_{j=1}^q H_j \cos(\omega_j t + \phi_j) \quad (27)$$

stands for the observed tides; H_j is the observed amplitude and ϕ_j is the observed phase of the tidal wave of frequency ω_j . The sum of the instrumental drift and the long period tides is denoted by d_t while ϵ_t describes the random noise process.

Figure 1 shows the power spectrum of part of a record by the horizontal pendulum Verbaandert - Melchior N° 28, East-West component (station Dourbes, Belgium). It consists of a superposition of the diurnal (D), semi-diurnal (SD) and ter-diurnal (TD) oscillations upon a continuum of non-tidal origin. The power spectrum is seen to be almost flat for frequencies f larger than 0.17 cph (cycles/hour); if the white noise level at the high-frequency end of the spectrum is

maintained throughout the entire Nyquist interval $0 \leq f \leq 0.5$ cph, the square root of the total integrated power would be 1 msec. This value may be interpreted as the mean square error of a single reading and it corresponds to 0.2 mm on the record.

Since it is commonly assumed that tides, drift and random errors are mutually uncorrelated, the power spectrum $P_{yy}(f)$ of the observed record can be written as the sum

$$P_{yy}(f) = P_{ss}(f) + P_{nn}(f) \quad (28)$$

of the power spectrum $P_{ss}(f)$ of the observed tides plus the power spectrum $P_{nn}(f) = P_{dd}(f) + P_{\epsilon\epsilon}(f)$ of the coloured noise $n_t = d_t + \epsilon_t$. The presence of the instrumental drift utterly hampers an adequate harmonic analysis of the data since, in this context, the concept "noise" now stands for the sum of the drift, which is in general a smoothly varying function, plus random disturbances. The random error series appears in the power spectrum of Fig. 1 as a constant level at the higher frequencies, while the contribution of the drift is seen as a coloured noise at the low frequencies.

Most methods of harmonic analysis of earth tide records use numerical filtering to eliminate the frequencies external to the model accepted to describe the tidal observations, thus transforming the input y_t into the filtered sequence

$$\bar{y}_t = \bar{s}_t + \bar{n}_t \quad (29)$$

by means of a convolution filter with impulse response $\{h_k\}_p$; \bar{y}_t , \bar{s}_t and \bar{n}_t are given by the respective discrete convolutions

$$\bar{y}_t = \sum_{r=-p}^p h_r y_{t-r}, \quad \bar{s}_t = \sum_{r=-p}^p h_r s_{t-r} \quad (30)$$

$$\bar{n}_t = \bar{d}_t + \bar{\epsilon}_t = \sum_{r=-p}^p h_r d_{t-r} + \sum_{r=-p}^p h_r \epsilon_{t-r}$$

Since ϵ_t mainly contributes to the high-frequency part of the Nyquist interval, a band-pass filter for the diurnal band (say) may be expected to reduce effectively the output noise $\bar{\epsilon}_t$ of the random errors; the contribution of the drift \bar{d}_t outside the D-band also disappears, but inside the band the contribution of the drift is not eliminated. Band-pass filtering therefore is not fit to reduce the noise in the tidal wave bands. In addition, this technique has a very unattractive consequence since the output noise \bar{n}_t becomes highly autocorrelated even if the input noise were truly uncorrelated. Indeed, assuming the input noise to be stationary with zero mean, its autocovariance function is defined by

$$c_j = \mathbb{E}[n_t n_{t+j}] \quad (31)$$

and the autocovariance function of the filtered noise will be given by

$$\bar{c}_j = \mathbb{E}[\bar{n}_t \bar{n}_{t+j}] = \sum_{r=-p}^p \sum_{s=-p}^p h_r h_s c_{j+r-s} \quad (32)$$

In terms of the autocorrelations $\rho_j = c_j/c_0$, $\bar{\rho}_j = \bar{c}_j/\bar{c}_0$, with $c_0 = \sigma_n^2 = \mathbb{E}[n_t^2]$ and $\bar{c}_0 = \sigma_{\bar{n}}^2 = \mathbb{E}[\bar{n}_t^2]$, we obtain the relationship

$$\sigma_{\bar{n}}^2 \rho_j = \sigma_n^2 \sum_{r=-p}^p \sum_{s=-p}^p h_r h_s \rho_{j+r-s} \quad (33)$$

and, for $j=0$,

$$\sigma_{\bar{n}}^2 = \sigma_n^2 \left[\sum_{r=-p}^p h_r^2 + 2 \sum_{j=1}^{2p} \rho_j \sum_{r=-p}^{p-j} h_r h_{r+j} \right] \quad (34)$$

If n_t is a realization of a white noise process ($\rho_0 = 1$, $\rho_j = 0$ for $j \neq 0$) with variance σ_n^2 we conclude that the variance of the original noise process will be modified (and generally will be reduced) by the filtering with the factor $\sum_{r=-p}^p h_r^2$. But Eq. (33) can also be written

$$\sigma_{\bar{n}}^2 \bar{\rho}_j = \sigma_n^2 \sum_{r=-p}^p \mu_r \rho_{j-r} \quad (35)$$

where

$$\mu_r = \sum_{s=-p}^{p-|r|} h_s h_{s+r} \quad (36)$$

is the autocorrelation sequence of the filter coefficients h_k . Even in the absence of drift from the registration and purely white input noise, it follows that the autocorrelations of the output noise are precisely determined by the autocorrelations of the filterweights, i.e.

$$\sigma_{\bar{n}}^2 \bar{\rho}_j = \sigma_n^2 \mu_j$$

which shows that the output noise anyhow becomes highly autocorrelated by either band-pass filtering or any other smoothing technique.

To show the form of the correlation that can be expected, we refer to the fact that the autocovariance function is the Fourier transform of the power spectrum

$$c_j = \int_{-1/2}^{1/2} P_{nn}(f) e^{2\pi i j f} df \quad (37)$$

The power spectra of the input and output noise are then related by

$$P_{\bar{n}\bar{n}}(f) = |H(f)|^2 P_{nn}(f) \quad (38)$$

(Lee, 1960, p. 333), where

$$H(f) = \sum_{r=-p}^p h_r e^{-2\pi i r f} \quad (39)$$

is the frequency response of the filter $\{h_k\}$. For an ideal band-pass filter between the frequencies f_1 and f_2 and input white noise, $P_{nn}(f) = \sigma_n^2$, we obtain

$$\bar{c}_0 = 2 \sigma_n^2 (f_2 - f_1), \quad \bar{c}_j = 2 \sigma_n^2 \int_{f_1}^{f_2} \cos 2\pi j f df$$

Writing $\bar{c}_j = \sigma_n^2 g_j$, with g_j defined by

$$g_0 = 2(f_2 - f_1), \quad g_j = \frac{1}{\pi j} (\sin 2\pi j f_2 - \sin 2\pi j f_1)$$

we see that $\bar{\rho}_j = g_j / g_0$. From Figure 2, which shows the form of the function g_j / g_0 for the band-pass filter between the frequencies $f_1 = 0.034$ cph and $f_2 = 0.047$ cph, we infer that a severe autocorrelation can be expected in the output noise, even for white input noise.

Equation (26) can be linearized to write

$$y_t = \sum_{j=1}^q [\xi_j (h_j \cos \omega_j t) + \eta_j (h_j \sin \omega_j t)] + n_t \quad (40)$$

where h_j is the theoretical amplitude of the tidal wave with frequency ω_j (eventually modified by the amplitude factors of the digital filters used in the data preparation), and with

$$H_j = \gamma_j h_j, \quad \xi_j = \gamma_j \cos \phi_j, \quad \eta_j = -\gamma_j \sin \phi_j \quad (41)$$

The parameters in which we are interested are the ratios γ_j (or δ_j) of the observed to the theoretical amplitudes and the differences $\kappa_j = \phi_j - \phi_j^0$ between the observed and the theoretical phases ϕ_j of the tidal waves.

Comparing Eq. (40) with the general expression (2), and for $1 \leq j \leq q$, we identify

$$\begin{aligned} n = 2q, \quad b_j &= \xi_j, \quad x_{tj} = h_j \cos \omega_j t \\ b_{j+q} &= \eta_j, \quad x_{t,j+q} = h_j \sin \omega_j t \end{aligned} \quad (42)$$

Using the trigonometric relation (Blackman and Tukey, 1958, p. 80)

$$C_m(\omega) = \sum_{t=1}^m \cos \omega t = \frac{\sin m\omega/2}{\sin \omega/2} \cos (m+1)\omega/2 \quad (43)$$

$$S_m(\omega) = \sum_{t=1}^m \sin \omega t = \frac{\sin m\omega/2}{\sin \omega/2} \sin (m+1)\omega/2$$

the elements of the symmetrical normal matrix $A = X'X$ for m observations and $1 \leq i, j \leq q$ can be written

$$\begin{aligned} a_{ij} &= h_i h_j t_{ij}^{cc}(m), & a_{i,j+q} &= h_i h_j t_{ij}^{cs}(m) \\ a_{i+q,j} &= h_i h_j t_{ji}^{cs}(m), & a_{i+q,j+q} &= h_i h_j t_{ij}^{ss}(m) \end{aligned} \quad (44)$$

with

$$\begin{aligned} t_{ij}^{cc}(m) &= \sum_{t=1}^m \cos \omega_i t \cos \omega_j t = \frac{1}{2} [C_m(\omega_i - \omega_j) + C_m(\omega_i + \omega_j)] \\ t_{ij}^{cs}(m) &= \sum_{t=1}^m \cos \omega_i t \sin \omega_j t = \frac{1}{2} [S_m(\omega_i + \omega_j) - S_m(\omega_i - \omega_j)] \\ t_{ij}^{ss}(m) &= \sum_{t=1}^m \sin \omega_i t \sin \omega_j t = \frac{1}{2} [C_m(\omega_i - \omega_j) - C_m(\omega_i + \omega_j)] \end{aligned} \quad (45)$$

Since $C_m(\omega) \rightarrow m$ and $S_m(\omega) \rightarrow 0$ for $\omega \rightarrow 0$, and provided m is sufficiently large and $|\omega_i - \omega_j|$ is not too small for $i \neq j$, it is granted with a good approximation that the normal matrix A has a diagonal structure

$$a_{ij} \simeq \frac{m}{2} h_i^2 \delta_{ij}, \quad 1 \leq i, j \leq 2q$$

so that the elements of A^{-1} can be approximated by

$$a^{ij} \simeq \frac{2}{m} \frac{1}{h_i^2} \delta_{ij}$$

Consequently,

$$\begin{aligned} \text{var} [\xi_i] = \text{var} [\eta_i] &\simeq \frac{2}{m} \frac{\sigma_n^2}{h_i^2} \\ \text{var} [\gamma_i] &\simeq \frac{2}{m} \frac{\sigma_n^2}{h_i^2}, \quad \text{var} [\kappa_i] \simeq \frac{2}{m} \frac{\sigma_n^2}{h_i^2 \gamma_i^2} \end{aligned} \quad (46)$$

In the case of a trigonometric model we conclude that the least squares method has an efficiency factor $\sqrt{\frac{2}{m}}$; this means that the standard errors of the regression parameters, obtained by a least squares analysis over a period of one year, can be reduced by a factor 4 if 16 years of observations are used.

The relation ship (46) has another important consequence : if $\Delta\gamma_{K_1}$ denotes the standard error of the γ -factor of the wave K_1 and if $\Delta\gamma_i$ is the standard error of the γ -factor of a tidal wave other than K_1 , we get the relation ship ,

$$\Delta\gamma_i = \frac{h_{K_1}}{h_i} \Delta\gamma_{K_1} \quad (47)$$

which is independent from both the number of observations and the standard deviation of the noise in the observations. If, for example, in a least squares analysis for the diurnal band the amplitude of the wave K_1 is estimated with an error of 1%, the amplitude of the wave J_1 can be expected to be estimated with an error of $0.53011/0.02964 \simeq 18\%$. Also, if the amplitude of the wave ψ_1 is to be estimated with an error of 1% this would require an accuracy of 0.01% for the γ -factor of the wave K_1 .

5. Venedikov's method.

The first step in Venedikov's method (1966b) consists of a band-pass filtering of the hourly observations in order to eliminate the long period tides and to reduce the contributions of the instrumental drift outside the tidal wave bands. For each of the diurnal ($r=1$), semi-diurnal ($r=2$) and ter-diurnal ($r=3$) bands two filters, $C_t^{(r)}$ and $S_t^{(r)}$, are applied on a sequence of 48 hourly readings without gaps and then shifted from 48 hours to avoid any superposition of data so that independent output points are obtained. If we have m series of 48 hourly readings we thus end up with six new series $M_i^{(r)}$ and $N_i^{(r)}$ of m independent data, $1 \leq i \leq m$, $r=1, 2, 3$, and it readily follows that the $M_i^{(r)}$ and $N_i^{(r)}$ are not correlated. For the construction of the filters and a complete description of Venedikov's method the reader is referred to Venedikov (1966 a, 1966 b), Melchior and Vene-

dikov (1968) and Melchior (1978).

On the ground of geophysical considerations it can reasonably be accepted that the tidal development can be combined into a number of wave groups and that the Love numbers are not different for waves having near frequencies within the same group, which means that the γ - and κ - factors can safely be taken to be constant for waves in the same group.

Since Venedikov's coefficients $M_i^{(r)}$ and $N_i^{(n)}$ can be written in the form (40) of a trigonometric model, the second step is evidently the application of the least squares method to each tidal wave band, thus obtaining the estimates $\hat{\gamma}_j$ and $\hat{\kappa}_j$ and the standard errors $\Delta\gamma_j$ and $\Delta\kappa_j$ by Eqs. (4) and (6). It should be noted that the errors in the $M_i^{(r)}$ and $N_i^{(r)}$ series mainly arise from the imperfect elimination of the instrumental drift by the band-pass filters $C_t^{(r)}$ and $S_t^{(r)}$, from the fluctuations of the sensitivity of the instrument between two calibrations, and from non-tidal contributions in the wave bands. In view of the fact that the three tidal bands are analyzed separately and that the filtering is performed on non-overlapping data, Venedikov's method implicitly assumes that the error series in each of the $M_i^{(r)}$ and $N_i^{(r)}$ are uncorrelated and also presumes a constant noise level for each tidal frequency band. If this is not the case great care must be taken in estimating the standard errors through Eq. (6), as indeed the influence of autocorrelated noise may lead to underestimation of the computed mean square errors. Table 1 shows the results of Venedikov's method for the period 1/1/1969 - 31/12/1977 using the observations made with the Verbaandert - Melchior pendulum N° 28, East-West component at the station Dourbes (50.06N, 4.36E, H 233M, P 46M); the complete Cartwright-Tayler-Edden potential development is used. All subsequent analyses refer to this instrument and time interval.

Figure 3 shows the autocorrelation sequence and the power spectrum of the observed residuals after least squares adjustment for the coefficients $M_i^{(r)}$, $r = 1, 2, 3$; the 95% confidence limits for the autocorrelation functions are indicated by the dashed lines, and the 95% confidence band for the power spectrum is given by the vertical bar. The power spectrum of the residuals of the $M_i^{(1)}$ series indicates a small peak at the period $T = (13.33 \pm 0.9)$ days, while the power spectrum of the residuals of the $M_i^{(2)}$ series shows an important peak at the period $T = (14.29 \pm 1)$ days. Both power spectra noticeably deviate from a white noise level, which is estimated from the mean-square errors of the harmonic analysis. For the ter-diurnal band a white noise spectrum assumption is more justified, although small peaks are indicated for the periods $T = (14.29 \pm 1)$ days and $T = (7.14 \pm 0.3)$ days.

It can be argued that these periods happen to appear as a result of an aliasing effect of the method. Barker (1978) drew the attention to the fact that non-linear waves induced by shallow water loading can be important in the main tidal bands and at higher frequencies for earth tide stations set up near to the ocean. In Section 10 we shall demonstrate that the residual spectrum after the tidal analysis comprises peaks at the frequencies where the waves OP_2 (together with MKS_2), SK_3 and M_4 are located; there is also an important residual power at the frequency of the wave L_2 . Since the station Dourbes is about 140 km away from the North Sea it may be concluded that these non-linear terms indeed affect the earth tide measurements by shallow water loading. Sampling with an interval $\Delta t = 48$ h defines a Nyquist frequency $f_N = \frac{1}{96}$ cph and will project the power at the frequencies of the non-linear waves, not included in the tidal model, to the low frequency range. The power in the vicinity of the wave M_2 with frequency $f_{M_2} = 0.0805114$ cph will be aliased to the frequencies around $0.0805114 - \frac{8}{96} = 0.0028219$ cph, which corresponds to a period $T = 14.77$ days. This already explains the fact that a peak at 14 days is observed in the residual series of $M_i^{(2)}$. Similarly, the residual power in the vicinity of the wave O_1 will be aliased to a period of about 14.19 days in the $M_i^{(1)}$ series

and the residual power at the frequencies surrounding the wave MK_3 are aliased to a period of about 15.38 days in the $M_i^{(3)}$ series. Since the filter $C_t^{(3)}$ imperfectly removes the wave M_4 from the observations, the power at this frequency is aliased to a period of about 7.38 days in the $M_i^{(3)}$ series, thus accounting for the second small peak in the power spectrum of the $M_i^{(3)}$ residuals. The filter gains of the Venedikov filters are shown by Schüller (1978).

In conclusion, it is anticipated that the method of Venedikov will give slightly biased results, especially for the semi-diurnal band. Wenzel (1977) on the contrary concludes that the results are unbiased on the basis of the observation that the computed autocorrelations are practically zero for non-zero lags but, unfortunately, the residual power spectra are not shown in his work. However, it can be safely stated that the effect of the peak in the residual spectrum of the $M_i^{(2)}$ series upon the estimation of the mean square errors of the tidal constants will be of minor importance. We shall return to this question in Section 6.

With a view to improving the results of the Venedikov method, Usandivaras and Ducarme (1976) propose the following test to eliminate the abnormal 48 hour-blocks : if the value of the parameter

$$PE_i = \{ [M_i^{(3)}]^2 + [N_i^{(3)}]^2 \}^{1/2}$$

is larger than three times the maximum theoretical amplitude of the wave M_3 , the block i is not considered in the harmonic analysis. Since the elimination of the drift is performed differently by the filters $C_t^{(r)}$ and $S_t^{(r)}$ we propose to work on the individual values of the $M_i^{(r)}$, $r = 1, 2, 3$, for each block of 48 hourly readings and for each tidal band concerned. A first application of Venedikov's method gives estimates $(\hat{\gamma}_j, \hat{\kappa}_j)$ of the tidal parameters and estimates $\hat{\sigma}_r$, $r = 1, 2, 3$ of the mean square errors for the three tidal bands. During a subsequent analysis of the band with index r , an estimated value $\hat{M}_i^{(r)}$ can be computed from the model $(\hat{\gamma}_j, \hat{\kappa}_j)$ and compared with the observed value $M_i^{(r)}$ for the block i . If $|M_i^{(r)} - \hat{M}_i^{(r)}| > 3 \hat{\sigma}_r$ the block i is dismissed from the analysis for the tidal band r . At the end of the least squares analysis the model $(\hat{\gamma}_j, \hat{\kappa}_j)$ can eventually be updated to be used in a next computation. It can of course be argued that the danger of this procedure lies in the trend of biasing the results of the analysis towards the original tidal model $(\hat{\gamma}_j, \hat{\kappa}_j)$.

Figure 4 shows sections of the differences $M_i^{(r)} - \hat{M}_i^{(r)}$, together with the limits $\pm 3 \hat{\sigma}_r$, referring to the same data interval. Table 2 demonstrates how the results of the harmonic analysis are improved with this test by rejecting 54 days out of 3194 days. The standard errors for the D- and the TD- band are slightly improved, but for the SD- band they are halved. Also note that the amplitude 1.0051 of the wave ψ_1 (Table 1) is changed to 0.5557 (Table 2) when this test for detecting anomalous observations is applied. It must be taken into account that the rejection of conspicuous data may drastically alter the γ -factors of the small waves.

6. Band- pass filtering with overlapping.

An obvious drawback of Venedikov's method is the severe limitation of the number of data usable for the tidal analysis since the initial set of m hourly observations is reduced to six series, each containing only $m/48$ points. A generalization of this approach evidently consists in constructing adequate band-pass filters for each tidal wave band and applying the filter weights with a shift of one hour (and not 48 hours as in Venedikov's method) and to perform a least squares analysis on the

three resulting time sequences.

The main problem in numerical filter design is to obtain a good frequency cut-off with a small number of coefficients. Let us consider an even function $D_j(f)$, $j = 0, 1, 2, \dots$, having the property of being zero outside the frequency interval $-\epsilon \leq f \leq \epsilon$ and $D_j(0) = 1$. The frequency response of the band-pass filter with central frequency f_0 and width 2ϵ is now defined as

$$H_j(f) = D_j(f - f_0) \quad (48)$$

with a corresponding filter function

$$\begin{aligned} h_j(t) &= \int_{-\infty}^{\infty} H_j(f) e^{2\pi i f t} df \\ &= 2 \cos 2\pi f_0 t d_j(t) \end{aligned} \quad (49)$$

and with $d_j(t)$ the Fourier transform of the function $D_j(f)$

$$d_j(t) = 2 \int_0^{\epsilon} D_j(f) \cos 2\pi f t df \quad (50)$$

Possible choices for $D_j(f)$ can be found in Table 3, together with the corresponding $d_j(t)$. The continuous impulse response $h_j(t)$ of infinite length must be shortened to a finite extent and the discrete weighting sequence $\{h_k\}$, $-p \leq k \leq p$, is taken as the set of ordinates of the function $h_j(t)$. The filter length p is chosen as the time point above which $d_j(t)$ is essentially zero and it is entirely controlled by the band-width of the filter. The truncation points of the kernels $d_j(t)$ are also indicated in Table 3.

As pinpointed in Section 4, band-pass filtering forces the output noise to become highly autocorrelated even if the input noise is a realization of a white noise process. However, the standard errors of the least squares analysis can be corrected by using Eq. (8) in the case of autocorrelated residuals. If the autocorrelations $\hat{\rho}_k$ of the observed residuals may be neglected for lags k greater than some k_0 , then the elements of the matrix C in Eq. (11) are defined by

$$c_{ij} = \hat{\sigma}_e^2 \left\{ x_{ij}(0) + \sum_{k=1}^{k_0} \hat{\rho}_k [x_{ij}(k) + x_{ji}(k)] \right\} \quad (51)$$

and k_0 is supposed to be small in respect of the number m of observations. For the trigonometric model (40) we obtain from Eqs. (12), (42), (43) and (45), for $1 \leq i, j \leq q$,

$$\begin{aligned} x_{ij}(k) &= h_i h_j [t_{ij}^{cc}(m-k) \cos k \omega_j - t_{ij}^{cs}(m-k) \sin k \omega_j] \\ x_{i,j+q}(k) &= h_i h_j [t_{ij}^{cs}(m-k) \cos k \omega_j + t_{ij}^{cc}(m-k) \sin k \omega_j] \\ x_{i+q,j+q}(k) &= h_i h_j [t_{ij}^{ss}(m-k) \cos k \omega_j + t_{ji}^{cs}(m-k) \sin k \omega_j] \end{aligned} \quad (52)$$

For a sufficiently large value of m and $k_0 \ll m$ we can make the approximation $t_{ij}(m-k) \simeq t_{ij}(m)$, and from the definition (44) we find

$$c_{ij} \simeq \hat{\sigma}_e^2 \left\{ a_{ij} [1 + R_c(\omega_i) + R_c(\omega_j)] - a_{i+q,j} R_s(\omega_i) - a_{i,j+q} R_s(\omega_j) \right\}$$

$$c_{i,j+q} \simeq \hat{\sigma}_\epsilon^2 \left\{ a_{i,j+q} [1 + R_c(\omega_i) + R_c(\omega_j)] + a_{ij} R_s(\omega_j) - a_{i+q,j+q} R_s(\omega_i) \right\} \quad (53)$$

$$c_{i+q,j+q} \simeq \hat{\sigma}_\epsilon^2 \left\{ a_{i+q,j+q} [1 + R_c(\omega_i) + R_c(\omega_j)] + a_{i,j+q} R_s(\omega_i) + a_{i+q,j} R_s(\omega_j) \right\}$$

with

$$R_c(\omega) = \sum_{k=1}^{k_0} \hat{\rho}_k \cos k \omega, \quad R_s(\omega) = \sum_{k=1}^{k_0} \hat{\rho}_k \sin k \omega \quad (54)$$

Equations (53) show how the elements of the matrix C can be computed explicitly using only the elements a_{ij} of the normal matrix $A = X'X$ and the cosine and sine Fourier transforms of the autocorrelations $\hat{\rho}_k$, $k \geq 1$, of the observed residuals. For large m the normal matrix becomes almost diagonal and the same holds for the correction matrix C , which then takes entirely account of the residual power spectrum $R(\omega)$, since the diagonal elements of C are, in a good approximation, given by

$$c_{ii} \simeq \hat{\sigma}_\epsilon^2 a_{ii} R(\omega_i) \quad (55)$$

with

$$R(\omega) = 1 + 2 \sum_{k=1}^{k_0} \hat{\rho}_k \cos k \omega \quad (56)$$

The conclusion is evident: if Δb_i denotes the standard error of the estimated unknown \hat{b}_i , obtained by Eq. (6) with the assumption of uncorrelated residuals, all we have to do is to replace Δb_i by $R(\omega_i)^{1/2} \Delta b_i$ to take full account of the autocorrelation in the residual series. The correction factors will be denoted by $R_i = R(\omega_i)^{1/2}$. Applying this rule to the results reached by the Venedikov method (Table 1 and Fig. 3) we note that the power spectra are computed from the autocovariance sequence $\hat{\sigma}_\epsilon^2 \hat{\rho}_k$ and not from the autocorrelations $\hat{\rho}_k$. We conclude that the tidal parameters $\hat{\gamma}_i$ and $\hat{\kappa}_i$ are underestimated by a factor $\sqrt{22/2.06} \simeq 2.3$ for the waves in the vicinity of M_2 , while the correction factors for the diurnal and ter-diurnal bands may safely be considered equal to 1.

During the construction of the normal matrix $A = X'X$ in the harmonic analysis for each tidal band, the value of the observed residual can be tested with the procedure mentioned in Section 5. Since Venedikov's method already provides for a good initial tidal model $(\hat{\gamma}_j, \hat{\kappa}_j)$, a theoretical value $\hat{l}_t^{(r)}$, $r = 1, 2, 3$, at the time instant t can be calculated with this model and compared with the filtered value $l_t^{(r)}$; for the computation of $\hat{l}_t^{(r)}$ the amplitude factors of the band-pass filters must be taken into account. If $|l_t^{(r)} - \hat{l}_t^{(r)}| > 3 \hat{\sigma}_r$ the value $l_t^{(r)}$ is rejected for the tidal band with index r . Since the output errors become highly correlated by the band-pass filtering, the effect of an erroneous observation will be spread out over the time axis and therefore 25 values on the left and on the right of each conspicuous observation are eliminated. The same procedure of data rejection will be used in all subsequent analyses.

The band-pass filters we used are characterized by the kernel $d_7(t)$, $\epsilon = 0.015$, $p + 1 = 200$ and central frequencies $f_0 = 0.040272$ cph, $f_0 = 0.080546$ cph, $f_0 = 0.120786$ cph for the D , SD and TD - bands, respectively. The results of this method are summarized in Table 4; it should be noted that the standard errors are corrected using Eq. (53). The autocorrelations of the observed residuals after least squares adjustment are shown in Fig. 5.

From column 6 in Table 4 it is clear that the standard errors of the amplitudes and phases of the tidal waves could be underestimated by a factor of the order of 10 in the case of strong correlation in the residual series when these are computed with Eq. (6) and not corrected as indicated in the above mentioned procedure.

7. Markov estimation on the original observations.

What is attempted by the band-pass filtering in Section 6 is the rejection of the contributions of the instrumental drift outside the tidal wave band in question, but yet, inside the band the influence of the drift is not removed and a severe autocorrelation is introduced in the residual series by the filtering process. A completely different view is indicated in Section 2. At present we have already a good model $(\hat{\gamma}_j, \hat{\kappa}_j)$ of the tidal parameters of all main waves. Using this model a reconstructed theoretical tide \hat{s}_t can be subtracted from the raw observations, yielding a time series $\hat{d}_t = y_t - \hat{s}_t = (s_t - \hat{s}_t) + d_t + \epsilon_t$, which comprises the real drift and the long period tides d_t , the original noise process ϵ_t , and small tidal residuals $s_t - \hat{s}_t$. This is in fact the first step of the method of Chojnicki (1972). The idea now is to adapt an autoregressive model of order p to this approximation \hat{d}_t of the instrumental drift

$$\sum_{k=0}^p \hat{\alpha}_k \hat{d}_{t-k} = \hat{v}_t \quad (57)$$

The estimated AR parameters $(\hat{\alpha}_0, \hat{\alpha}_1, \dots, \hat{\alpha}_p)$ can be computed with the Burg scheme, details on which will be found in Ulrych and Bishop (1975), Ulrych and Clayton (1976) and Smylie et al (1973). The optimum order of the AR model is estimated by Akaike's information theoretic criterion AIC (Akaike, 1974).

The next step is to apply the filter $(\hat{\alpha}_0, \hat{\alpha}_1, \dots, \hat{\alpha}_p)$ to the raw data in Eq. (26); the tidal constants can then be obtained from the transformed model (25) with nearly uncorrelated noise. In this way the drift is not eliminated from the record but transformed into a quasi white noise process. It will be noticed also that the three tidal bands are now analyzed in one step and not separately as they were in Venedikov's method or the technique suggested in Section 6.

If the order p is fairly low, the filter $(\hat{\alpha}_0, \hat{\alpha}_1, \dots, \hat{\alpha}_p)$ will be insensitive to the tidal residual $s_t - \hat{s}_t$. Denoting the Fourier transforms of $\hat{\alpha}_k$, \hat{d}_t and \hat{v}_t by $A(f)$, $D(f)$ and $N(f)$, respectively, it follows from Eq. (57) that

$$|A(f)|^2 = \frac{K^2}{|D(f)|^2} \quad (58)$$

since $|N(f)|^2 = K^2$, where K is a constant. The power transfer function $|A(f)|^2$ of the AR filter is therefore inversely proportional to the power spectrum of the drift and from Fig. 1 we see that the operator $(\hat{\alpha}_0, \hat{\alpha}_1, \dots, \hat{\alpha}_p)$ has essentially the properties of a high pass filter.

From Eq. (25) it follows that the Markov estimates \tilde{b}_i are computed by the matrix equation

$$\sum_{j=1}^n \tilde{a}_{ij} \tilde{b}_j = \tilde{c}_i, \quad 1 \leq i \leq n \quad (59)$$

where

$$\tilde{a}_{ij} = \sum_{t=1}^m \tilde{x}_{ti} \tilde{x}_{tj}, \quad \tilde{c}_i = \sum_{t=1}^m \tilde{y}_t \tilde{x}_{ti} \quad (60)$$

and taking the \tilde{x}_{ti} and \tilde{y}_t defined in Eq. (24). In the case of the trigonometric model (40) the matrix elements \tilde{a}_{ij} can be obtained in a different way than indicated by the discrete convolutions in Eq. (24). Indeed, from Eqs. (60) and (24) it follows that

$$\tilde{a}_{ij} = \sum_{t=1}^m \left(\sum_{r=0}^p \hat{\alpha}_r x_{t-r,i} \right) \left(\sum_{s=0}^p \hat{\alpha}_s x_{t-s,j} \right)$$

Using Eq. (42) we obtain, for $1 \leq i, j \leq q$

$$\begin{aligned} \tilde{a}_{ij} &= \sum_{t=1}^m [h_i A_c(\omega_i) \cos \omega_i t + h_i A_s(\omega_i) \sin \omega_i t] \cdot \\ &\quad [h_j A_c(\omega_j) \cos \omega_j t + h_j A_s(\omega_j) \sin \omega_j t] \\ \tilde{a}_{i,j+q} &= \sum_{t=1}^m [h_i A_c(\omega_i) \cos \omega_i t + h_i A_s(\omega_i) \sin \omega_i t] \cdot \\ &\quad [h_j A_c(\omega_j) \sin \omega_j t - h_j A_s(\omega_j) \cos \omega_j t] \\ \tilde{a}_{i+q,j+q} &= \sum_{t=1}^m [h_i A_c(\omega_i) \sin \omega_i t - h_i A_s(\omega_i) \cos \omega_i t] \cdot \\ &\quad [h_j A_c(\omega_j) \sin \omega_j t - h_j A_s(\omega_j) \cos \omega_j t] \end{aligned} \quad (61)$$

where

$$A_c(\omega) = \sum_{k=0}^p \hat{\alpha}_k \cos k \omega, \quad A_s(\omega) = \sum_{k=0}^p \hat{\alpha}_k \sin k \omega \quad (62)$$

are the cosine and sine Fourier transforms, respectively, of the AR filter.

Similarly it is shown that

$$\begin{aligned} \tilde{c}_i &= \sum_{t=1}^m \left(\sum_{k=0}^p \hat{\alpha}_k y_{t-k} \right) [h_i A_c(\omega_i) \cos \omega_i t + h_i A_s(\omega_i) \sin \omega_i t] \\ \tilde{c}_{i+q} &= \sum_{t=1}^m \left(\sum_{k=0}^p \hat{\alpha}_k y_{t-k} \right) [h_i A_c(\omega_i) \sin \omega_i t - h_i A_s(\omega_i) \cos \omega_i t] \end{aligned} \quad (63)$$

Although we have written $\omega_i t$ for the argument of the trigonometric functions we refer to Venedikov (1966 b) and Melchior (1978) for an exact computation of the arguments of the tidal waves. Comparing Eqs. (61) and (63) with Eqs. (40) and (44) we conclude that the computation of functions such as $h_j \text{trig } \omega_j t$ (where "trig" stands for cos or sin) in the least squares analysis is replaced by the calculation of function such as $h_j A_c(\omega_j) \text{trig } \omega_j t$ and $h_j A_s(\omega_j) \text{trig } \omega_j t$ in the Markov estimation, which means that the theoretical amplitudes merely need to be replaced by $h_j A_c(\omega_j)$ and $h_j A_s(\omega_j)$. In the least squares analysis we have to add up expressious like $h_i h_j \text{trig } \omega_i t \text{ trig } \omega_j t$ at the time instants t to obtain the matrix elements a_{ij} ; Eq. (61) shows how the matrix $\tilde{A} = \tilde{X}'\tilde{X}$ can be computed without performing explicitly the discrete convolutions of the AR filter ($\hat{\alpha}_0, \hat{\alpha}_1, \dots, \hat{\alpha}_p$) with the x_{tj} . The only convolution that has to be executed is the computation of the trans-

formed observations \tilde{y}_t in Eq. (24).

For the instrument and observing interval concerned we found that an AR model of the order $p = 8$ effectively reduces the approximation \hat{d}_t of the instrumental drift to a nearly uncorrelated time sequence. However it should be stated that the AR model of order $p = 8$ for \hat{d}_t is obtained from 3000 consecutive data and that it describes the drift fairly well in this restricted time interval, but in view of the fact that the actual instrumental drift must be regarded as a nonstationary phenomenon, the performance of the filter $(\hat{\alpha}_0, \hat{\alpha}_1, \dots, \hat{\alpha}_p)$ could be quite different for other observing intervals.

Certainly, advantages of this method are, first, that we work with the original data spaced $\Delta t = 1$ hour in time which thus increases considerably the number of data available for the analysis, and, second, that we can have access also to the series of observed residuals. An evident drawback in comparison with Venedikov's method is the important increase of computer time required.

The results of this method are summarized in Table 5 and the autocorrelations of the observed residuals \hat{v}_t are shown in Fig. 6. The standard deviation now stands for the root-mean-square error of the noise process \hat{v}_t and it estimates the white noise level at the end of the Nyquist interval. From Table 5 we conclude that the corrected standard errors are not essentially different from those obtained by the assumption of uncorrelated residuals; it is accordingly safe to regard the \hat{v}_t as a realization of a white noise process. This conclusion is further confirmed by the form of the autocorrelation sequence in Fig. 6.

The method of Usandivaras and Ducarme (1969) clearly belongs to this class. As an observation equation the difference between two successive readings is considered

$$z_t = y_t - y_{t-1} = (s_t - s_{t-1}) + (d_t - d_{t-1}) + (\epsilon_t - \epsilon_{t-1})$$

This corresponds to the application of the causal filter $h_0 = 1$, $h_{-1} = -1$ to the raw observations, with a transferfunction

$$H(\omega) = 1 - \cos \omega + i \sin \omega, \quad i^2 = -1,$$

having essentially the properties of a high-pass filter. If the drift is almost linear it may be expected to be sufficiently suppressed by the filter, together with the long period tides (the amplitude factor at the frequency of the wave M_f is 0.01916), but for a rapidly changing drift there will be an important drift residual in the error series of z_t . A disadvantage of the method is the fact that the error series $\epsilon_t - \epsilon_{t-1}$ becomes more correlated and the method therefore tends to underestimate slightly the standard errors of the tidal constants; this effect, however, can be eliminated by considering only every second point in the output series z_t .

8. Chojnicki's method.

The method of Chojnicki (1972) starts with a model $(\hat{\gamma}_j, \hat{\kappa}_j)$ of the tidal constants of all main waves in the diurnal, semi-diurnal and ter-diurnal bands, from which a theoretical tide \hat{s}_t is reconstructed. When this series \hat{s}_t is subtracted from the raw observations y_t in Eq. (26) a first approximation \hat{d}_t of the drift is obtained:

$$\hat{d}_t = y_t - \hat{s}_t = (s_t - \hat{s}_t) + n_t \quad (64)$$

where the noise process, $n_t = d_t + l_t + \epsilon_t$, comprises the actual instrumental drift d_t , the long period tides l_t , and the random disturbances ϵ_t . To eliminate the small tidal residuals $s_t - \hat{s}_t$, the Pertzev filter (Melchior, 1978, p. 168) with coefficients p_k , $-18 \leq k \leq 18$, is applied to \hat{d}_t and the result of this filtering is considered as an approximation to both the actual instrumental drift and the long period variations

$$\bar{d}_t = \sum_{k=-18}^{18} p_k \hat{d}_{t-k} = \sum_{k=-18}^{18} p_k (s_{t-k} - \hat{s}_{t-k}) + \sum_{k=-18}^{18} p_k n_{t-k} \quad (65)$$

The Pertzev filter is symmetrical ($p_{-k} = p_k$) with coefficients $p_0 = p_2 = p_3 = p_5 = p_8 = p_{10} = p_{18} = 1/15$ and all other weights are zero.

The time series d_t is next subtracted from the original data y_t and a least squares analysis is started on the modified observations

$$\begin{aligned} \bar{y}_t = y_t - \bar{d}_t &= s_t + n_t - \sum_{k=-18}^{18} p_k (s_{t-k} - \hat{s}_{t-k}) - \sum_{k=-18}^{18} p_k n_{t-k} \\ &= \sum_{k=-18}^{18} q_k s_{t-k} + \sum_{k=-18}^{18} p_k \hat{s}_{t-k} + \sum_{k=-18}^{18} q_k n_{t-k} \end{aligned} \quad (66)$$

where the filter coefficients q_k are defined by $q_0 = 1 - p_0$, $q_k = -p_k$ for $k \neq 0$. The filter q_k has essentially the properties of a high-pass filter.

Denoting by $P(f)$ and $Q(f) = 1 - P(f)$ the respective amplitude responses of the filters p_k and q_k , Eq. (66) can likewise be expressed in terms of the Fourier transforms

$$\bar{Y}(f) = Q(f) S(f) + P(f) \hat{S}(f) + Q(f) N(f) \quad (67)$$

The frequency response $Q(f)$ is shown by De Meyer (1973, p.3537, Fig. 1.3) and can be computed easily from

$$Q(f) = q_0 + 2 \sum_{k=1}^{18} q_k \cos 2\pi k f \quad (68)$$

Equation (67) clearly shows that the amplitudes of the observed tides are slightly modified by the value of the amplitude response $Q(f)$ at the frequencies of the tidal waves and that the noise process n_t in the original observations is transformed to the weighted sum of ordinates

$$\sum_{k=-18}^{18} q_k n_{t-k} = \sum_{k=-18}^{18} q_k (d_{t-k} + l_{t-k} + \epsilon_{t-k})$$

in the output data \bar{y}_t . Resulting from the fact that q_k is not a good high-pass filter, the drift is not entirely eliminated from the low-frequency part of the Nyquist interval (and certainly not from the tidal wave bands), but modified to $Q(f) D(f)$. For linearly changing drifts this effect can be expected to be small, but for rapidly changing drifts, as we observe for horizontal pendulum data, there can be an important drift residual in the series \bar{y}_t . Besides this imperfect attenuation of the low-frequency components in the noise process the Pertzev filter also introduces a strong autocorrelation in the residuals.

The residuals $P(f) \hat{S}(f)$ of the theoretical model may safely be regarded as being zero in

view of the fact that the Pertzev filter p_k behaves like an adequate band-reject filter for the three tidal wave bands in question. From the point of view of filter theory Chojnicki's method therefore is equivalent to a high-pass filtering scheme with coefficients q_k , and to the execution of an harmonic analysis on the filtered data

$$\bar{y}_t = \sum_{k=-18}^{18} q_k y_{t-k} = \sum_{k=-18}^{18} q_k s_{t-k} + \sum_{k=-18}^{18} q_k n_{t-k}$$

This conclusion corroborates the opinion of Schüller (1975) that the use of a theoretical model \hat{s}_t is not needed a priori.

The results achieved with Chojnicki's method are summarized in Table 6 and the autocorrelations of the observed residuals are shown in Fig. 7. We conclude that the uncorrected standard errors of the tidal parameters are underestimated by a factor of the order 3 in the D-band but the root-mean square errors for the SD-band are not essentially changed when the autocorrelations of the residuals are taken into account. The standard deviation 5.60 m sec estimates the white noise level in the frequency interval $0.03 \leq f \leq 0.05$ cph; its relatively large value indicates that there is an important drift residual left in the filtered observations \bar{y}_t .

9. A modification of Chojnicki's method.

The fact that the instrumental drift can be inadequately estimated from the observations by the Pertzev filter is illustrated in Fig. 8, where a well selected observation interval with a rapidly changing trend is shown for the instrument concerned. We note the relatively large differences between the drift \bar{d}_t , obtained by the method of Chojnicki, and the first approximation $\hat{d}_t = y_t - \hat{s}_t$. If the tidal model \hat{s}_t is fairly good it can be argued intuitively that \bar{d}_t should follow the curve \hat{d}_t more closely. Therefore we have tested a method of drift correction, described below, which is not based on the principle of filtering.

Starting from the time series $\hat{d}_t = y_t - \hat{s}_t$ we select $(2p + 1)$ consecutive values of \hat{d}_t at each time instant t , such that p values are on the left of t and p values are on the right of t . In this time interval of $(2p + 1)$ values \hat{d}_{t+k} , $-p \leq k \leq p$, the curve \hat{d}_t is approximated in the least squares sense by a quadratic expression

$$\hat{d}_t \simeq D_t = a + bt + ct^2 \quad (68)$$

and the constants a, b, c can be estimated from the $(2p + 1)$ values of \hat{d}_t by the least squares method, thus obtaining the value of D_t at the time t . Shifting the origin with 1 hour and repeating this procedure, the time sequence D_t is obtained. Figure 8 shows that D_t is much closer to \hat{d}_t than the drift \bar{d}_t obtained by the Pertzev filter. This new D_t is now supposed to be an approximation of the actual instrumental drift and a tidal analysis can be started on the differences $y_t - D_t$.

The results of this method are given in Table 7 and the autocorrelations of the observed residuals are shown in Fig. 9. We conclude that the standard errors under the assumption of uncorrelated noise should be corrected by a factor of the order of 2 in the D-band and by a factor of the order of 3 in the SD-band; for the TD-band the correction does not seem to have an appreciable effect. For this analysis $p = 12$ is chosen. Furthermore it is seen that the standard deviation for this method is about

one half of the standard deviation for Chojnicki's method and that the corrected root-mean-square errors of the tidal parameters for the diurnal band are about three times smaller than those in Table 6. The standard errors are nearly equivalent in the SD-band for both methods.

Although it is tempting to claim that this method is superior to the other techniques we have mentioned, we must clearly point out that it is not evident how this drift elimination affects the Fourier spectrum and especially the amplitudes of the observed tidal waves. In addition it can be argued that the final tidal model will be biased towards the model originally selected for constructing the theoretical tides. This method must be seen in the context of a better determination of the fine structure of the tidal spectrum and especially as concerns the diurnal band (wave ψ_1). Therefore further investigation of this procedure is required.

Since the use of a theoretical tidal sequence \hat{s}_t does not seem essential for eliminating the drift the logical improvement of the method of Chojnicki can be outlined in the following steps :

- (1) low-pass filtering of the data with cut - off frequency
 $f_c = 0.14$ cph, $\Delta t = 1$ h, 50 coefficients,
- (2) decimation of the filtered output by taking every third point in order to reduce the number of computations,
- (3) high-pass filtering of the decimated series with cut - off frequency
 $f_c = 0.03$ cph, $\Delta t = 3$ h, 50 coefficients,
- (4) execution of a least-squares analysis on the resulting output.

This rather simple technique gives very reliable results as can be seen in Table 8; the autocorrelations of the observed residuals are shown in Fig. 10. The correction factors R_i are of the order of 4 and 2 for the diurnal and semi-diurnal band, respectively.

10. The residual spectrum.

Lecolazet and Melchior (1977), Wenzel (1977) and Barker (1978) have advocated for a careful inspection of the residual spectrum after least squares adjustment. Indeed the ultimate goal of any method of tidal analysis is to end up with a constant power spectrum of the observed residuals over the entire Nyquist interval, from which the conclusion would be reached that the noise process in the residual series should be white and that nothing could be gained after this stage for the same observing interval. In practice it is found that the residual spectra deviate considerably from this ideal situation. A non-constant power spectrum arises if the instrumental drift is not perfectly eliminated from the data, if some waves are inadequately described or not included in the linear model or if the amplitudes of some tidal waves suffer from modulation effects. Examples can be seen in Figs. 2 and 3 of Barker (1978, p. 4609-4610), where the residual spectra of data from an Askania tiltmeter are shown for two different periods and in Fig. 3 of Lecolazet and Melchior (1977, p. 16) for observations from two gravimeters. In both cases the method of Chojnicki was used to perform the harmonic analysis. A coloured noise spectrum with important contributions at the low frequencies and increased noise levels in the main tidal bands are observed.

An incomplete description of the linear model arises for example when earth tide measurements from areas affected by shallow water loading are analyzed, thus introducing non-linear waves which disturb the astronomical components. Non-linear waves can also be generated by a non-linear response of the instrument and by inhomogeneities in the site geology. The fact that these shallow water waves ac-

tually disturb the records at the station Dourbes (140 km from the North Sea) is clearly demonstrated in Fig. 11, where we show the residual power spectra for the method of the Markov estimation, Chojnicki's method and the two modifications of the method of Chojnicki. The autocovariances for lags up to $m = 1024$ are calculated from $n = 8192$ observations with sampling interval $\Delta t = 2$ hours for Fig. 11 a, b, c, thus giving the frequency resolution $\Delta f = 1/4096$ cph and the equivalent number of degrees of freedom $2n/m = 16$. Fig. 11 d corresponds to the parameters $m = 1024$, $n = 5970$, $\Delta t = 3$ h, $\Delta f = 1/6144$ cph. Figure 12 shows the periodogram of the residual series for the least squares method of Section 9 (modified Chojnicki's method, sliding least squares), computed from $n = 4096$ data with $\Delta t = 2$ h and giving a frequency resolution $\Delta f = 1/16384$ cph. For the identification of the shallow water constituents the terminology of Rossiter and Lennon (1968) is used.

From Fig. 12 it is evident that the noise is far from uniform and it is maximum in the tidal wave bands in which we are precisely interested. Except for a small S_1 the diurnal group of tidal lines appears to be adequately represented in the linear model and the noise is low in the D-band (possibly due to the numerical method itself). The same conclusion is reached for the Markov estimation, but Figs. 12 b and 12d show exactly the opposite effect. The general impression for the diurnal band is of an increased background noise, almost certainly of meteorological origin and there seem to be no significant constituents other than those derived from the harmonic development of the tide-generating potential.

The largest residual power in Figs. 12 and 11c is found in the semi-diurnal band and a number of lines surrounding M_2 is indicated. Their position in the spectrum suggests that they may be generated by modulations of M_2 by long period terms, i.e. transient equivalents of OP_2 and MKS_2 which are the pair of lines representing semi-annual perturbations of M_2 . Also lines at the frequencies of the waves MNS_2 (and OQ_2), MSN_2 (and KJ_2), $2SM_2$ and SKN_2 can be identified as peaks on the periodogram. We also note non-negligible residual power at the frequencies where the tidal waves $2N_2 + \mu_2$, $N_2 + \nu_2$ and especially L_2 are situated, respectively disturbed by $2MK_2$, $2ML_2$ and $2MN_2$.

In the ter-diurnal and quarter diurnal bands the background noise is fairly low and the waves SK_3 , MN_4 , M_4 and MS_4 can be identified.

Table 9 shows the magnitudes α_i of some important non-linear waves in percentages of the observed amplitude of the wave M_2 for the oceanic tides at the Ostend harbour (Melchior et al, 1967). The corresponding coefficients α_i' denote the amplitudes of the residual waves in percentages of the observed magnitude of M_2 for the earth tide observations and they are obtained from the periodogram of Fig. 12. It is clear that the non-linear terms affect the earth tide observations by shallow water loading for the station in question (140 km from the North Sea). The amplitude of the wave M_4 is about 0.5% of the observed amplitude of M_2 ; the residual amplitudes in the astronomical components $3N_2$, $2N_2$, N_2 and η_2 are about 0.4% of M_2 , while the residual amplitudes in M_2 and L_2 are estimated as 0.8% of M_2 . Much of the variance of the noise process therefore goes into these non-linear disturbances; the shallow water constituents not coinciding with the astronomical components could be included into the harmonic analysis, but the perturbations at the tidal frequencies constitute a problem.

11. Results for the nearly diurnal free wobble.

Tesseral forces of the diurnal tides generate the precession-nutation torque, which tends to rotate the equator towards the ecliptic, thus creating core motions with respect to the earth's mantle.

The hydrodynamical theory demonstrates that a resonance effect due to these motions in the liquid core is imposed on the tidal waves in the vicinity of K_1 , and a resonant amplification of the amplitudes factors as a function of frequency takes place. The resonance frequency has been calculated for a few earth models and it is found to be very near the solar wave ψ_1 . The tilt factors γ for four theoretical models, together with the results of Table 7 and the values obtained by Melchior (1978, Chap. 13), are given in Table 10: MO_1 is the Molodensky model 1 (liquid, homogeneous core), MO_2 is the Molodensky model 2 (inner core), JV_1 is the Jeffreys-Vicente model 1 (homogeneous, incompressible core with central particle) and JV_2 is the Jeffreys-Vicente model 2 (Roche density law); ω_r stands for the associated resonance frequency (Melchior, 1978). The columns P.Y.S. and T.S. give the theoretical results of $P_0 - Yu$ Shen and Mansinha (1976) and T. Sasao et al (1977) respectively.

The results of the observations are in good agreement with the theory of the dynamical effects of a liquid core on the principal diurnal waves O_1 , P_1 , K_1 . A nearly diurnal resonance effect undoubtedly exists, but the factors $\gamma(O_1)/\gamma(K_1)$ and $[1 - \gamma(O_1)]/[1 - \gamma(K_1)]$ are significantly different from the corresponding factors for the theoretical models.

As to the exact location of the resonance frequency the observations are actually controversial. Since the wave O_1 is relatively far from the resonance frequency the tilt factor $\gamma(O_1)$ must be practically insensitive to the exact structure of the resonance band. It seems that $\gamma(O_1)$ is systematically somewhat smaller than the value predicted by the models, while $\gamma(K_1)$ is slightly larger. A value $\gamma(O_1)/\gamma(K_1) = 0.914$ can be explained by a Molodensky model 2 with $\omega_r = 15^\circ.060$; this in turn gives $\gamma(O_1) = 0.686$, $\gamma(K_1) = 0.756$, $\gamma(O_1)/\gamma(K_1) = 0.91$ and $[1 - \gamma(O_1)]/[1 - \gamma(K_1)] = 1.29$. In this respect ω_r should be slightly shifted to the lower frequencies; however, this value for ω_r would give even smaller values for the tilt factors for the waves ψ_1 and Q_1 .

The comparison of Tables 1 and 2 teaches that the value of $\gamma(\psi_1)$ can be drastically changed when even only a small amount of data is rejected from the observations. This effect should impose stringent restrictions in the interpretation of the observational results as they are obtained at present. All harmonic analyses in this study indicate quite large $\gamma(\psi_1)$ and $\gamma(\varphi_1)$, supporting the idea that the resonance frequency is displaced towards the higher frequencies, but this would yield smaller values for $\gamma(K_1)$. A large $\gamma(\varphi_1)$ and relatively small $\gamma(K_1)$ is reported by Blum et al (1973), but our results are not so coherent from this point of view. It is a matter of fact that the observations are not sufficiently accurate to determine the location of the resonant frequency but, nevertheless, the idea turns up that the resonance band is more complicated in its structure than is indicated by the theory of Molodensky (Sasao et al, 1977).

With the exception of the core resonance the amplitude factors are expected to be a smoother function of the frequency than the corresponding parameters for the oceanic tides. All analyses clearly indicate that the results in the semi-diurnal band are anomalous for the waves ϵ_2 , μ_2 , ν_2 , λ_2 , L_2 and T_2 . This shows once more the presence of the loading signal, of non-linearities and of perturbations of non-tidal origin.

Table 1

Method Venédikov without the application of the test

Wave group	Wave	γ	$\Delta\gamma$	κ	$\Delta\kappa$
115-119	SIGMQ1	0.6145	0.4222	- 84.69	39.39
124-126	2Q1	0.5193	0.1283	- 1.90	14.16
127-129	SIGMA1	0.2200	0.1056	- 17.85	27.50
133-136	Q1	0.5965	0.0164	5.30	1.57
137-139	RH ϕ 1	0.4817	0.0856	14.96	10.18
143-145	ϕ 1	0.6484	0.0031	6.73	0.27
146-149	TAU1	1.1133	0.2343	- 41.15	12.06
152-155	N ϕ 1	0.6508	0.0356	6.26	3.13
156-158	KI1	1.1102	0.1989	6.97	10.27
161-162	PI1	0.6650	0.1142	- 5.97	9.83
163-163	P1	0.7156	0.0067	3.07	0.54
164-164	S1	2.4484	0.4106	18.98	9.52
165-165	K1	0.7452	0.0022	- 0.42	0.17
166-166	PSI1	1.0051	0.2778	- 0.83	15.83
167-168	PHI1	0.9666	0.1575	- 22.20	9.34
172-174	TETA1	0.6569	0.2010	12.66	17.54
175-177	J1	0.6026	0.0385	0.87	3.66
181-183	S ϕ 1	0.7853	0.2348	- 28.29	17.14
184-186	$\phi\phi$ 1	0.5540	0.0594	- 8.46	6.15
191-195	NU1	0.5573	0.3111	28.92	31.98
215-226	3N2	0.8713	0.4101	20.13	26.98
227-229	EPS2	1.3994	0.1722	8.29	7.05
233-236	2N2	0.8215	0.0492	8.81	3.43
237-239	MU2	1.2072	0.0405	- 6.10	1.92
243-245	N2	0.8211	0.0063	4.92	0.44
246-248	NU2	0.7905	0.0329	10.85	2.38
252-258	M2	0.8137	0.0012	3.58	0.08
262-264	LAMB2	1.0652	0.1566	48.27	8.42
265-265	L2	0.9037	0.0380	12.50	2.41
267-272	T2	0.7699	0.0420	3.77	3.13
273-273	S2	0.8225	0.0025	- 3.46	0.17
274-277	K2	0.8090	0.0085	- 3.26	0.60
282-285	ETA2	0.6661	0.1431	- 18.96	12.31
292-295	2K2	0.3424	0.3929	- 57.77	65.75
335-347		0.5601	0.0772	8.04	7.89
353-365	M3	0.8608	0.0214	8.20	1.42
375-375		0.8939	0.1413	- 1.39	9.05

Standard deviation D 2.75 , SD 2.06 , TD 0.45 m seca

Number of days 3194 (1/1/1969-31/12/1977)

 $\gamma(O_1)/\gamma(K_1) = 0.8701$ $[1 - \gamma(O_1)]/[1 - \gamma(K_1)] = 1.3799$

Table 2

Method Venedikov with the application of the test

Wave group	Wave	γ	$\Delta\gamma$	κ	$\Delta\kappa$
115-119	SIGMQ1	0.6605	0.3657	- 83.14	31.72
124-126	2Q1	0.4814	0.1113	- 6.27	13.25
127-129	SIGMA1	0.1829	0.0916	8.31	28.68
133-136	Q1	0.6033	0.0142	5.25	1.35
137-139	RH ϕ 1	0.5058	0.0742	7.91	8.41
143-145	ϕ 1	0.6510	0.0027	6.59	0.23
146-149	TAU1	0.8295	0.2034	- 37.70	14.05
152-155	N ϕ 1	0.6630	0.0309	4.58	2.67
156-158	KI1	0.9605	0.1725	5.65	10.29
161-162	PI1	0.6305	0.0991	2.93	9.00
163-163	P1	0.7097	0.0058	2.39	0.47
164-164	S1	2.1067	0.3561	25.61	9.61
165-165	K1	0.7450	0.0019	- 0.27	0.14
166-166	PSI1	0.5597	0.2410	- 0.52	24.85
167-168	PHI1	0.8902	0.1367	- 11.35	8.80
172-174	TETA1	0.5984	0.1744	17.85	16.70
175-177	J1	0.6090	0.0334	1.26	3.14
181-183	S ϕ 1	0.7666	0.2036	- 19.07	15.22
184-186	$\phi\phi$ 1	0.5360	0.0515	- 10.75	5.51
191-195	NU1	0.4862	0.2695	28.93	31.75
215-226	3N2	0.8953	0.2099	19.89	13.44
227-229	EPS2	1.2911	0.0881	4.51	3.91
233-236	2N2	0.8431	0.0252	7.59	1.71
237-239	MU2	1.1990	0.0207	- 5.65	0.99
243-245	N2	0.8256	0.0032	4.34	0.22
246-248	NU2	0.7782	0.0168	6.72	1.24
252-258	M2	0.8152	0.0006	3.40	0.04
262-264	LAMB2	1.0894	0.0800	46.98	4.21
265-265	L2	0.8930	0.0194	14.18	1.24
267-272	T2	0.8079	0.0215	4.13	1.52
273-273	S2	0.8243	0.0013	- 3.18	0.09
274-277	K2	0.8158	0.0043	- 2.87	0.30
282-285	ETA2	0.7308	0.0731	- 13.06	5.73
292-295	2K2	0.4024	0.2008	- 49.93	28.59
335-347		0.5901	0.0717	10.95	6.96
353-365	M3	0.8760	0.0198	8.26	1.30
375-375		1.0477	0.1315	- 4.71	7.19

Standard deviation D 2.37 , SD 1.05 , TD 0.41 m seca

Number of days 3140 (1/1/1969-31/12/1977)

 $\gamma(O_1)/\gamma(K_1) = 0.8738$ $[1 - \gamma(O_1)]/[1 - \gamma(K_1)] = 1.3686$

Table 3

j	$D_j(f)$	$d_j(t)$	Truncation point
0	1, $ f < \epsilon$ 0, $ f > \epsilon$	$\frac{1}{\pi t} \sin 2\pi \epsilon t$	$\epsilon p = 10$
1	$(1 - \frac{ f }{\epsilon}) D_0(f)$	$\epsilon (\frac{\sin \pi \epsilon t}{\pi \epsilon t})^2$	$\epsilon p = 5$
2	$\frac{1}{2} (1 + \cos \frac{\pi f}{\epsilon}) D_0(f)$	$\frac{1}{2} d_0(t) + \frac{1}{4} [d_0(t - \frac{1}{2\epsilon}) + d_0(t + \frac{1}{2\epsilon})]$	$\epsilon p = 3$
3	$(0.54 + 0.46 \cos \frac{\pi f}{\epsilon}) D_0(f)$	$0.54 d_0(t) + 0.23 [d_0(t - \frac{1}{2\epsilon}) + d_0(t + \frac{1}{2\epsilon})]$	$\epsilon p = 3$
4	$(0.42 + 0.50 \cos \frac{\pi f}{\epsilon})$ $+ 0.08 \cos \frac{2\pi f}{\epsilon}) D_0(f)$	$0.42 d_0(t) + 0.25 [d_0(t - \frac{1}{2\epsilon}) + d_0(t + \frac{1}{2\epsilon})]$ $+ 0.04 [d_0(t - \frac{1}{\epsilon}) + d_0(t + \frac{1}{\epsilon})]$	$\epsilon p = 2$
5	$(1 - \frac{f^2}{\epsilon^2})^2 D_0(f)$	$16 \sqrt{\frac{\pi}{2}} \epsilon \frac{J_{5/2}(2\pi \epsilon t)}{(2\pi \epsilon t)^{5/2}}$	$\epsilon p = 3$
6	$(1 - \frac{f^2}{\epsilon^2}) D_0(f)$	$4 \sqrt{\frac{\pi}{2}} \epsilon \frac{J_{3/2}(2\pi \epsilon t)}{(2\pi \epsilon t)^{3/2}}$	$\epsilon p = 3$
7	$1 - 6 \frac{f^2}{\epsilon^2} + 6 \frac{ f ^3}{\epsilon^3}$, $ f \leq \frac{1}{2} \epsilon$ $2(1 - \frac{ f }{\epsilon})^3$, $\frac{1}{2} \epsilon \leq f \leq \epsilon$ 0, $ f > \epsilon$	$\frac{3}{4} \epsilon (\frac{\sin \pi \epsilon t/2}{\pi \epsilon t/2})^4$	$\epsilon p = 1.7$

Table 4

Band - pass filtering with overlapping

Wave group	Wave	γ	$\Delta\gamma$	κ	$\Delta\kappa$	R_i
115-119	SIGMQ1	0.7289	0.0688	- 58.22	5.41	4.54
124-126	2Q1	0.4974	0.0160	- 9.75	1.84	4.03
127-129	SIGMA1	0.4146	0.0126	- 1.69	1.74	4.16
133-136	Q1	0.6068	0.0016	7.07	0.15	6.15
137-139	R ϕ 1	0.5336	0.0082	12.18	0.88	6.34
143-145	ϕ 1	0.6522	0.0003	6.18	0.02	5.76
146-149	T ϕ 1	0.7832	0.0199	- 12.60	1.46	5.57
152-155	N ϕ 1	0.6452	0.0029	3.08	0.26	7.41
156-158	KI1	0.8092	0.0163	- 2.33	1.16	7.99
161-162	PI1	0.6142	0.0097	9.97	0.91	9.83
163-163	P1	0.7167	0.0006	1.47	0.05	9.88
164-164	S1	1.7132	0.0352	23.44	1.18	9.88
165-165	K1	0.7446	0.0002	0.03	0.01	9.84
166-166	PSI1	0.6264	0.0243	7.54	2.22	9.75
167-168	FI1	0.7733	0.0139	- 2.01	1.03	9.62
172-174	TETA1	0.6118	0.0198	4.95	1.85	6.63
175-177	J1	0.6246	0.0038	- 1.49	0.35	5.89
181-183	S ϕ 1	0.5705	0.0291	3.21	2.92	3.71
184-186	$\phi\phi$ 1	0.5762	0.0076	0.60	0.76	3.91
191-195	NU1	0.4367	0.0562	11.39	7.37	3.01
215-266	3N2	1.0019	0.0502	19.56	2.87	2.76
227-229	EPS2	1.3164	0.0195	0.30	0.85	2.90
233-236	2N2	0.8444	0.0046	5.47	0.31	5.35
237-239	MU2	1.2122	0.0037	- 5.96	0.18	5.80
243-245	N2	0.8266	0.0005	4.02	0.04	8.02
246-248	NU2	0.7964	0.0027	8.42	0.20	8.28
252-258	M2	0.8162	0.0001	3.31	0.01	9.83
262-264	LAMB2	1.1038	0.0133	46.97	0.69	9.74
265-265	L2	0.7686	0.0033	11.03	0.25	9.40
267-272	T2	0.7957	0.0041	4.65	0.29	5.49
273-273	S2	0.8247	0.0002	- 3.13	0.02	4.99
274-277	K2	0.8076	0.0009	- 2.86	0.06	3.98
282-285	ETA2	0.6443	0.0183	- 18.75	1.62	2.50
292-295	2K2	0.6829	0.0731	- 60.90	6.13	2.86
335-347		0.5659	0.0110	13.24	1.11	7.02
353-365	M3	0.8776	0.0030	8.22	0.19	6.59
375-375		0.9586	0.0248	4.41	1.48	5.79

Standard deviation D 2.27 , SD 1.70 , TD 0.70 msec

Number of observations D 63151 , SD 62941 , TD 68582 (1/1/1969-31/12/1977)

 $\gamma(O_1)/\gamma(K_1) = 0.8759$ $[1 - \gamma(O_1)]/[1 - \gamma(K_1)] = 1.3618$

Table 5

Markov estimation

Wave group	Wave	γ	$\Delta\gamma$	κ	$\Delta\kappa$	R_i
115-119	SIGMQ1	0.8571	0.2782	- 73.51	18.59	1.08
124-126	2Q1	0.7752	0.0829	- 45.05	6.13	0.59
127-129	SIGMA1	0.4565	0.0680	- 16.69	8.53	0.62
133-136	Q1	0.6074	0.0103	6.37	0.97	1.01
137-139	R ϕ 1	0.5072	0.0534	- 4.66	6.03	1.01
143-145	ϕ 1	0.6536	0.0018	6.54	0.16	0.59
146-149	T ϕ 1	0.8393	0.1401	- 33.62	9.56	0.54
152-155	N ϕ 1	0.6917	0.0204	12.23	1.69	1.15
156-158	KI1	0.7166	0.1134	0.09	9.07	1.26
161-162	PI1	0.6728	0.0628	22.51	5.34	1.54
163-163	P1	0.7193	0.0037	2.38	0.29	1.55
164-164	S1	2.1580	0.2226	31.28	5.91	1.55
165-165	K1	0.7473	0.0012	0.19	0.09	1.54
166-166	PSI1	0.6239	0.1499	0.40	13.77	1.53
167-168	FI1	0.7307	0.0846	2.58	6.64	1.52
172-174	TETA1	0.6416	0.1032	17.30	9.21	1.31
175-177	J1	0.6194	0.0196	- 0.26	1.81	1.28
181-183	S ϕ 1	0.7375	0.1121	- 36.91	8.71	1.23
184-186	$\phi\phi$ 1	0.5524	0.0281	2.06	2.91	1.22
191-195	NU1	0.6162	0.1353	22.21	12.57	1.07
215-226	3N2	0.8666	0.1083	- 23.21	7.16	1.29
227-229	EPS2	1.3202	0.0459	- 2.91	1.99	1.33
233-236	2N2	0.8326	0.0134	1.94	0.92	1.14
237-239	MU2	1.2094	0.0110	- 4.96	0.52	1.08
243-245	N2	0.8272	0.0017	3.91	0.12	1.57
246-248	NU2	0.7773	0.0091	- 3.56	0.67	1.74
252-258	M2	0.8167	0.0003	3.38	0.02	2.39
262-264	LAMB2	1.0545	0.0431	44.54	2.34	1.77
265-265	L2	0.8972	0.0104	19.02	0.67	1.60
267-272	T2	0.7925	0.0114	5.84	0.82	0.96
273-273	S2	0.8259	0.0007	- 3.23	0.05	0.97
274-277	K2	0.8189	0.0023	- 3.05	0.16	1.03
282-285	ETA2	0.7459	0.0376	- 12.63	2.89	1.49
292-295	2K2	0.5907	0.0994	- 47.94	9.64	1.32
335-347		0.5909	0.0622	14.56	6.03	0.94
353-365	M3	0.8745	0.0176	7.32	1.15	0.90
375-375		1.0756	0.1172	3.26	6.25	1.05

Standard deviation 2.53 msec

Number of observations 75698 (1/1/1969-31/12/1977)

 $\gamma(O_1)/\gamma(K_1) = 0.8746$ $[1 - \gamma(O_1)]/[1 - \gamma(K_1)] = 1.3708$

Table 6

Chojnicki's method

Wave group	Wave	γ	$\Delta\gamma$	κ	$\Delta\kappa$	R_i
115-119	SIGMQ1	0.9380	0.0789	- 53.56	4.82	2.69
124-126	2Q1	0.5031	0.0250	- 4.06	2.85	1.68
127-129	SIGMA1	0.4555	0.0208	7.24	2.62	1.75
133-136	Q1	0.6064	0.0033	7.22	0.31	2.29
137-139	R ϕ 1	0.5924	0.0175	7.70	1.69	2.25
143-145	ϕ 1	0.6548	0.0006	6.32	0.06	1.44
146-149	T ϕ 1	0.6976	0.0482	- 13.51	3.96	1.38
152-155	N ϕ 1	0.6998	0.0074	1.80	0.60	2.40
156-158	KI1	0.8041	0.0420	12.80	2.99	2.59
161-162	PI1	0.7082	0.0239	6.02	1.93	3.08
163-163	P1	0.7220	0.0014	1.49	0.11	3.09
164-164	S1	1.7459	0.0854	19.31	2.80	3.08
165-165	K1	0.7464	0.0005	0.07	0.04	3.07
166-166	PSI1	0.7427	0.0582	3.46	4.49	3.05
167-168	FI1	0.6779	0.0329	2.48	2.78	3.02
172-174	TETA1	0.6693	0.0421	5.65	3.61	2.51
175-177	J1	0.6443	0.0080	- 0.27	0.71	2.42
181-183	S ϕ 1	0.5241	0.0486	- 10.88	5.31	2.13
184-186	$\phi\phi$ 1	0.5483	0.0124	2.09	1.30	2.11
191-195	NU1	0.6309	0.0624	2.08	5.70	1.83
215-226	3N2	0.9625	0.1003	13.39	5.97	1.06
227-229	EPS2	1.2685	0.0425	3.36	1.92	1.10
233-236	2N2	0.8369	0.0126	6.69	0.86	0.92
237-239	MU2	1.2152	0.0105	- 5.57	0.49	0.86
243-245	N2	0.8259	0.0017	4.28	0.12	1.24
246-248	NU2	0.7966	0.0088	8.14	0.63	1.38
252-258	M2	0.8178	0.0003	3.38	0.02	1.86
262-264	LAMB2	1.1151	0.0433	46.44	2.23	1.34
265-265	L2	0.8629	0.0106	13.77	0.70	1.21
267-272	T2	0.7787	0.0118	3.85	0.86	0.73
273-273	S2	0.8272	0.0007	- 3.23	0.05	0.74
274-277	K2	0.8202	0.0024	- 2.87	0.17	0.78
282-285	ETA2	0.7670	0.0403	- 10.82	3.01	1.04
292-295	2K2	0.5283	0.1089	- 55.66	11.81	0.94
335-347		0.5088	0.0884	16.48	9.95	0.49
353-365	M3	0.8797	0.0252	6.97	1.64	0.50
375-375		1.1113	0.1758	12.07	9.07	0.59

Standard deviation 5.60 m seca

Number of observations 59828 (1/1/1969-31/12/1977)

 $\gamma(O_1)/\gamma(K_1) = 0.8773$ $[1 - \gamma(O_1)]/[1 - \gamma(K_1)] = 1.3612$

Table 7.

Modified Chojnicki's method (sliding least-squares).

Wave group	Wave	γ	$\Delta\gamma$	κ	$\Delta\kappa$	R_i
115-119	SIGMQ1	0.8101	0.0374	- 78.88	2.65	1.01
124-126	2Q1	0.5151	0.0119	- 8.05	1.32	0.65
127-129	SIGMA1	0.3532	0.0099	- 0.84	1.60	0.68
133-136	Q1	0.5954	0.0016	7.62	0.15	1.07
137-139	R ϕ 1	0.5150	0.0083	17.88	0.92	1.08
143-145	ϕ 1	0.6517	0.0003	6.55	0.03	0.75
146-149	T ϕ 1	0.9880	0.0230	- 28.10	1.33	0.70
152-155	N ϕ 1	0.6515	0.0035	4.59	0.31	1.42
156-158	KI1	0.8208	0.0199	15.01	1.39	1.57
161-162	PI1	0.6603	0.0114	2.66	0.99	2.03
163-163	P1	0.7215	0.0007	2.26	0.05	2.05
164-164	S1	0.7613	0.0407	- 9.60	3.07	2.06
165-165	K1	0.7468	0.0002	- 0.18	0.02	2.07
166-166	PSI1	0.9396	0.0277	0.49	1.69	2.07
167-168	FI1	0.8210	0.0157	- 18.32	1.09	2.06
172-174	TETA1	0.6762	0.0200	9.91	1.70	1.82
175-177	J1	0.6263	0.0038	- 0.93	0.35	1.78
181-183	S ϕ 1	0.5025	0.0230	- 9.08	2.62	1.81
184-186	$\phi\phi$ 1	0.5564	0.0058	- 1.19	0.60	1.82
191-195	NU1	0.5824	0.0296	- 3.50	2.91	1.67
215-226	3N2	0.9602	0.0477	11.57	2.84	2.98
227-229	EPS2	1.2707	0.0203	2.49	0.91	3.06
233-236	2N2	0.8337	0.0060	5.98	0.41	2.58
237-239	MU2	1.2068	0.00	- 5.12	0.24	2.46
243-245	N2	0.8280	0.0008	4.30	0.06	3.63
246-248	NU2	0.7867	0.0042	8.63	0.31	4.00
252-258	M2	0.8171	0.0002	3.36	0.01	5.41
262-264	LAMB2	1.0325	0.0207	46.56	1.15	4.03
265-265	L2	0.8643	0.0051	13.41	0.34	3.64
267-272	T2	0.7876	0.0056	3.85	0.41	2.08
273-273	S2	0.8256	0.0003	- 3.18	0.02	2.10
274-277	K2	0.8170	0.0011	- 3.05	0.08	2.22
282-285	ETA2	0.7317	0.0190	- 12.05	1.49	3.23
292-295	2K2	0.5356	0.0514	- 47.87	5.50	2.81
335-347		0.5775	0.0423	14.05	4.20	1.16
353-365	M3	0.8963	0.0121	8.34	0.77	1.04
375-375		1.0152	0.0831	2.14	4.69	1.13

Standard deviation 2.75 m seca

Number of observations 63188 (1/1/1969-31/12/1977)

 $\gamma(O_1)/\gamma(K_1) = 0.8727$ $[1 - \gamma(O_1)]/[1 - \gamma(K_1)] = 1.3756$

Table 8.

Modified Chojnicki's method (high-pass filtering)

Wave group	Wave	γ	$\Delta\gamma$	κ	$\Delta\kappa$	R_i
115-119	SIGMQ1	0.6515	0.0972	- 69.36	8.54	2.04
124-126	2Q1	0.4874	0.0300	- 3.78	3.53	2.26
127-129	SIGMA1	0.5129	0.0249	5.01	2.78	2.32
133-136	Q1	0.6034	0.0039	8.34	0.37	1.99
137-139	R ϕ 1	0.5838	0.0206	14.50	2.02	1.91
143-145	ϕ 1	0.6537	0.0007	6.25	0.07	1.75
146-149	T ϕ 1	0.8125	0.0568	- 26.09	4.00	1.84
152-155	N ϕ 1	0.7093	0.0086	1.91	0.69	1.79
156-158	KI1	0.7507	0.0493	12.12	3.76	1.44
161-162	PI1	0.7023	0.0282	14.58	2.30	3.70
163-163	P1	0.7273	0.0016	1.78	0.13	3.97
164-164	S1	1.2453	0.1008	14.83	4.63	4.06
165-165	K1	0.7452	0.0005	- 0.09	0.04	3.96
166-166	PSI1	0.9180	0.0685	4.02	4.28	3.69
167-168	FI1	0.6887	0.0387	1.00	3.22	3.27
172-174	TETA1	0.6387	0.0493	2.51	4.43	2.17
175-177	J1	0.6464	0.0094	- 1.82	0.83	1.86
181-183	S ϕ 1	0.4173	0.0568	- 3.60	7.82	2.32
184-186	$\phi\phi$ 1	0.5557	0.0145	2.84	1.49	2.23
191-195	NU1	0.5332	0.0722	8.39	7.76	1.54
215-226	3N2	1.0285	0.1161	16.53	6.46	1.19
227-229	EPS2	1.2353	0.0494	1.62	2.29	0.92
233-236	2N2	0.8489	0.0147	5.11	0.99	1.27
237-239	MU2	1.1883	0.0122	- 5.33	0.51	1.23
243-245	N2	0.8268	0.0020	4.22	0.14	1.71
246-248	NU2	0.7925	0.0103	9.72	0.74	1.58
252-258	M2	0.8176	0.0004	3.36	0.03	2.68
262-264	LAMB2	1.1070	0.0507	49.11	2.63	1.60
265-265	L2	0.8636	0.0126	14.06	0.84	1.70
267-272	T2	0.7941	0.0138	3.53	0.99	1.15
273-273	S2	0.8264	0.0008	- 3.24	0.06	1.21
274-277	K2	0.8170	0.0028	- 2.79	0.20	1.14
282-285	ETA2	0.6987	0.0467	- 10.74	3.83	0.93
292-295	2K2	0.4710	0.1246	- 59.28	15.16	1.06
335-347		0.6166	0.1027	23.43	9.53	0.60
353-365	M3	0.8878	0.0296	8.05	1.91	0.31
375-375		0.9028	0.2063	6.68	13.11	0.37

Standard deviation 2.94 m sec

Number of observations 12192 (1/1/1969-31/12/1977)

 $\gamma(O_1)/\gamma(K_1) = 0.8772$ $[1 - \gamma(O_1)]/[1 - \gamma(K_1)] = 1.3591$

Table 9 — The magnitudes of some non-linear waves.

Astronomical component	Shallow water component	α_i	α'_i	α'_i/α_i
$3N_2, \epsilon_2$	$OQ_2 + MNS_2$	2.08	0.43	0.21
$2N_2, \mu_2$	$2MS_2$		0.42	
N_2, ν_2	$2ML_2$		0.46	
M_2	$OP_2 + MKS_2$	1.45	0.83	0.57
L_2	$2MN_2$		0.84	
η_2	$MSN_2 + KJ_2$	1.70	0.34	0.20
	$2SM_2$	1.95	0.63	0.32
	SK_3	0.50	0.36	0.72
	MN_4	1.89	0.25	0.13
	M_4	5.84	0.50	0.09
	MS_4	3.58	0.30	0.08

Table 10 — Theoretical and observed tilt factors.

Wave	MO2	MO2	JV1	JV2	P.Y.S.	T.S.	Table 7	Mechior
Q ₁	0.688	0.686			0.690	0.681	0.5954	0.6590
O ₁	0.688	0.686	0.658	0.658	0.691	0.681	0.6517	0.6788
π_1	0.696	0.694			0.699	0.690	0.6603	
P ₁	0.700	0.697	0.676	0.696	0.702	0.693	0.7215	0.7054
S ₁	0.707	0.703			0.709	0.701	0.7613	
165.545	0.730	0.723			0.731	0.723		
K ₁	0.732	0.726	0.714	0.693	0.734	0.726	0.7468	0.7429
165.565	0.736	0.729			0.737	0.729		
ψ_1	0.523	0.529			0.521	0.466	0.9396	0.450
φ_1	0.657	0.658			0.660	0.648	0.8210	0.712
J ₁	0.684	0.682			0.686	0.677	0.6263	0.6690
OO ₁	0.685	0.684	0.654	0.661	0.688	0.679	0.5564	0.6690
$\gamma(O_1)/\gamma(K_1)$	0.937	0.945	0.922	0.949	0.941	0.938	0.873	0.914
$[1 - \gamma(O_1)]/[1 - \gamma(K_1)]$	1.172	1.146	1.196	1.114	1.162	1.146	1.376	1.249
ω_r (deg/h)	15.07327	15.07361	15.07476	15.10168				

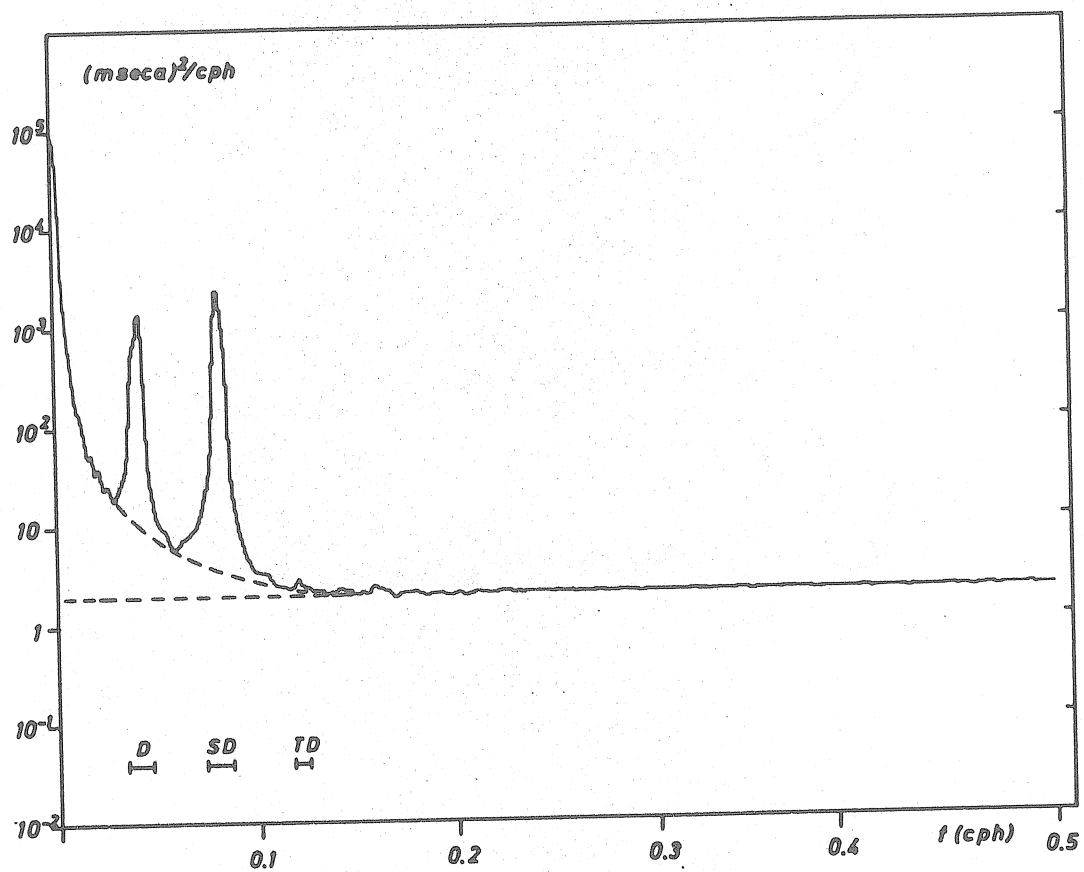


Fig. 1 - Power spectrum of the horizontal pendulum VM 28 EW.

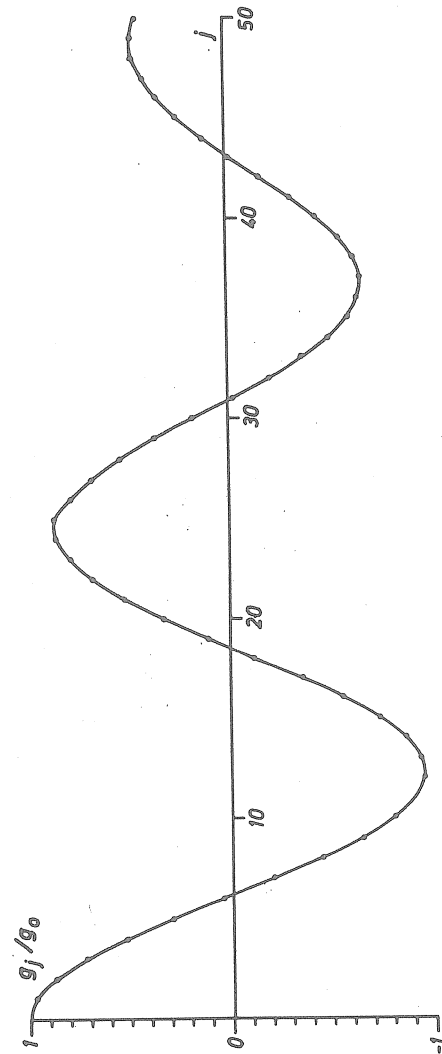


Fig. 2 - The function g_j/g_0 for the band-pass filter with $f_1 = 0.034$ cph and $f_2 = 0.047$ cph.

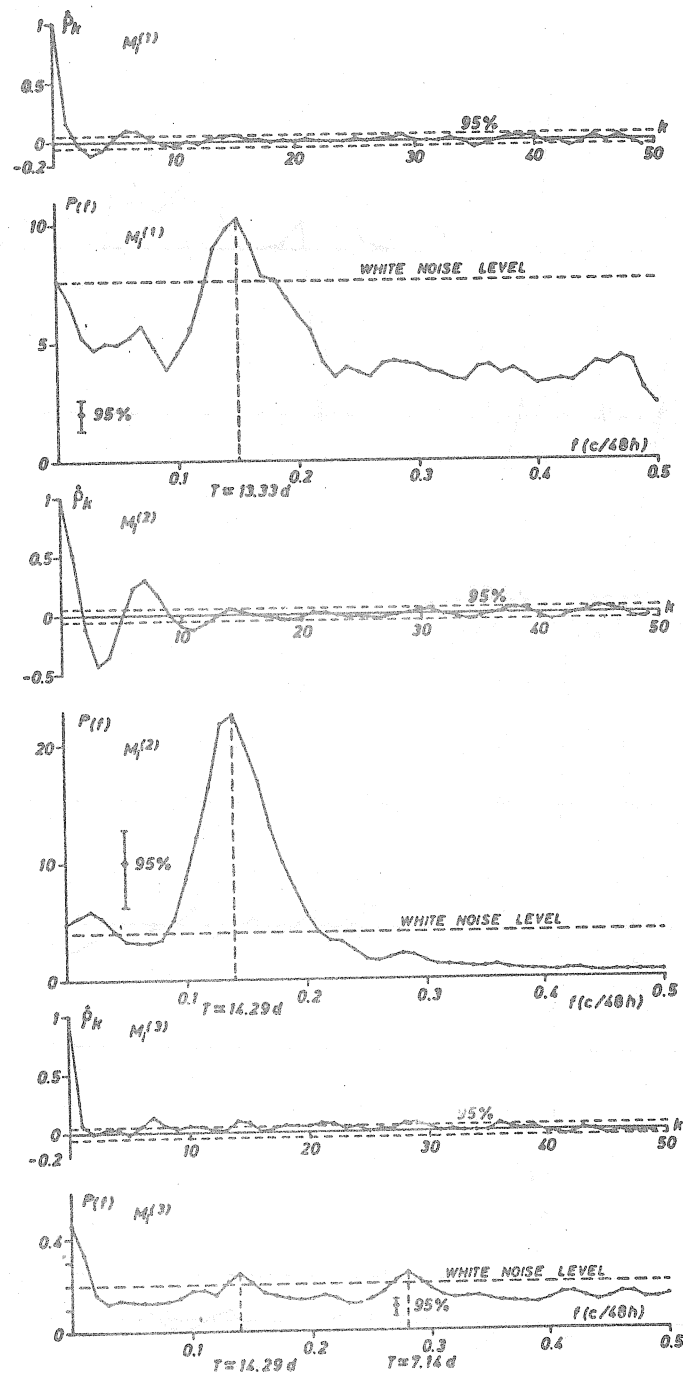


Fig. 3 - Autocorrelation function $\hat{\rho}_k$ and power spectrum $P(f)$ of the observed residuals of the $M_i^{(r)}$ series.

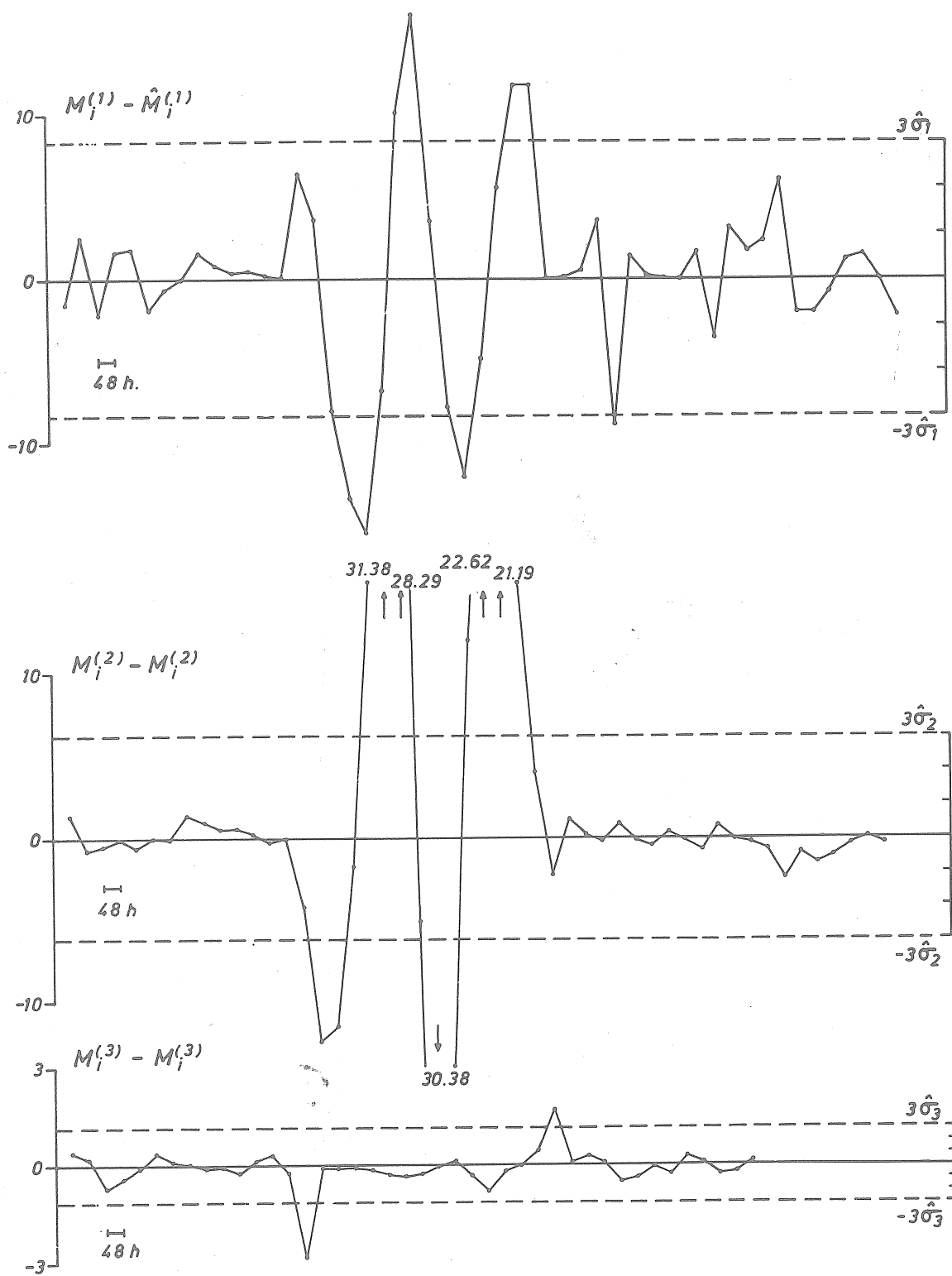


Fig. 4 - Differences $M_i^{(r)} - \hat{M}_i^{(r)}$ for the tidal band $r = 1, 2, 3$.

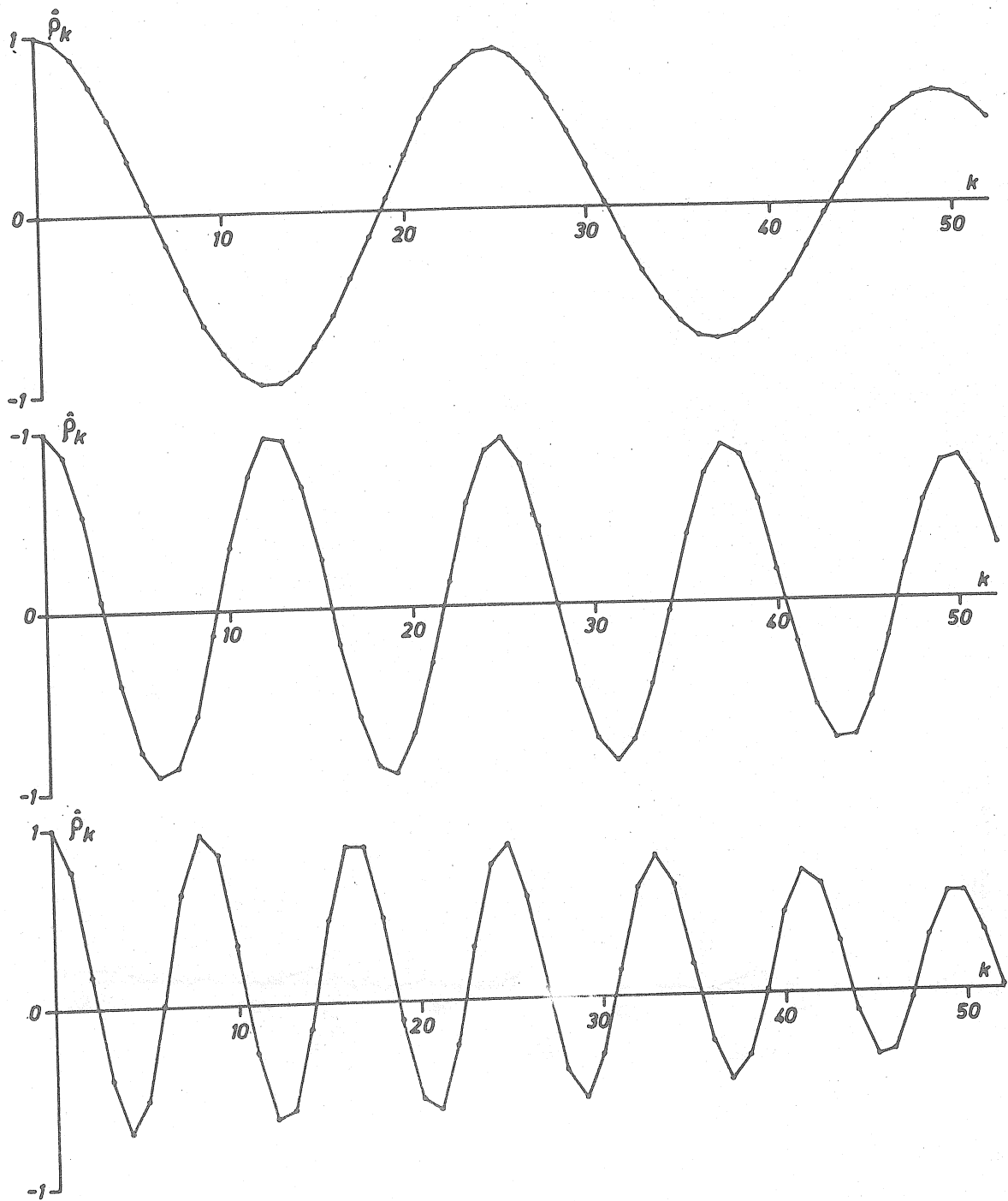


Fig. 5 - Band-pass filtering with overlapping. Autocorrelations of the observed residuals (a) D-band, (b) SD-band, (c) TD-band.

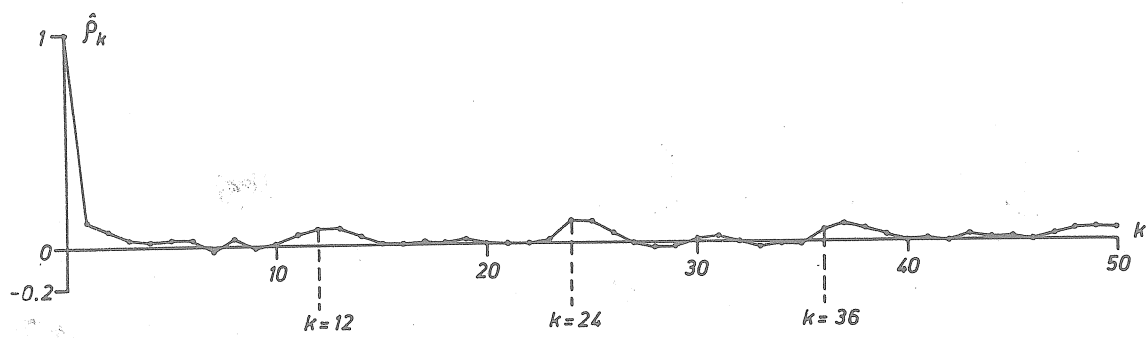


Fig. 6 - Markov estimation. Autocorrelations of the observed residuals.

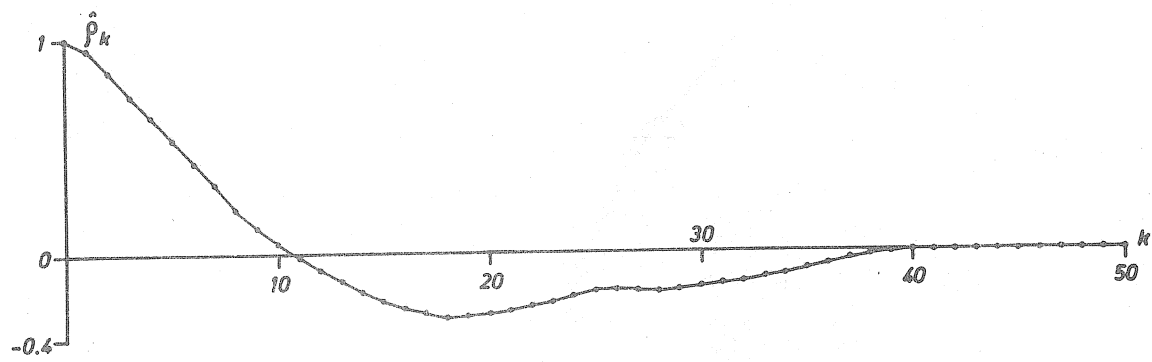


Fig. 7 - Chojniki's method. Autocorrelations of the observed residuals.

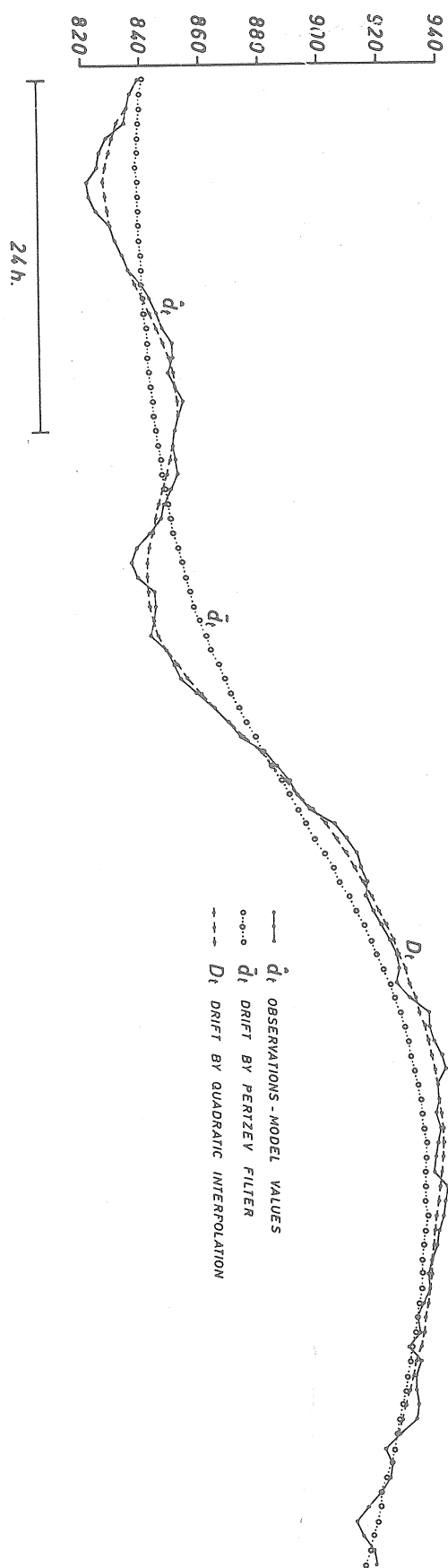


Fig. 8 - Different trend estimations. Drift $\hat{d}_t = y_t - \hat{s}_t$ (full curve); drift \bar{d}_t of Chojnicki's method (dotted curve); drift D_t of sliding least squares method (dashed curve).

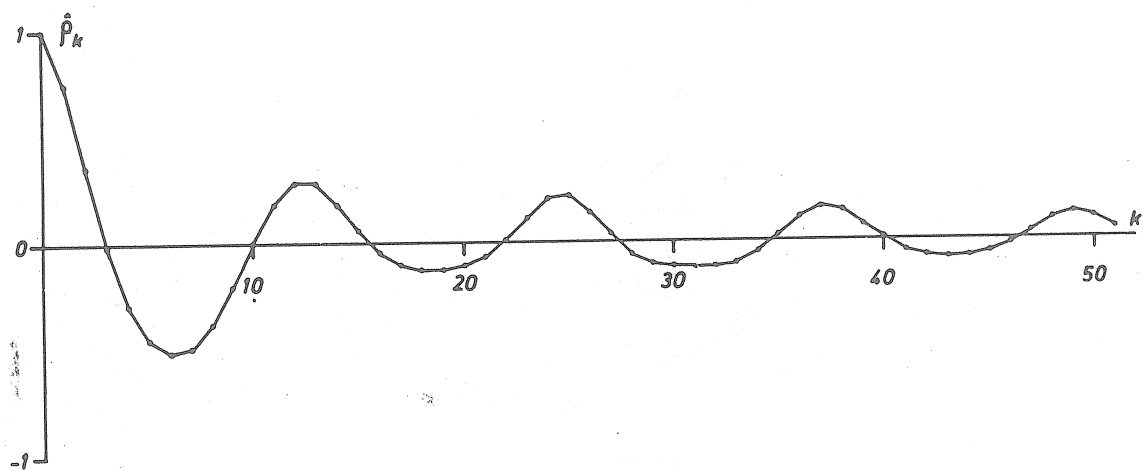


Fig. 9 - Modified Chojnicki's method (sliding least-squares). Autocorrelations of the observed residuals.

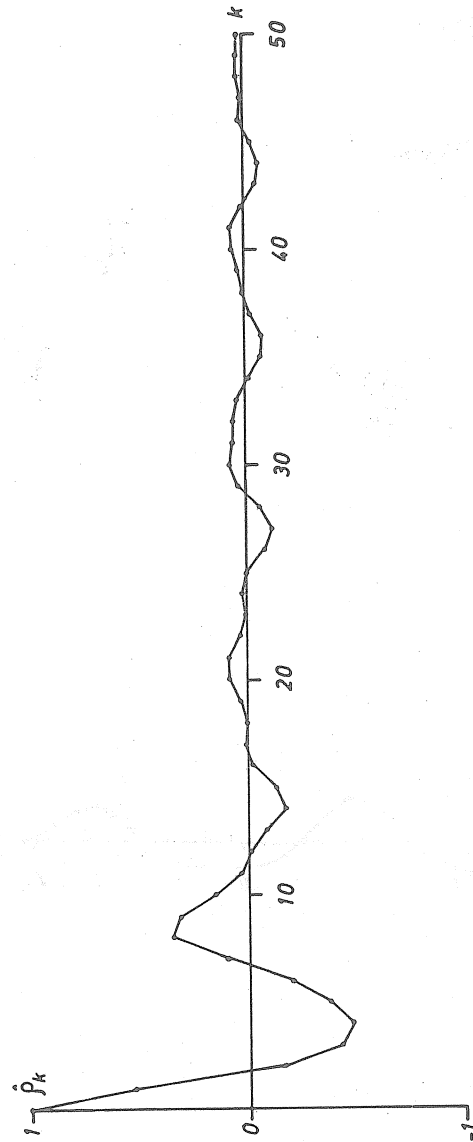


Fig. 10 - Modified Chojnicki's method (high-pass filtering). Autocorrelations of the observed residuals.

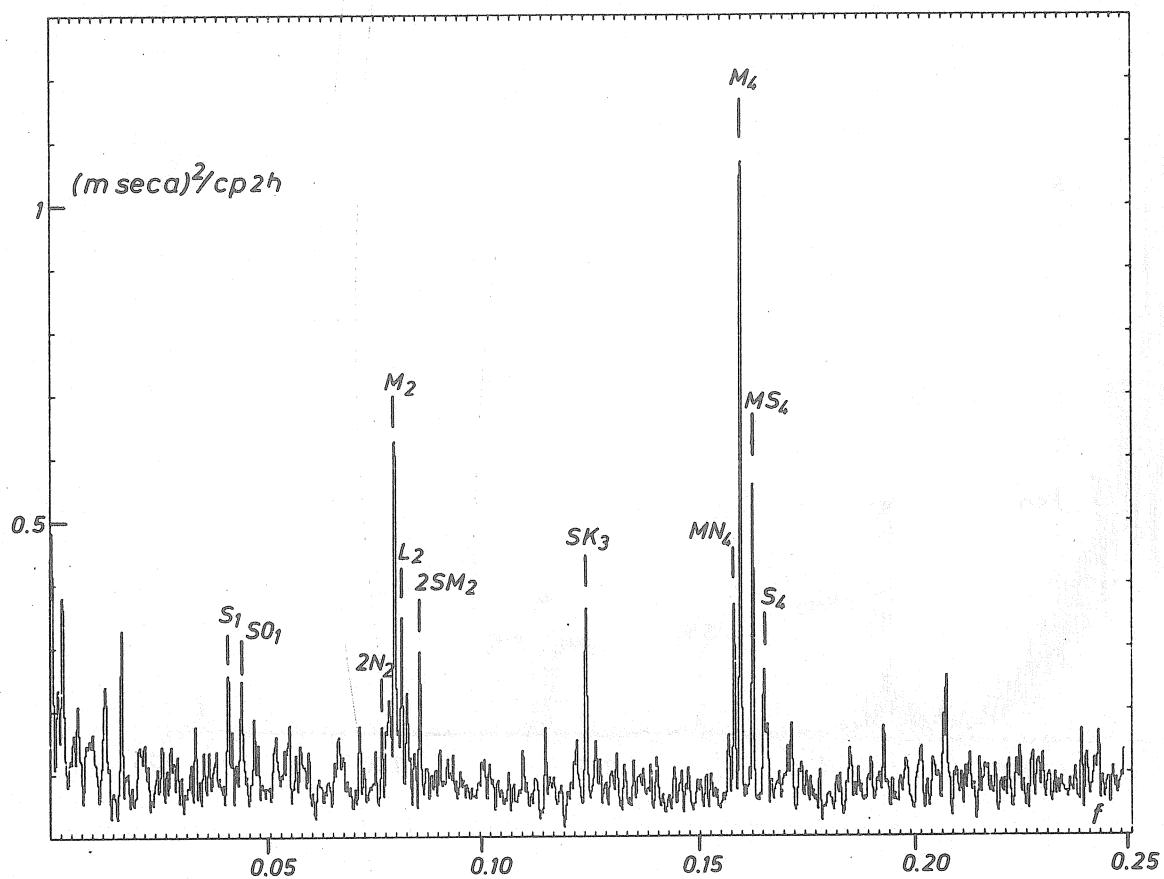


Fig. 11a - Markov estimation; residual power spectrum.

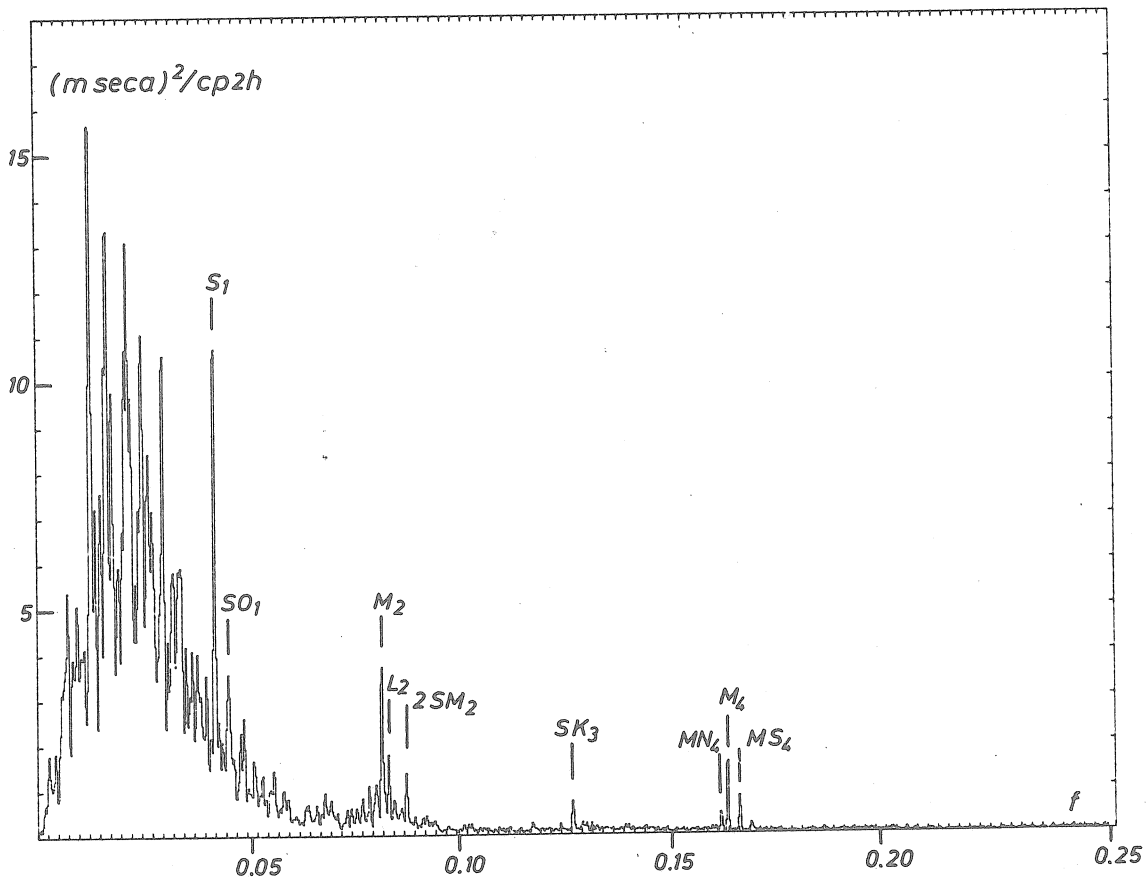


Fig. 11b - Chojnicki's method; residual power spectrum.

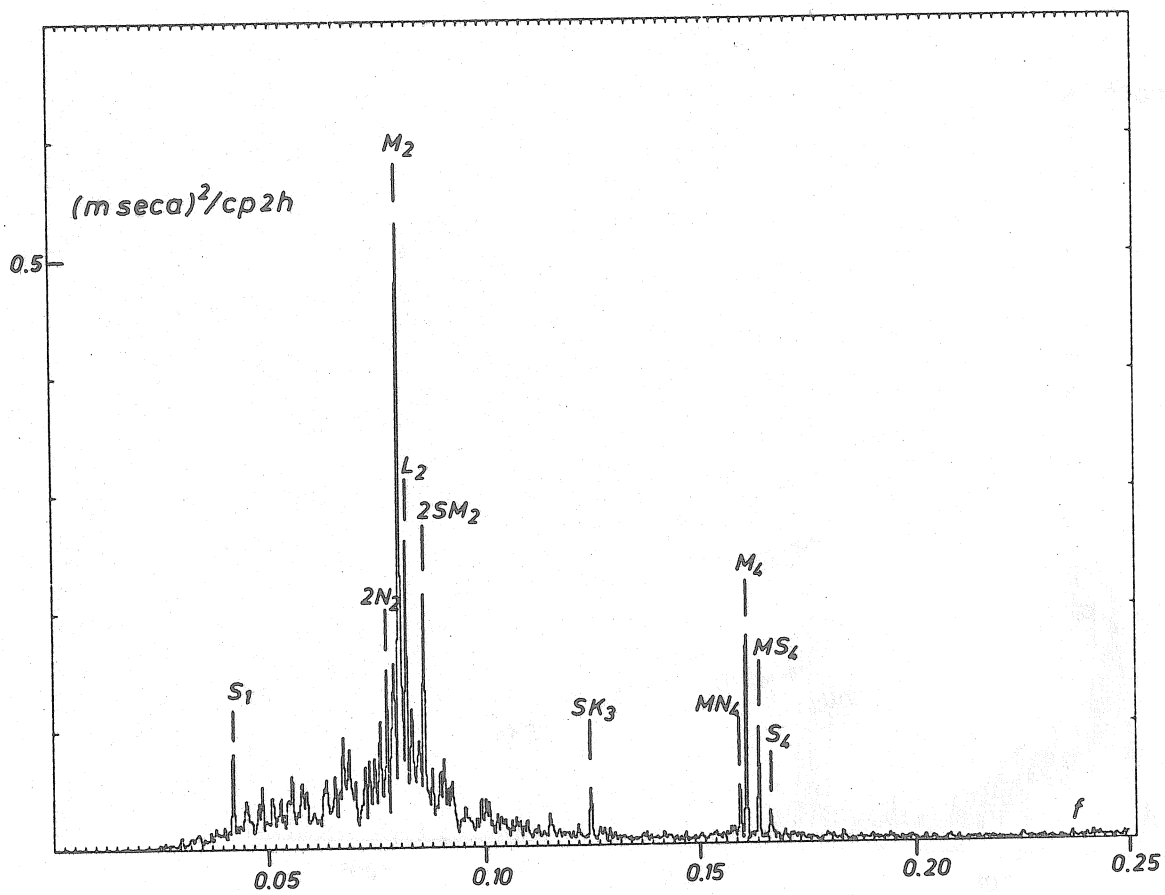


Fig. 11c - Modified Chojnicki's method (sliding least squares); residual power spectrum.

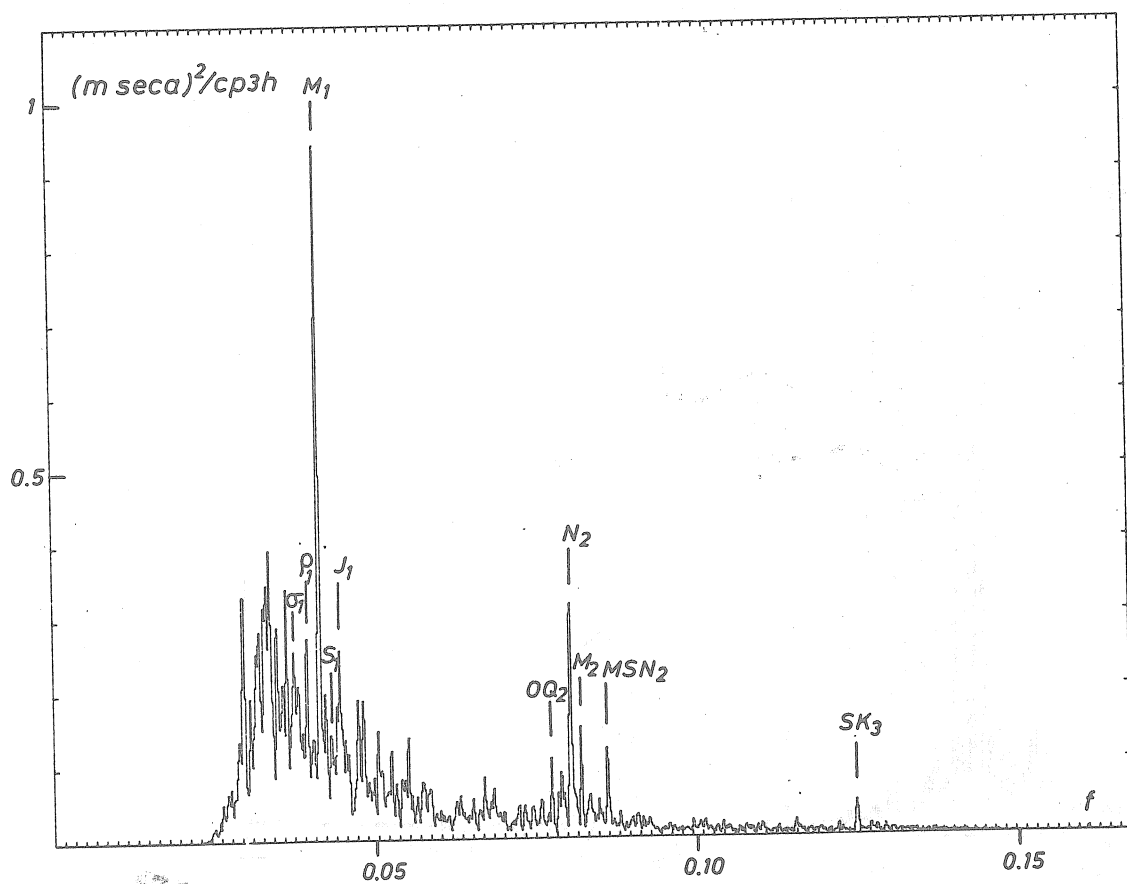


Fig. 11d - Modified Chojniki's method (high-pass filtering); residual power spectrum.

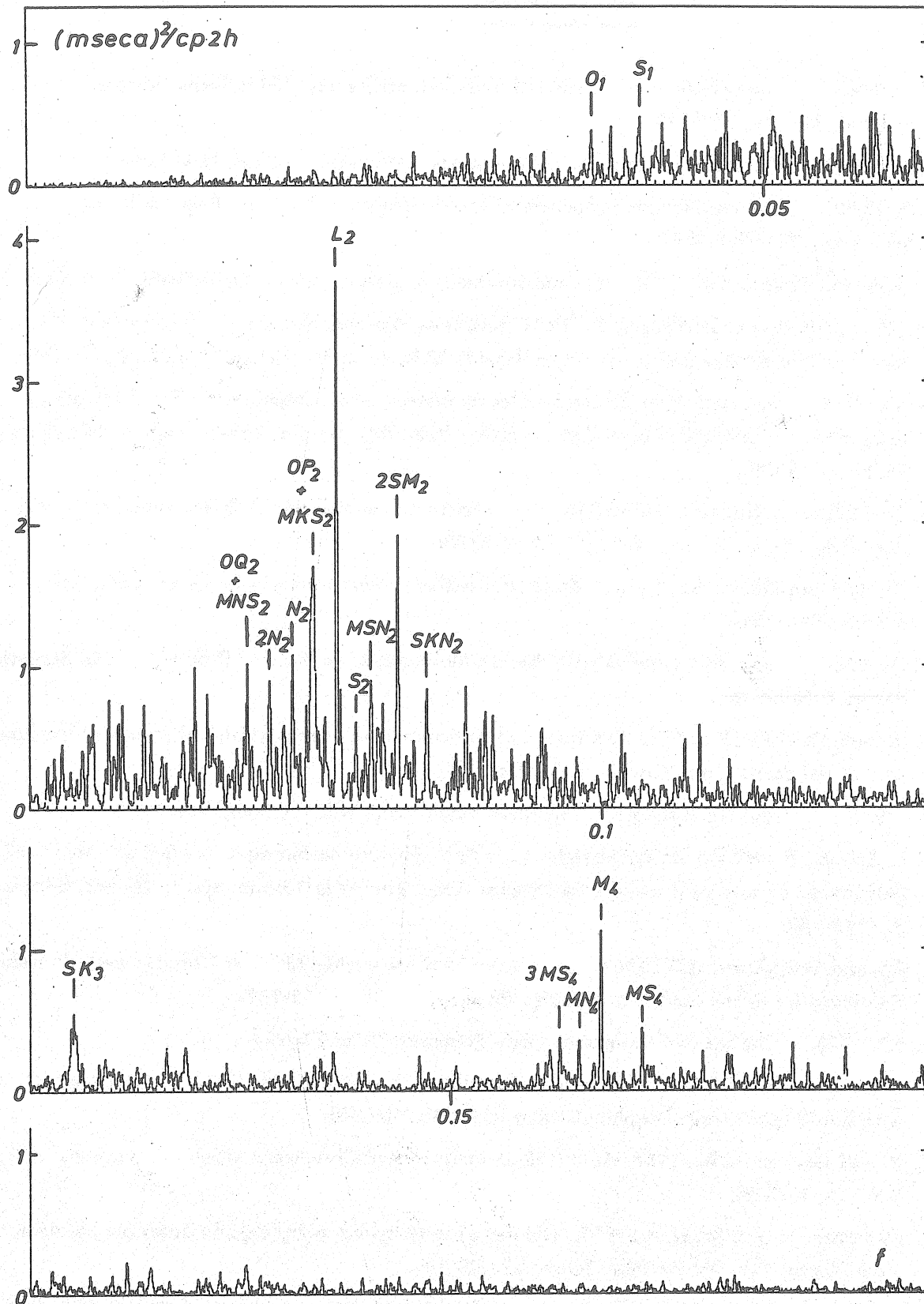


Fig. 12 - Residual periodogram of the modified Chojnicki method (sliding least-squares).

REFERENCES.

- Akaike, H., 1974. A new look at the statistical model identification. *IEEE Trans. Autom. Control*, AC - 19, 716-723.
- Anderson, T.W., 1971. *The statistical analysis of time series*. John Wiley & Sons, New York.
- Barker, T.F., 1978. Non-equilibrium influences of the tidal signal. *Obs. Roy. Belg., Bull. Inf. Mar. Terr.*, 78, 4596-4610.
- Blackman, R.B. and Tukey, J.W., 1958. *The measurement of power spectra*. Dover Publ., New York.
- Blum, P.A., Hatzfield, D. and Wittlinger, G., 1973. Résultats expérimentaux sur la fréquence de résonance due à l'effet dynamique du noyau liquide. *C.R. Acad. Sc. Paris*, 277, Série B, 241-244.
- Chojnicki, T., 1972. Détermination des paramètres de marée par la compensation des observations au moyen de la méthode des moindres carrés. *Publ. Inst. Geoph. Polish Acad. Sc. Mar. Terr.*, 55, N° 15, 43-80.
- De Meyer, F., 1973. Estimation and automatic correction of the individual observational error. *Obs. Roy. Belg., Bull. Inf. Mar. Terr.*, 65, 3526-3550.
- Grenander, U. and Rosenblatt, M., 1966. *Statistical analysis of stationary time series*. John Wiley & Sons, New York.
- Hannan, E.J., 1960. *Time series analysis*. Methuen's Monographs in Applied Probability and Statistics, Barnes & Noble Inc.
- Lecolazet, R. and Melchior, P., 1977. Experimental determination of the dynamical effects of the liquid core of the earth. *Ann. Géoph.*, t. 33, fasc. 1/2, 11-22.
- Lee, Y.W., 1960. *Statistical theory of communication*. John Wiley & Sons, New York.
- Melchior, P., Paquet, P. and Van Cauwenberghe, C., 1967. Analyse harmonique de vingt années d'enregistrements de marées océaniques à Ostende. *Obs. Roy. Belg. Comm. Sér. B*, 20, Sér. Géoph. 82, 123-130.
- Melchior, P.J. and Venedikov, A.P., 1968. Derivation of the wave $M_3/8H.279/$ from the periodic tidal deformations of the earth. *Phys. Earth. Plan. Int.*, 1, n° 6, 363-372.
- Melchior, P.J., 1978. *The tides of the planet earth*. Pergamon Press, Oxford.
- Po-Yu-Shen and Mansinha, L., 1976. Oscillation, nutation and wobble of an elliptical rotating earth with liquid outer core. *Geoph. J.R. Astr. Soc.*, 46, 467-496.
- Rositer, J.R. and Lennon, G.W., 1968. An intensive analysis of shallow water tides. *Geoph. J. R. Astr. Soc.*, 16, 275-293.
- Sasao, T., Okamoto, J., and Sakai, S., 1977. Dissipative core-mantle coupling and nutational motion of the earth. *Pub. Astron. Soc. Japan*, 29, 83-105.
- Schüller, K., 1975. Ein Vorschlag zur Beschleunigung des Analysenverfahrens Chojnicki. *Obs. Roy. Belg., Inf. Mar. Terr.*, 70, 3976-3981.
- Schüller, K., 1978. About the sensitivity of the Venedikov tidal parameter estimates to leakage effects. *Obs. Roy. Belg., Bull. Inf. Mar. Terr.*, 78, 4635-4648.
- Smylie, D.E., Clarke, G.K.C. and Ulrych, T.J., 1973. *Analysis of irregularities in the earth's rotation*. *Methods in Computational Physics*, v. 13, Academic Press, New York.

- Ulrych, T.J. and Bishop, T.N., 1975. Maximum entropy spectral analysis and autoregressive decomposition. *Rév. Geophys*, 13, 183-200.
- Ulrych, T.J. and Clayton, R.W., 1976. Time series modelling and maximum entropy. *Phys. Earth. Planet. Int.*, 12, N°2/3, 188-200.
- Usandivaras, J.C. and Ducarme, B., 1969. Analyse des enregistrements de marée terrestre par la méthode des moindres carrés. *Obs. Roy. Belg. Comm. Sér. B*, 45, S. Geoph. 95, 560-569.
- Usandivaras, J. C. and Ducarme, B., 1976. Etude de la structure du spectre diurne des marées terrestres par la méthode de moindres carrés. *Bull. Géod.*, 50, 139-157.
- Venedikov, A.P., 1966. Sur la constitution de filtres numériques pour le traitement des enregistrements des marées terrestres. *Acad. Roy. Belg. Bull, Cl. Sc.* 5, 6, 827-845.
- Venedikov, A.P., 1966. Une méthode pour l'analyse des marées terrestres à partir d'enregistrements de longueur arbitraire. *Obs. Roy. Belg. Comm.*, 250, Sér. Géoph., 71, 437-459.
- Wenzel, H.G., 1977. Estimation of the accuracy for the earth tide analysis results. *Obs. Roy. Belg., Bull, Inf. Mar. Terr.*, 76, 4427-4445.

M Ø D P Ø L - PROGRAMME NUMERIQUE PERMETTANT DE REPRESENTER
DES MODELES TERRESTRES, PLANETAIRES ET STELLAIRES DE MANIERE
COHERENTE

Carlo Denis
Institut d'Astrophysique
Université de Liège
Liège, Belgique

&

Aysel İbrahim
Physics Department
M. E. T. U.
Ankara, Turquie

1. Introduction

Dans une note récente (Denis & İbrahim, 1980) nous avons attiré l'attention sur la nécessité de pouvoir disposer, dans certains cas, d'un modèle terrestre, planétaire ou stellaire représenté de manière entièrement cohérente, sous forme paramétrique simple de préférence, et nous y avons fourni les algorithmes permettant d'arriver à une telle représentation cohérente. Cette nécessité se présente notamment lorsqu'on désire calculer les nombres de Love statiques ou quasistatiques, car dans ce cas un paramètre faisant intervenir le gradient de densité peut jouer un rôle essentiel (Pekeris & Accad, 1972 ; Denis, 1979). Or, si la densité à l'intérieur de la Terre est assez bien connue et tabulée, le gradient n'en est généralement pas donné et les valeurs locales adoptées par différents auteurs dans leurs calculs d'oscillations et de déformations de marée varient parfois grandement pour le même modèle initial; par ailleurs, il est souvent difficile de savoir quelles sont exactement les valeurs qu'ils ont adoptées. Il devient alors difficile de comparer leurs résultats et de juger s'ils sont significatifs.

Dans ce qui suit nous présentons un programme numérique basé sur les algorithmes publiés dans la note mentionnée. Ce programme est écrit en langage FØRTRAN tel qu'il est accepté par tous les compilateurs FØRTRAN du système d'ordinateurs IBM 360/370; l'adaptation à des ordinateurs d'un type différent est aisée. Nous avons par ailleurs visé dans ce

programme une grande généralité, une grande précision et une grande flexibilité, au détriment bien-entendu d'un encombrement minimum de mémoires et, dans une moindre mesure, au détriment d'une rapidité maximum des calculs. Là encore, les adaptations selon des besoins spécifiques ne devraient soulever aucun problème majeur.

La séismologie permet d'évaluer, avec une excellente précision, les vitesses des ondes P et S à différentes profondeurs dans la Terre. Elle fournit en outre des courbes de dispersion pour les ondes de Love et de Rayleigh et un grand nombre de périodes propres, ainsi que des estimations du facteur d'atténuation spécifique (grandeur que nous ne considérerons pas dans la suite). Ces informations, complétées par des données astrogéodésiques et gravimétriques, par des considérations physiques et physico-chimiques et par des hypothèses simplificatrices de sphéricité, d'équilibre hydrostatique, e.a. sont utilisées dans la formulation d'un problème mathématique inverse dont la solution - non unique il est vrai - fournit un modèle mécanique de la Terre, c'est-à-dire essentiellement les valeurs de la densité à différents niveaux à l'intérieur de la Terre (voir p.ex.: Bullen, 1975).

De ces trois grandeurs primaires :

- densité : ρ
- vitesse des ondes P : α
- vitesse des ondes S : β

on peut alors déduire tout un ensemble de grandeurs secondaires dont la connaissance précise est indispensable dans les études géodynamiques. Avant de décrire en détail le programme MØDPØL et son emploi, il nous a paru judicieux de rassembler ci-dessous les principales relations existant entre les grandeurs considérées (section 2) et les algorithmes employés dans le programme (section 3). Pour ce qui est de ces algorithmes, nous ne donnons ici aucun détail quant à leur dérivation, renvoyant le lecteur pour cela à notre note mentionnée plus haut.

2. Relations entre les principales grandeurs considérées

Pour un modèle à symétrie sphérique en équilibre hydrostatique, ne tournant pas sur lui-même et se comportant comme un corps élastique linéaire isotrope, on a les relations suivantes :

coefficients élastiques

$$1^{\text{er}} \text{ paramètre de Lamé} \dots\dots\dots \lambda = \rho (\alpha^2 - 2\beta^2) \quad (1)$$

$$\text{module de rigidité} \dots\dots\dots \mu = \rho \beta^2 \quad (2)$$

$$\begin{aligned} \text{module de compression} \dots\dots\dots \kappa &= \lambda + \frac{2}{3}\mu \quad (3) \\ &= \rho (\alpha^2 - \frac{4}{3}\beta^2) \quad (3') \end{aligned}$$

$$\begin{aligned} \text{module de Young} \dots\dots\dots E &= \mu(3\lambda + 2\mu)/(\lambda + \mu) \quad (4) \\ &= \rho \beta^2 (3\alpha^2 - 4\beta^2)/(\alpha^2 - \beta^2) \quad (4') \end{aligned}$$

$$\begin{aligned} \text{coefficient de Poisson} \dots\dots\dots \sigma &= \frac{1}{2}\lambda/(\lambda + \mu) \quad (5) \\ &= \frac{1}{2}(\alpha^2 - 2\beta^2)/(\alpha^2 - \beta^2) \quad (5') \end{aligned}$$

coefficients cinétiques

$$\text{masse comprise dans une sphère de rayon } r \dots\dots\dots M(r) = 4\pi \int_0^r \rho(y) y^2 dy \quad (6)$$

$$\text{densité moyenne d'une sphère de rayon } r \dots\dots\dots D(r) = M(r)/(\frac{4}{3}\pi r^3) \quad (7)$$

$$\text{moment d'inertie d'une sphère de rayon } r \text{ autour d'un axe polaire} \dots\dots\dots C(r) = \frac{8}{3}\pi \int_0^r \rho(y) y^4 dy \quad (8)$$

$$\begin{aligned} \text{moment d'inertie réduit au niveau } r \dots\dots\dots j(r) &= C(r)/(M(r)r^2) \quad (9) \\ &= C(r)/(\frac{4}{3}\pi D(r)r^5) \quad (9') \end{aligned}$$

coefficients dynamiques

$$\text{accélération gravifique} \dots\dots\dots g(r) = G M(r)/r^2 \quad (10)$$

$$\text{pression hydrostatique} \dots\dots\dots p(r) = p(R) + \int_r^R \rho(y) g(y) dy \quad (11)$$

coefficient de stabilité dynamique

$$A(r) = \frac{1}{\rho} \frac{d\rho}{dr} + \frac{\rho g}{\kappa} \quad (12)$$

coefficients géométriques

Pour des raisons de simplicité et de capacité de calcul les modèles de Terre publiés jusqu'à présent sont sphériques, c'est-à-dire les différentes surfaces de niveau internes sont des sphères concentriques. Mais à cause de la rotation de la Terre sur elle-même et de la présence de toutes sortes d'inhomogénéités latérales, les surfaces équipotentielles ne sont en réalité pas parfaitement sphériques, bien que dans l'ensemble les écarts à la sphéricité restent assez faibles ; les modèles terrestres sphériques constituent une approximation d'ordre zéro. Dans l'étude de certains effets géodynamiques cette approximation d'ordre zéro ne suffit pas, mais dans de nombreux cas l'approximation du premier ordre est satisfaisante; celle-ci consiste à représenter les surfaces de niveau par des ellipsoïdes de révolution, ou sphéroïdes. Pour repérer ces divers sphéroïdes emboîtés les uns dans les autres, c'est-à-dire pour numéroter en quelque sorte les différentes surfaces de niveau, on utilise le paramètre r représentant le rayon d'une sphère fictive possédant le même volume que l'ellipsoïde considéré. Le programme MØDPØL calcule, parmi d'autres quantités, l'ellipticité (ou aplatissement) géométrique f grâce à la théorie de Clairaut et Radau.

$$\text{paramètre de Radau} \dots\dots\dots \eta(r) = \left(\frac{5}{2} - \frac{15}{4} f(r) \right)^2 - 1 \quad (13)$$

$$\text{aplatissement géométrique interne} \dots\dots\dots f(r) = f(R) \exp\left(-\int_r^R \frac{\eta(y)}{y} dy\right) \quad (14)$$

$$\text{ellipticité en surface} \dots\dots\dots f(R) = 10 \left(\frac{\pi}{T} \right)^2 \frac{R}{(\eta(R)+2) g(R)} \quad (15)$$

T représente ici la période de rotation propre, R est le rayon total du modèle.

3. Algorithmes employés

Nous divisons le modèle en N couches sphériques concentriques et nous utilisons les conventions suivantes : si x désigne la distance au centre r mesurée en unités du rayon total R , alors la frontière inférieure de la $k^{\text{ième}}$ couche sera notée x_k et la frontière supérieure x_{k+1} . Ainsi, x_1 correspondra au centre ($x_1 = 0$) et x_{N+1} désignera la surface extérieure ($x_{N+1} = 1$).

Dans une couche k quelconque, définie par $x_k \leq x \leq x_{k+1}$ ($k = 1, 2, \dots, N$) on utilise la représentation cohérente suivante :

vitesse des ondes P
$$\alpha_k(x) = \sum_{j=1}^{A(k)} \alpha_{k,j} x^{j-1} \quad (16)$$

$$\alpha_{k,m} = 0 \text{ si } m > A(k)$$

vitesse des ondes S
$$\beta_k(x) = \sum_{j=1}^{B(k)} \beta_{k,j} x^{j-1} \quad (17)$$

$$\beta_{k,m} = 0 \text{ si } m > B(k)$$

densité
$$\rho_k(x) = \sum_{j=1}^{P(k)} \rho_{k,j} x^{j-1}, \quad \rho_{k,m} = 0 \text{ si } m > P(k) \quad (18)$$

coefficients de masse
$$\mathcal{M}_k = \mathcal{M}_{k-1} + \sum_{j=1}^J (\rho_{k-1,j} - \rho_{k,j}) \frac{x_k^{j+2}}{j+2}, \quad k \geq 2 \quad (19)$$

$$\mathcal{M}_1 = 0, \quad J = \text{Max}(P(k-1), P(k))$$

coefficients d'inertie
$$\mathcal{C}_k = \mathcal{C}_{k-1} + \sum_{j=1}^J (\rho_{k-1,j} - \rho_{k,j}) \frac{x_k^{j+4}}{j+4}, \quad k \geq 2 \quad (20)$$

$$\mathcal{C}_1 = 0, \quad J = \text{Max}(P(k-1), P(k))$$

masse de la boule de rayon x
$$\mathcal{M}_k(x) = 4\pi R^3 \left(\mathcal{M}_k + \sum_{j=1}^{P(k)} \rho_{k,j} \frac{x^{j+2}}{j+2} \right) \quad (21)$$

moment d'inertie de la boule de rayon x
$$\mathcal{C}_k(x) = \frac{8}{3}\pi R^5 \left(\mathcal{C}_k + \sum_{j=1}^{P(k)} \rho_{k,j} \frac{x^{j+4}}{j+4} \right) \quad (22)$$

accélération gravifique en x
$$g_k(x) = 4\pi G R \left(\mathcal{M}_k x^{-2} + \sum_{j=1}^{P(k)} \rho_{k,j} \frac{x^j}{j+2} \right) \quad (23)$$

densité moyenne de la boule de rayon x
$$D_k(x) = 3 \left(\mathcal{M}_k x^{-3} + \sum_{j=1}^{P(k)} \rho_{k,j} \frac{x^{j-1}}{j+2} \right) \quad (24)$$

densité moyenne du modèle
$$\bar{\rho} = D_N(1) = 3 \left(\mathcal{M}_N + \sum_{j=1}^{P(N)} \frac{\rho_{N,j}}{j+2} \right) \quad (25)$$

densité centrale
$$\rho_c = \rho_1(0) = \rho_{1,1} = D_1(0) \quad (26)$$

coefficients de pression

$$R_{k,j} = \sum_{m=1}^j \frac{\rho_{k,j-m+1} \rho_{k,m}}{m+2} \quad (27)$$

$$Q_k(x) = M_k (-\rho_{k,1} x^{-1} + \rho_{k,2} \ln x + \rho_{k,3} x) + \sum_{j=1}^{2P(k)-1} (M_k \rho_{k,j+3} + R_{k,j}) \quad (28)$$

$$\int \rho_k(y) g_k(y) dy = 4\pi G R Q_k(y) \quad (29)$$

pression

$$P_k(x) = P_N(1) + 4\pi G R^2 (Q_k(x_{k+1}) - Q_k(x) + \sum_{\substack{j=k+1 \\ (k < N)}}^N (Q_j(x_{j+1}) - Q_j(x_j))) \quad (30)$$

Sous réserve que la représentation de $\rho(x)$ soit (physiquement) significative :

gradient de densité

$$\rho'_k(x) = \left(\sum_{j=1}^{P(k)-1} j \rho_{k,j+1} x^{j-1} \right) \frac{1}{R} \quad (31)$$

paramètre séismologique

$$\phi_k(x) = \alpha_k^2(x) - \frac{4}{3} \beta_k^2(x) \quad (32)$$

coefficient de stabilité

$$A_k(x) = \frac{\rho'_k(x)}{\rho_k(x)} + \frac{g_k(x)}{\phi_k(x)} \quad (33)$$

La représentation (31) fournit des valeurs numériques non significatives pour le gradient de densité, il convient de fournir une représentation indépendante pour le coefficient de stabilité, et éventuellement adapter le paramètre séismologique et les vitesses des ondes P et S en conséquence:

coefficient de stabilité

$$A_k(x) = \sum_{j=1}^{a(k)} A_{k,j} x^{j-1} \quad (33')$$

On trouve aussi

mètre de Radau dans la couche centrale

$$\eta_1(x) = -\frac{49}{36} \frac{\rho_{1,2}}{\rho_{1,1}} x + O(x^2) \quad (34)$$

4. Description et utilisation du programme numérique 'MØDPØL'

Le programme que nous proposons ici et duquel nous fournissons un listage complet en annexe, est écrit en FØRTRAN IV/IBM. Il peut être appelé tel quel par l'instruction

```
| ~~~~~CALL MØDPØL (jtab)
```

suivie éventuellement des instructions

```
|      STØP  
|      END
```

La valeur 'jtab' à pourvoir doit être entière.

' M Ø D P Ø L '

La fonction essentielle du (sous-)programme 'MØDPØL' est l'impression, selon l'un des deux formats pourvus ici ou, éventuellement, selon d'autres formats à définir par l'utilisateur lui-même au moyen du sous-programme 'MØDDAT' laissé ineffectif ici, de diverses grandeurs caractérisant un modèle particulier; accessoirement, il permet de simplement implanter effectivement en mémoire centrale les divers algorithmes permettant de calculer ces grandeurs. En effet, lorsqu'on désire seulement initialiser les coefficients polynomiaux de la représentation sans rien imprimer à ce niveau, il faut donner à 'jtab' une valeur entière plus petite ou égale à 1. L'instruction

```
|      CALL MØDPØL (1)
```

est essentiellement équivalente à la séquence d'instructions

```
|      CALL MØDELE  
|      CALL RHØF (0.DO,1,RHØC)  
|      CALL RHØF (1.DO,NBC,RHØS)
```

Si jtab = 2 on obtient une impression sous forme de table des grandeurs suivantes, dans l'ordre : numéro de couche, rayon fractionnaire, rayon en km, densité en g/cm³, vitesse des ondes P en km/s, vitesse des ondes S en km/s, module de compression en kb, module de rigidité en kb, premier paramètre de Lamé en kb, pression en kb, accélération gravifique en cm/s², masse fractionnaire en g, densité moyenne en g/cm³, moment d'inertie réduit, paramètre de Radau, ellipticité géométrique multipliée par mille, profondeur en km.

Si $jtab = 3$ l'impression se fait sous forme d'un tableau différent, particulièrement adapté à une unité de sortie dont le nombre de caractères par ligne n'excède pas 72. Les grandeurs suivantes sont imprimées, dans l'ordre: rayon en km, densité en g/cm^3 , vitesse des ondes P en km/s, vitesse des ondes S en km/s, pression en kb, accélération gravifique en cm/s^2 , densité moyenne en g/cm^3 , moment d'inertie réduit, paramètre de Radau, ellipticité géométrique multipliée par mille. (Des exemples correspondant aux valeurs 2 et 3 de jtab sont donnés en annexe, avec le listage du programme.)

Si $jtab \geq 4$ le contrôle est passé au sous-programme 'MØDDAT' après initialisation des paramètres de représentation du modèle, au moyen de l'instruction

```
|.....CALL MØDDAT (jtab)
```

Nous avons laissé le sous-programme 'MØDDAT' intentionnellement vide, pour permettre aux utilisateurs, s'ils le désirent, d'agir à leur guise sans toucher à 'MØDPØL' et éventuellement d'en déranger le bon fonctionnement. Ce sous-programme 'MØDDAT' peut par exemple s'employer pour imprimer diverses grandeurs, notamment le paramètre de stabilité, le gradient de densité, etc. en plus de celles déjà citées, selon un format adéquat.

'MØDPØL' appelle explicitement les sous-programmes suivants:

'CELAST', 'DENMOY', 'FLATG', 'GF', 'MASSE', 'MØDDAT',
'MØDELE', 'PRESS', 'RADAU', 'RHØF'.

' M Ø D E L E '

'MØDELE' constitue le sous-programme central du présent programme numérique. Il initialise les coefficients nécessaires à la représentation cohérente du modèle considéré, et permet de déterminer les grandeurs suivantes : densité, accélération gravifique, masse, densité moyenne, vitesse des ondes P, vitesse des ondes S, pression, moment d'inertie, gradient de densité (et éventuellement d'autres grandeurs, voir ci-dessous). Accessoirement, il permet également l'impression de certains paramètres du modèle.

Il s'agit en fait d'un sous-programme à entrées multiples, dont la structure est la suivante :

```

SUBROUTINE MØDELE
ENTRY RHØF (x,ic,rho)
ENTRY GF (x,ic,g)
ENTRY MASSE (x,ic,amasse)
ENTRY DMØY (x,ic,d)
ENTRY CPF (x,ic,cp)
ENTRY CSF (x,ic,cs)
ENTRY PRESS (x,ic,p)
ENTRY MØMIN (x,ic,ai)
ENTRY GRADRØ (x,ic,derrho)

```

Nous allons passer maintenant ces différents points d'entrée en revue.

La fonction essentielle de 'MØDELE' est de pourvoir des valeurs aux coefficients polynomiaux

$\rho_{k,j}$ ($k = 1, 2, \dots, N$; $j = 1, 2, \dots, P(k)$) (cfr. (18))

$\alpha_{k,j}$ ($k = 1, 2, \dots, N$; $j = 1, 2, \dots, A(k)$) (cfr. (16))

$\beta_{k,j}$ ($k = 1, 2, \dots, N$; $j = 1, 2, \dots, B(k)$) (cfr. (17))

à partir de modèles fournis sous forme de tables ou autrement. C'est cette opération que nous appelons "initialisation des coefficients de la représentation". Nous stockons ces coefficients en double précision sous la forme de trois tableaux à double entrée de dimensions 7×200 :

$\rho_{k,j} \longleftrightarrow$ tableau 'crho' : CRHØ(j,k)
 $\alpha_{k,j} \longleftrightarrow$ tableau 'cvp' : CVP(j,k)
 $\beta_{k,j} \longleftrightarrow$ tableau 'cvs' : CVS(j,k)

Dans ces tableaux le premier indice est 'j'; il est associé au terme de degré $j-1$ de la représentation polynomiale. Le second indice est 'k'; c'est l'indice de couche souvent noté 'ic' dans le programme. Celui-ci peut parcourir toutes les valeurs entières de 1 à N, où N désigne le nombre total de couches du modèle. N est désigné par 'nbc' dans le programme. Telle quelle, la place réservée est suffisante pour un modèle composé de 200 couches dans chacune desquelles on peut avoir une représentation polynomiale de degré 6 au maximum. Les degrés effectifs utilisés dans chaque couche pour 'crho', 'cvp', 'cvs' sont donnés par $P(k)-1$, $A(k)-1$, $B(k)-1$ respectivement. On a les correspondances

$P(k) \longleftrightarrow MRHØ(k) \leq 7$

$A(k) \longleftrightarrow MVP(k) \leq 7$

$B(k) \longleftrightarrow MVS(k) \leq 7$

Dans tous les cas 'MØDELE' commence par lire deux fichiers d'entrée.

Lecture du premier fichier, constitué d'un seul enregistrement (carte)
.....

```
*****REAL = 4 DT(20)
      READ (5,5000) DT
      5000 FØRMAT (20A4)
```

Le vecteur 'dt' à vingt composantes de longueur simple sert à stocker un texte composé de 80 caractères alphanumériques ou signes spéciaux. Toutefois, nous conseillons de n'utiliser effectivement qu'une chaîne de 72 caractères et signes, et de remplir les 8 dernières positions par des blancs. Le vecteur 'dt' sert à transmettre un titre relatif au nom et à certaines spécifications du modèle concerné, par exemple. La transmission se fait au moyen d'un bloc commun étiqueté appelé 'lin':

```
CØMMØN /LIN/ DT, .....
```

Ce bloc commun est transmis notamment dans le sous-programme d'impression 'MØDPØL'.

Lecture du deuxième fichier, constitué d'un nombre arbitraire de cartes
.....
respectant les spécifications d'une liste globale (NAMELIST)

```
REAL = 8 BIGG, DRKM, FSURF, PC, PSURF, RAYØN, RØTPER, XC, XM, XYZ
DIMENSION DRKM(200), MRHØ(200), MVP(200), MVS(200), NC(200)
DIMENSION NØ(200), NP(200), XC(201), XYZ(100)
NAMELIST /MØDEL/ BIGG, DRKM, FSURF, INITMØ, IPMØD, IPU, JEP, JX,
1 MRHØ, MVP, MVS, NBC, NC, NØ, NP, NREG, PC, PSURF, RAYØN,
2 RØTPER, XC, XM, XYZ
```

```
C
      READ (5,MØDEL)
```

La signification des différents arguments de cette liste est la suivante:

- 'bigg' = constante de gravitation G en unités CGS; si on ne la spécifie pas explicitement dans la liste globale /MØDEL/ le programme 'MØDELE' pourvoit automatiquement la valeur 6.6720D-8;
- 'drkm' = vecteur à 200 composantes double longueur transmis vers le sous-programme 'MØDPØL' à l'aide du bloc commun étiqueté 'jwx'; DRKM(k) est le pas de tabulation des grandeurs du modèle dans la couche 'k', en kilomètres, lorsque 'jtab' vaut 3;
- 'fsurf' = ellipticité géométrique en surface transmis vers le sous-programme 'FLATG' à l'aide du bloc commun étiqueté 'ellip'; si on n'en fournit pas explicitement la valeur dans /MØDEL/ le programme 'MØDELE' pourvoit automatiquement la valeur obser-

- vée pour la Terre, soit $3.35282D-3$ correspondant à $f^{-1} = 298,256$ (Stacey, 1977, p. 332); toutefois, si 'jep'=1, la valeur de 'fsurf' est redéterminée dans le sous-programme 'FLATG' grâce à la théorie de Clairaut-Radau développée au premier ordre (voir formule (15) ci-dessus), et alors il est inutile d'initialiser 'fsurf' dans la liste /MØDEL/;
- 'initmo' = paramètre d'aiguillage à définir selon la présentation du troisième fichier d'entrée; 'initmo' doit prendre une valeur entière strictement positive; la forme détaillée que doit prendre ce troisième fichier en fonction des différentes valeurs 'initmo' possibles sera discutée ci-dessous;
- 'ipmod' = paramètre servant à indiquer si oui ou non il faut imprimer diverses données caractérisant le modèle
 si 'ipmod' < 1 : pas d'impression;
 si 'ipmod' ≥ 1 : il y a impression;
- 'ipu' = paramètre servant à indiquer si oui ou non il faut perforer un fichier selon les normes du fichier 3,1 spécifiées ci-dessous
 si 'ipu' < 1 : pas de perforation;
 si 'ipu' ≥ 1 : il y a perforation;
- 'jep' = paramètre transmis par le bloc commun 'ellip' vers le sous-programme 'FLATG', où il sert à déterminer la manière d'évaluer 'fsurf'
 si 'jep' ≠ 1 : on utilise la valeur 'fsurf' fournie dans la liste /MØDEL/ ou, à défaut, la valeur $3.35282D-3$ de la Terre;
 si 'jep' = 1 : on calcule 'fsurf' par la théorie de Clairaut-Radau, formule (15) ci-dessus;
- 'jx' = paramètre servant à indiquer si oui ou non il convient de diviser toutes les composantes du vecteur 'xc' fournies dans /MØDEL/ par 'rkm' = 'rayon'/ 10^5 , c'est-à-dire par le rayon total du modèle exprimé en kilomètres
 si 'jx' ≠ 1 : pas de division par 'rkm'; dans ce cas 'xc' doit représenter une liste de rayons fractionnaires dans /MØDEL/;
 si 'jx' = 1 : division par 'rkm'; dans ce cas 'xc' est fourni en kilomètres dans /MØDEL/;
- 'mrho' = vecteur de dimension maximum 200, dont toutes les composantes sont des nombres entiers compris entre 1 et 7 et indiquent le degré moins un de la représentation polynomiale dans chaque couche pour la distribution de la densité;

-
- 'mvp' - vecteur analogue à 'mrho', mais pour la vitesse des ondes P;
- 'mvs' - idem, pour la vitesse des ondes S;
- 'nbc' - nombre total de couches constituant le modèle (au maximum: 200);
- 'nc' - vecteur de dimension maximum 200, dont les composantes doivent être des nombres entiers strictement positifs; sert à exprimer le nombre de couches contenues dans chacune des 'nreg' régions : 'nc(ir)', 'ir' variant de 1 à 'nreg' ;
- 'no' - vecteur de dimension maximum 200, dont les composantes doivent être des nombres entiers strictement positifs, généralement 2, 4 ou 6; sert à désigner l'ordre du système différentiel régissant les déformations du modèle dans chacune des régions: 'no(ir)', 'ir' variant de 1 à 'nreg' ; est sans effet dans le programme listé en annexe, mais intervient dans l'emploi du programme 'MØDPØL' dans des calculs ultérieurs (détermination des nombres de Love ou des nombres en charge caractéristiques, calcul des fréquences et fonctions propres, par exemple):
 'no(ir)' = 2 pour des déformations toroïdales ou radiales, ou pour des déformations sphéroïdales (région fluide) dans l'approximation de Cowling;
 'no(ir)' = 4 pour des déformations sphéroïdales (région fluide), ou pour des déformations sphéroïdales (région solide) dans l'approximation de Cowling;
 'no(ir)' = 6 pour des déformations sphéroïdales (région solide);
- 'np' - vecteur de dimension maximum 200, dont les composantes doivent être des nombres entiers strictement positifs; sert à indiquer le nombre de pas à considérer dans chaque couche, soit dans le cas de la tabulation (avec impression) du modèle, soit éventuellement lors d'une intégration numérique fournissant par exemple les nombres de Love théoriques; 'np(ic)', 'ic' de 1 à 'nbc';
- 'nreg' - nombre de régions constituant le modèle (au maximum: 200); nous appelons "région" un ensemble de couches consécutives toutes solides limité par des couches fluides, ou vice-versa;
- 'pc' - paramètre en double longueur n'intervenant pas effectivement dans le programme tel qu'il se présente ici; est prévu pour servir éventuellement de constante de normalisation représentant une pression caractéristique à l'intérieur du modèle, par exemple la pression centrale;
- 'psurf' - pression à la surface du modèle; si elle n'est pas spécifiée autre, le programme pourvoit automatiquement une pression nulle;

- 'rayon' = rayon total du modèle, exprimé en centimètres; si la valeur n'en est pas spécifiée au moyen de la liste /MØDEL/, le programme adopte automatiquement la valeur du rayon moyen de la Terre, soit $6,3710 \times 10^8$ cm ;
- 'rotper' = période de rotation sidérale du modèle, exprimée en secondes de temps; si la valeur n'en est pas spécifiée explicitement, le programme adopte automatiquement la durée du jour sidéral (terrestre), soit 86164 s ;
- 'xc' = vecteur de dimension maximum 201, servant à stocker en double précision les distances au centre des différents interfaces entre couches successives: 'xc(ic)', 'ic' = 1,2,...,'nbc'+1; si 'jx' ≠ 1 : les distances sont normalisées; si 'jx' = 1 : les distances sont en kilomètres;
- 'xm' = distance au centre en unités du rayon total à partir de laquelle on arrête le développement en série des solutions modales au voisinage du centre, s'il y a lieu; ce paramètre est sans effet dans le programme 'MØDPØL' tel quel;
- 'xyz' = vecteur de stockage auxiliaire de 100 composantes en double longueur, transmissible au moyen du bloc commun étiqueté 'zyx'; reste inutilisé dans le programme 'MØDPØL' tel quel.

Examinons maintenant l'effet produit par les différentes valeurs possibles du paramètre 'initmo' :

Lecture du troisième fichier, version 1
.....

Si 'initmo' = 1 on lit les paramètres primaires du modèle dans un fichier (appelé fichier 3,1) généralement préparé par l'ordinateur lui-même lors d'un passage précédent du programme 'MØDPØL' avec l'option 'ipu' ≥ 1. La séquence de lecture est la suivante :

```

^^510 READ (5,5101) NREG, NBC, (NC(J), J=1,NREG),
  1 ((MRHØ(IC), MVP(IC), MVS(IC)), IC=1,NBC)
  READ (5,5101) (NØ(J), J=1,NREG), (NP(IC), IC=1,NBC)
5101 FORMAT (20I4)
DØ 511 IC = 1,NBC
I = MRHØ(IC)
J = MVP(IC)
K = MVS(IC)
  READ (5,5102) (CRHØ(IJ,IC), IJ=1,I),
  1 (CVP(IJ,IC), IJ=1,J),
  2 (CVS(IJ,IC), IJ=1,K)
511 CØNTINUE

```



```

      K = NBC + 1
      READ (5,5103) (XC(I), I=1,K)
C   LES XC SONT DONNES ICI COMME FRACTIONS DU RAYON TOTAL
5102 FORMAT (3D25.16)
5103 FORMAT (4D20.13)

```

Les éléments du tableau 'crho' seront toujours exprimés en g/cm^3 , tandis que les éléments des tableaux 'cvp' et 'cvs' seront donnés en cm/s .

Lecture du troisième fichier, version 2

Si 'initmo' = 2 on initialise les tableaux 'crho', 'cvp' et 'cvs' (en g/cm^3 , cm/s et cm/s respectivement) au moyen d'une liste globale appelée /CØEF/. Cette façon de procéder est sans doute la plus pratique lorsqu'il s'agit de modèles très simples (par exemple de modèles à une ou plusieurs couches homogènes) ou lorsque les modèles sont déjà fournis dans la littérature sous forme paramétrisée, tels ceux de Dziewonski et al. (1975). L'initialisation se fait comme suit :

```

      REAL * 8 CRHØ(7,200), CVP(7,200), CVS(7,200)
      NAMELIST /CØEF/ CRHØ, CVP, CVS
520 READ (5,CØEF)

```

La liste globale /CØEF/ constitue le fichier 3,2.

Lecture du troisième fichier, version 3

Si 'initmo' = 3 le fichier d'entrée (appelé fichier 3,3) doit contenir le modèle sous forme d'un tableau à deux entrées, ainsi que toutes les informations nécessaires pour lire ce tableau et en déduire une représentation paramétrique complète. La séquence des instructions de lecture de ce fichier 3,3 est la suivante :

```

      REAL * 4 XR(250), DENSIT(250), VITP(250), VITS(250)
530 READ (5,5300) NLTB, NBC, NREG
      READ (5,5101) (NC(J), J=1,NREG)
      READ (5,5101) (NØ(J), J=1,NREG)
      READ (5,5302) ((IC, ICINF(IC), ICSUP(IC), ICIND(IC)), IC=1,NBC)
      READ (5,5301) ((XR(J), DENSIT(J), VITP(J), VITS(J)), J=1,NLTB)
5101 FORMAT (20I4)
5300 FORMAT (8I10)
5301 FORMAT (4E18.6)
5302 FORMAT (4I10)

```

Chaque ligne du tableau contient une composante du vecteur 'xr' donnant la distance au centre (en km), et la composante correspondante de chacun des vecteurs 'densit', 'vitp', 'vits' représentant les valeurs de la densité (en g/cm^3) et des vitesses des ondes P et S (en km/s) à ce niveau.

La signification de 'nbc', 'nreg', 'nc', 'no' est connue, celle des autres paramètres est la suivante :

'nltb' = nombre de lignes du tableau représentant le modèle brut ≤ 250
 'icind' = vecteur stockant au maximum 200 indices d'aiguillage, un par couche:
 si 'icind(ic)' = 0 : couche homogène, valeurs prises sur l'interface inférieur;
 si 'icind(ic)' = 1 : couche homogène, valeurs prises sur l'interface supérieur;
 si 'icind(ic)' = 2 : couche homogène, valeurs prises comme moyennes arithmétiques dans la couche;
 si 'icind(ic)' = 3 : couche stratifiée continûment; ajustement polynomial dans la couche;
 valeur prise par défaut si 'icind(ic)' < 0 ou > 3 : 2 ;
 'icinf' et 'icsup' = vecteurs dont les composantes (au maximum 200 par vecteur) contiennent les numéros des interfaces inférieur et supérieur, respectivement, pour chacune des couches.

S'il y a lieu, l'ajustement polynomial est effectué par le programme 'AJUPØL'.

Lecture du troisième fichier, version 4

Si 'initmo' = 4 on introduit le modèle brut au moyen d'une liste globale appelée /CØUCHE/, que l'on répète 'nbc' fois par groupes de trois, donc en tout trois 'nbc' fois. C'est le fichier 3,4. Dans chaque groupe de trois, lequel est associé à une couche déterminée, la première liste globale /CØUCHE/ est associée à la densité, la deuxième à la vitesse des ondes P, la troisième à la vitesse des ondes S. Chaque liste contient les valeurs de l'une de ces trois grandeurs en un nombre 'numb' = F de points, 'numb' pouvant varier pour chaque grandeur à l'intérieur d'une couche déterminée. Plus précisément, chacune des listes globales /CØUCHE/ doit contenir une valeur entière 'numb' = F ($1 \leq F \leq 7$), F abscisses quelconques appartenant à la couche n° k stockées comme vecteur 'xif' = (X_1, X_2, \dots, X_F) , et les F ordonnées correspondantes stockées comme vecteur 'deum' = $(f_k(X_1), \dots, f_k(X_F))$. Accessoirement, la liste peut aussi contenir un numéro de code 'noc' dont nous laissons entièrement le choix à l'utilisateur. Comme notre programme réserve un place suffisante pour 600 polynômes de degré 6 au maximum, F ne devrait pas dépasser 7, à moins de modifier les dimensions de 'crho', 'cvp' et 'cvs'. Si par erreur F dépasse 7, le programme y pourvoit en rejetant F-7 points, et en ne retenant que les 1^{er}, (F-5)^e, (F-4)^e, (F-3)^e, (F-2)^e, (F-1)^e et F^e points, et en redéfinissant F = 7. Ensuite, le programme 'MØDELE' (dans l'option 'initmo'=4) fait passer un polynôme de degré F-1 par les F valeurs de chaque liste globale /CØUCHE/, et pose : 'mrho(ic)' ou 'mvs(ic)' ou 'mvs(ic)' = 'numb' (= F), selon le cas. ('ic'=1,...,'nbc')

$$f_k(x) = f_{k,1} + f_{k,2} x + f_{k,3} x^2 + \dots + f_{k,F} x^{F-1}$$
$$\left\{ \begin{aligned} f_k(X_1) &= f_{k,1} + f_{k,2} X_1 + f_{k,3} X_1^2 + \dots + f_{k,F} X_1^{F-1} \\ f_k(X_2) &= f_{k,1} + f_{k,2} X_2 + f_{k,3} X_2^2 + \dots + f_{k,F} X_2^{F-1} \\ &\dots\dots\dots \\ f_k(X_F) &= f_{k,1} + f_{k,2} X_F + f_{k,3} X_F^2 + \dots + f_{k,F} X_F^{F-1} \end{aligned} \right.$$

```

*****REAL * 4  DEUM(10), XIF(10), CØA(10,10), SØL(10)
      NAMELIST /CØUCHE/ XIF, DEUM, NUMB, NØC

```

```

DØ 110 IC = 1,NBC
K = 0
101 READ (5,CØUCHE)
IF (NUMB.LT. 8) GØTØ 112
DØ 111 J = 2,7
JJ = J + NUMB - 7
XIF(J) = XIF(JJ)
111 DEUM(J) = DEUM(JJ)
NUMB = 7
112 WRITE (6,CØUCHE)
DØ 113 J = 1,NUMB
DØ 113 I = 1,NUMB
113 CØA(I,J) = XIF(I) * (J-1)
CALL ELIMIN (CØA,NUMB,DEUM,SØL,...)
K = K + 1
GØTØ (104,106,108), K
104 DØ 105 I = 1,NUMB
105 CRHØ(I,IC) = SØL(I)
GØTØ 101
106 DØ 107 I = 1,NUMB
107 CVP(I,IC) = SØL(I) * 1.D5
GØTØ 101
108 DØ 109 I = 1,NUMB
109 CVS(I,IC) = SØL(I) * 1.D5
110 CØNTINUE

```

Il convient de remarquer que dans les listes d'entrée /CØUCHE/ les valeurs de 'xif' et 'deum' à introduire sont en simple précision; les densités ('deum' pour la première liste d'un groupe de trois) sont à fournir en g/cm^3 , alors que les vitesses des ondes P et S ('deum' pour les deux dernières listes d'un groupe de trois) sont à donner en km/s .

Dans la programmation actuelle nous avons traité les cas $F=1$ et $F=2$ à part:

$$\text{si } F=1 : \quad f_{k,1} = f_k(X_1) \quad \longleftrightarrow \text{'sol(1)'}$$

$$\text{si } F=2 : \quad \begin{cases} f_k(X_1) = f_{k,1} + f_{k,2} X_1 \\ f_k(X_2) = f_{k,1} + f_{k,2} X_2 \end{cases}$$

$$\text{d'où} \quad \begin{cases} f_{k,2} = \frac{f_k(X_2) - f_k(X_1)}{X_2 - X_1} & \longleftrightarrow \text{'sol(2)'} \\ f_{k,1} = f_k(X_1) - f_{k,2} X_1 & \longleftrightarrow \text{'sol(1)'} \end{cases}$$

Lecture du troisième fichier, version 5
.....

Si 'initmo' = 5 on lit un fichier composé essentiellement d'un tableau à 'nlbt' lignes contenant comme informations les valeurs respectives : 'xr', distance au centre en km; 'densit', densité correspondante en g/cm^3 ; 'vitp' et 'vits', vitesses correspondantes des ondes P et S en km/s . Le premier enregistrement du fichier doit contenir une valeur entière strictement positive fournissant le nombre de lignes 'nlbt' du tableau :

```

^550 READ (5,5300) NLTB
      READ (5,5301) ((XR(J),DENSIT(J),VITP(J),VITS(J)), J=1,NLTB)
C
5300 FORMAT (8I10)
5301 FORMAT (4E18.6)

```

Ce fichier 3,5 se présente donc essentiellement de la même façon que le fichier 3,3. La seule différence en est que les informations concernant 'nbc', 'nreg', 'nc', 'no', 'icinf', 'icsup', 'icind' sont absentes ici. En effet, ces informations seront déduites automatiquement moyennant l'hypothèse que les valeurs intermédiaires entre deux lignes s'obtiennent toujours par interpolation linéaire.

Lecture du troisième fichier, version utilisateur

Si 'initmo' > 6 le programme 'MØDELE' passe le contrôle au programme 'MØDELL', à pourvoir par l'utilisateur. L'ordre d'appel de 'MØDELL' est le suivant :

| 600 CALL MØDELL (INITMØ)

Dans ce programme 'MØDELL', l'utilisateur pourra définir éventuellement une ou plusieurs autres manières d'initialiser les tableaux 'crho', 'cvp', 'cvs'. Il pourra aussi se servir de 'MØDELL' pour calculer d'autres grandeurs physiques que celles incorporées dans 'MØDELE' par entrées multiples, sans pour cela devoir toucher directement à 'MØDELE' et risquer d'en déranger le bon fonctionnement.

Ayant initialisé les tableaux 'crho', 'cvp', 'cvs', autrement dit les coefficients polynomiaux $\rho_{j,k}$, $\alpha_{j,k}$, $\beta_{j,k}$ des formules (18), (16) et (17), respectivement, le programme 'MØDELE' détermine

les coefficients de masse : 'gmr(k)' $\longleftrightarrow \mathcal{M}_k$

et les coefficients d'inertie: 'gir(k)' $\longleftrightarrow \mathcal{I}_k$

$1 \leq k \leq \text{NBC}$; $1 \leq \text{NBC} \leq 200$, à l'aide des formules (19) et (20), respectivement. Il évalue alors la densité moyenne du modèle :

'rhom' $\longleftrightarrow \bar{\rho}$

grâce à la formule (25), ainsi que les paramètres suivants :

'pigrho' $\longleftrightarrow \pi G \bar{\rho}$
 'amass' $\longleftrightarrow M = \frac{4}{3} \pi \bar{\rho} R^3$... masse totale
 'enrond' $\longleftrightarrow \mathcal{N} = \frac{G M}{R} = \frac{4}{3} \pi G \bar{\rho} R^2$
 'enne' $\longleftrightarrow N = \frac{3}{4} \mathcal{N} = \pi G \bar{\rho} R^2$
 'en' $\longleftrightarrow \frac{N}{R} = \pi G \bar{\rho} R$
 'amasr2' $\longleftrightarrow M R^2$

transmissibles par les blocs communs étiquetés : 'CØNST1', 'CØNST2' et 'CØNST3'. Ensuite, il détermine les coefficients de pression des formules (27), (28), (29) :

'rkj(k,j)' $\longleftrightarrow R_{k,j}$
 'pk(1,k)' $\longleftrightarrow Q_k(x_k)$
 'pk(2,k)' $\longleftrightarrow Q_k(x_{k+1})$

et, après une impression (si $IPMØD \geq 1$) et une perforation (si $IPU \geq 1$) d'un fichier de sortie éventuelles, le sous-programme 'MØDELE' retourne au programme appelant, 'MØDPØL' dans le cas envisagé ici.

Les autres points d'entrée dans 'MØDELE' sont les suivants :

' R H Ø F '

fonction : calcule la valeur de la densité ρ , en g/cm^3 , au point dont la distance au centre exprimée en unités du rayon total R est x , d'après la formule (18);

emploi : CALL RHØF (X,K,RHØ)

RHO = valeur de la densité au point de rayon normalisé X situé dans la couche n° K (entrer: X,K ; sortie: RHØ);

' G F '

fonction : calcule la valeur de l'accélération gravifique g , en cm/s^2 , en fonction de la distance centrale normalisée, par (23);

emploi : CALL GF (X,K,G)

G = valeur de la gravité au point de rayon normalisé X situé dans la couche n° K (entrer: X,K ; sortie: G);

' M A S S E '

fonction : calcule la valeur de la masse M , en g , en fonction de la distance centrale normalisée, par la relation (21);

emploi : CALL MASSE (X,K,AMASSE)

AMASSE = valeur de la masse d'une boule de rayon normalisé X dont la surface est comprise dans la couche n° K (entrer: X,K ; sortie: AMASSE);

' D M Ø Y '

fonction : calcule la densité moyenne D , en g/cm^3 , en fonction de la distance centrale normalisée, par la relation (24);

emploi : CALL DMØY (X,K,D)

D = valeur de la densité moyenne d'une boule de rayon normalisé X dont la surface est contenue dans la couche n° K (entrer: X,K ; sortie: D);

' C P F '

fonction : calcule la vitesse des ondes P : α , en cm/s, en fonction de la distance centrale normalisée, par la relation (16);

emploi : CALL CPF (X,K,CP)

CP = valeur de la vitesse des ondes P au point de rayon normalisé X situé dans la couche n° K (entrer: X,K; sortie: CP);

' C S F '

fonction : calcule la vitesse des ondes S : β , en cm/s, en fonction de la distance centrale normalisée, par la relation (17);

emploi : CALL CSF (X,K,CS)

CS = valeur de la vitesse des ondes S au point de rayon normalisé X situé dans la couche n° K (entrer: X,K; sortie: CS);

' P R E S S '

fonction : calcule la pression hydrostatique p, en dyn/cm², en fonction de la distance centrale normalisée, par la relation (30);

emploi : CALL PRESS (X,K,P)

P = valeur de la pression au point de rayon normalisé X situé dans la couche n° K (entrer: X,K; sortie: P);

' M Ø M I N '

fonction : calcule le moment d'inertie C, en g cm², en fonction de la distance centrale normalisée, par la relation (22);

emploi : CALL MØMIN (X,K,C)

C = valeur du moment d'inertie d'une boule de rayon normalisé X dont la surface est contenue dans la couche n° K (entrer: X,X; sortie: C);

' G R A D R Ø '

fonction : calcule le gradient de densité ρ' , en g/cm³/cm, en fonction de la distance centrale normalisée, par la relation (31);

emploi : CALL GRADRØ (X,K,RP)

RP = valeur du gradient de densité au point de rayon normalisé X situé dans la couche n° K (entrer: X,K; sortie: RP).

C. Denis & A. Ibrahim : Programme M Ø D P Ø L

Le programme 'MØDELE' appelle explicitement les sous-programmes : 'AJUPØL', 'ELIMIN' et 'MØDELI'. 'AJUPØL' appelle lui-même 'GAUSID'.

' C E L A S T '

Ce programme très court appelle 'RHØF', 'CPF' et 'CSF', pour évaluer la densité, la vitesse des ondes P, et la vitesse des ondes S, respectivement, en un point de distance centrale normalisée 'x' situé dans la couche n° 'ic'. A partir de ces valeurs 'rho', 'cp' et 'cv' il calcule alors :

'phi', le paramètre séismologique ϕ , par la relation (32);
 'bulk', le module de compression κ , par la relation (3');
 'rig', le module de rigidité μ , par la relation (2);
 'clame', le 1^{er} paramètre de Lamé λ , par la relation (3);
 'poiss', le coefficient de Poisson σ , par la relation (5);
 'young', le module de Young E, par la relation (4).

Toutes ces valeurs sont fournies en double précision.

Emploi :

```
REAL * 8 X,RHØ,CP,CS,BULK,RIG,CLAME,YØUNG,PØISS,PHI
CALL CELAST (X,IC,RHØ,CP,CS,BULK,RIG,CLAME,YØUNG,PØISS,PHI)
```

' R A D A U '

Ce programme détermine la valeur 'eta' du paramètre η de Radau au point 'x' dans la couche n° 'ic' grâce à la relation (13), ainsi que la valeur de la fonction η/x , soit 'etap'. Tout près du centre on se sert du développement (34) pour le paramètre de Radau, qui implique qu'au centre-même on a : 'eta' = 0, 'etap' = 'etap0' = $-1,36111 \rho_{1,2}/\rho_{1,1}$. La valeur de 'eta0' est calculée dans 'MØDELE' et transmise à 'RADAU' au moyen du bloc commun étiqueté /REDMØM/. Accessoirement, le programme 'RADAU' évalue aussi le moment d'inertie 'ai', la densité moyenne 'd' et le moment d'inertie réduit 'redin' à chaque niveau, et ces valeurs sont transmises de même par le commun étiqueté /REDMØM/. Toutes les variables réelles considérées sont en double précision.

Emploi :

```
REAL * 8 X,ETA,ETAP
CALL RADAU (X,IC,ETA,ETAP)
```


' F L A T G '

Emploi :
 REAL π 8 X, F
 CALL FLATG (X,K,F,IND)

Ce programme calcule la valeur 'f' de l'aplatissement interne de la surface de niveau repérée par 'x' et située dans la couche n° 'k'; les approximations faites sont celles de la théorie au premier ordre de Clairaut et Radau. 'FLATG' fait explicitement appel aux sous-programmes 'RADAU', 'GF' et 'DGQ4'. Nous avons préconisé ailleurs (Denis & Ibrahim, 1980) l'intérêt d'utiliser, de préférence à toute méthode analytique, une quadrature de Gauss-Legendre d'ordre relativement peu élevé combinée à la méthode des trapèzes, pour évaluer l'intégrale intervenant dans la formule (14). C'est en fait le seul endroit dans notre programme où nous recourons à une méthode d'intégration numérique, très rapide et très précise dans ce cas-ci.

L'argument 'ind' est un paramètre d'aiguillage, lequel peut seulement prendre l'une quelconque des trois valeurs entières 1, 2 ou 3. Avant tout emploi ultérieur de 'FLATG' il faut nécessairement faire un appel préalable à 'FLATG' avec la valeur 'ind'=1. Le programme 'FLATG' permet d'évaluer l'aplatissement f de deux manières légèrement différentes, selon que l'indice 'ind' vaut deux ou trois. En effet, supposant que $x \in (x_k, x_{k+1})$ écrivons la formule (14) sous la forme

$$f(x) = f(1) \exp [Y(x)] \quad (35)$$

où

$$Y(x) = \int_1^x \frac{\eta(y)}{y} dy \quad (36)$$

Tout d'abord, en posant 'ind'=1 on évalue les intégrales successives

$$\mathcal{F}_k = \int_1^{x_k} \frac{\eta(y)}{y} dy, \quad k=1, 2, \dots, N, N+1 \quad (37)$$

dont on range les valeurs dans le vecteur 'fOk' de dimension 201 au maximum. ($N \longleftrightarrow \text{'nbc'}$) Le calcul de ces intégrales est fait de la manière suivante: Nous partitionnons l'intervalle (0,1) en sous-intervalles

(x_j, x_{j+1}) tels que

$$(0,1) = (x_1, x_2) \cup (x_2, x_3) \cup \dots \cup (x_{k-1}, x_k) \cup (x_k, x_{k+1}) \cup \dots \cup (x_N, x_{N+1})$$

où $x_1 = 0$ et $x_{N+1} = 1$. Puis nous divisons tous ces sous-intervalles

eux-mêmes en sous-sous-intervalles $(x-h_k, x)$ de longueur $h_k = \frac{x_{k+1} - x_k}{n_k}$, où n_k est le nombre de pas 'np(k)' dans la couche considérée, pris automatiquement égal à 4 s'il n'est pas fourni explicitement par l'utilisateur. Dans chacun de ces sous-sous-intervalles on intègre alors la fonction $\eta(x)/x$ par la méthode de Gauss-Legendre à 4 points (Stroud & Secrest, 1966) au moyen du sous-programme appelé 'DGQ4', et on somme successivement les valeurs intégrales ainsi obtenues :

$$\mathcal{F}'_1 = 0 \quad (38)$$

$$\mathcal{F}'_{k+1} = \mathcal{F}'_k + \int_{x_k}^{x_{k+1}} \frac{\eta(y)}{y} dy \quad (39)$$

$$= \mathcal{F}'_k + \sum_{j=1}^{n_k} \int_{x_k}^{x_k + jh_k} \frac{\eta(y)}{y} dy \quad (39')$$

On trouve ensuite les intégrales \mathcal{F}_k par

$$\mathcal{F}_k = \mathcal{F}'_k - \mathcal{F}'_{N+1}, \quad k = 1, 2, \dots, N, N+1 \quad (40)$$

La valeur $\mathcal{F}'_{N+1} = \int_0^1 (\eta/y) dy$ est rangée comme 'f01'. Le vecteur 'f0k' ainsi que la variable 'f01' peuvent être transmis à l'aide du bloc commun étiqueté /FRK/. En outre, toujours dans le cas 'ind'=1 et à condition que l'on ait 'jep'=1, le programme 'FLATG' détermine également la valeur de l'aplatissement en surface, $f(1) \longleftrightarrow \text{'fsurf'}$, au moyen de la relation (15).

Cela étant dit, 'FLATG' prévoit donc deux manières d'évaluer 'f':

D'une part, si 'ind'=2 on suppose les \mathcal{F}_k connus et on évalue la quantité

$$\delta \mathcal{F}_k(x) = \int_{x_k}^x \frac{\eta(y)}{y} dy, \quad x \in (x_k, x_{k+1}) \quad (41)$$

par une quadrature de Gauss-Legendre à 4 points au moyen de 'DGQ4'; on calcule ensuite l'aplatissement f , compte tenu de (35), (36), (37) et (41), par

$$f(x) = f(1) \exp[\mathcal{F}_k + \delta \mathcal{F}_k(x)] \quad (42)$$

D'autre part, si 'ind'=3 on suppose la quantité $Y(x-h)$ connue, et l'on évalue alors par quadrature au moyen de 'DGQ4' la quantité

$$\delta Y(x) = \int_{x-h}^x \frac{\eta(y)}{y} dy \quad (43)$$

puis

$$f(x) = f(1) \exp [Y(x-h) + \delta Y(x)] \quad (44)$$

En général, lorsqu'on désire connaître toute une distribution de valeurs de f pour un modèle, la deuxième manière (avec 'ind'=3) est avantageuse tant du point de vue rapidité que du point de vue précision, à condition que l'on ait au préalable déterminé une valeur de départ, par exemple par un appel à 'FLATG' avec 'ind'=2. Par contre, si l'on ne désire connaître qu'une valeur isolée de f associée à un niveau particulier du modèle, seule la première manière (relative à 'ind'=2) est généralement praticable.

' D G Q 4 '

Fonction : Sous-programme d'intérêt général permettant d'effectuer une quadrature de Gauss à quatre points d'appui utilisant des coefficients de Legendre; légèrement aménagé du "IBM Scientific Subroutine Package" (IBM Application Program, 1968, p.300), où il porte le nom 'DQG4' (noter l'inversion des lettres G et Q);

Emploi : REAL * 8 XL, XU, FY
EXTERNAL FCT
CALL DGQ4 (XL,XU,K,FCT,FY)

' A J U P Ø L '

Fonction : Sous-programme d'intérêt général permettant d'ajuster un polynome de degré M-1 à un ensemble de N points donnés :

si $N > M$: solution par moindres carrés; le polynome passe "au mieux" par les N points;
si $N = M$: solution unique; le polynome passe exactement par les N points;
si $N < M$: infinité de solutions; dans ce cas 'AJUPØL' réduit automatiquement M à la valeur N, et produit alors une solution unique correspondant à un polynome de degré N-1;

Emploi : REAL * 8 C(7,nbc), XR(nv), V(nv)
CALL AJUPØL (C,XR,V,N,K,M)

Note : Il faut que
 $N \leq 'nv'$
 $K \leq 'nbc'$
 $M \leq 7$ (dans la version actuelle);

Sous-programme appelé : 'GAUSID' ;

Adapté de Pennington (1967), pp. 363-374.

' E L I M I N '

Fonction : Sous-programme d'intérêt général permettant de déterminer la solution x d'un système algébrique linéaire d'ordre n :

$$A x = b$$

adapté de Pennington (1967), pp. 290-295 ;

méthode utilisée: éliminations successives;

Emploi : REAL ≥ 8 A(n,n), B(n), X(n), EPS, AA(n,n+1), BB(n)
 DIMENSION ID(n)
 NDPl = ND + 1
 CALL ELIMIN (A,N,B,X,EPS,ND,NDPl,AA,BB,ID,JELIM)

Notes : Il faut que $N \leq 'n' = ND$;

'jelim' est défini par le programme :

si 'jelim' vaut 1, le retour est normal;

si 'jelim' vaut 2, il n'y a pas de solution unique;

'eps' est lié au nombre de chiffres significatifs dont on admet la perte par soustraction de deux nombres voisins; si l'on admet la perte jusqu'à m chiffres, on pose : 'eps' = $1.D-m$.

' G A U S I D '

Fonction : Sous-programme d'intérêt général permettant de déterminer la solution x d'un système algébrique linéaire d'ordre n :

$$A x = b$$

adapté de Pennington (1967), pp. 295-303 ;

méthode utilisée: itérations successives (Gauss-Seidel);

Emploi : REAL ≥ 8 A(n,n), B(n), X(n), ERR, AA(n,n+1)
 NDPl = ND + 1
 CALL GAUSID (A,N,B,X,ERR,ND,NDPl,AA,JGAUS,NIT)

Notes : Il faut que $N \leq 'n' = ND$;

'jgaus' est défini par le programme :

si 'jgaus' vaut 1, le retour est normal;

si 'jgaus' vaut 2, pas de convergence;

'err' est la précision absolue souhaitée;

'nit' est le nombre maximum d'itérations admis.

5. Répertoire alphabétique des blocs communs du programme

```

*****IMPLICIT REAL * 8 (A-H,Ø-Z)
      REAL * 4 LINE, DT
      CØMMØN /CØFPØL/ CRHØ(7,200), CVP(7,200), CVS(7,200), GMR(201),
1      GIR(201), MVP(200), MVS(200)
      CØMMØN /CØNST1/ PI, QPI2, PIGRHØ, EN, ENNE, RHØC, PC, RHØS, PSURF
      CØMMØN /CØNST2/ BIGG, RAYØN, RHØM, GSR2, QPIGR, QPIGR2, QTPIGR
      CØMMØN /CØNST3/ AMASS, AMASR2, ENRØND, HPS3R5
      CØMMØN /ELLIP/ FSURF, RØTPER, FLAT, MRHØ(200), JEP
      CØMMØN /FRK/ FOK(201), FØ1, XU, FY
      CØMMØN /JWX/ XC(201), XM, DRKM(200), JX, NC(200), NØ(200),
1      NP(200), NLTB, NREG, NBC
      CØMMØN /LIN/ DT(20), LINE(33), KØUNT1
      CØMMØN /QTP/ QTPIR3, QTPIR5
      CØMMØN /REDMØM/ REDIN, AINERT, DMØYEN, ETAPO      dans 'MØDELE'
                  ou AI      ou D      dans 'MØDPØL' et 'RADAU'
      CØMMØN /ZYX/ XYZ(100)

/CØFPØL/   intervient dans 'MØDELE'
/CØNST1/   est commun à 'MØDPØL', 'MØDELE' et 'FLATG'
/CØNST2/   est commun à 'MØDPØL', 'MØDELE' et 'FLATG'
/CØNST3/   intervient dans 'MØDELE'
/ELLIP/    est commun à 'MØDPØL', 'MØDELE' et 'FLATG'
/FRK/      intervient dans 'FLATG'
/JWX/      est commun à 'MØDPØL', 'MØDELE' et 'FLATG'
/LIN/      est commun à 'MØDPØL' et 'MØDELE'
/QTP/      est commun à 'MØDELE' et 'RADAU'
/REDMØM/    est commun à 'MØDPØL', 'MØDELE' et 'RADAU'
/ZYX/      intervient dans 'MØDELE'

```

Arguments non définis dans ce qui précède, mais définis par le programme :

```

'flat'      :   adresse reste disponible;
'gsr2'      ↔    $G/R^2$ 
'hps3r5'    ↔    $\frac{8}{3} \pi R^5$ 
'line'      :   vecteur à 33 composantes renfermant chacune la chaîne '++++';
'kount1'    :   compteur du nombre de lignes imprimées avant saut de page;
'pi'        ↔   3.141592653589793200

```

'qp12'	—	$4 \pi^2$
'qpigr'	—	$4 \pi G R$
'qpigr2'	—	$4 \pi G R^2$
'qtpigr'	—	$\frac{4}{3} \pi G R$
'qtpir3'	—	$\frac{4}{3} \pi R^3$
'qtpir5'	—	$\frac{4}{3} \pi R^5$
'rhoc'	:	valeur de la densité au centre
'rhos'	:	valeur de la densité à la surface

6. Répertoire alphabétique des sous-programmes listés

```
'AJUPØL',      'CELAST',      'DGQ4',      'ELIMIN',      'FLATG',      'GAUSID',
'MØDDAT',
'MØDELE'      entrées:      'CPF',      'CSF',      'DMØY',      'GF',
                'GRADRØ',      'MASSE',      'MØMIN',      'PRESS',
                'RHØF',
'MØDELL',
'MØDMAI'      (programme principal :  MAIN ) ,
'MØDPØL',      'RADAU'.
```

7. Références

- Bullen K.E. (1975) "The Earth's Density", Chapman & Hall, London.
- Denis C. (1979) "Static and dynamic effects in theoretical Love numbers", Proc. 8th Int. Symp. Earth Tides, published by M. Bonatz & P. Melchior, Institut für Theoretische Geodäsie, Bonn, pp. 709-729.
- Denis C. & Ibrahim A. (1980) "Sur la représentation de modèles terrestres, planétaires et stellaires, avec application au calcul de l'aplatissement interne", soumis au Bull. géodés.
- Dziewonski A.M., Hales A.L. & Lapwood E.R. (1975) "Parametrically simple Earth models consistent with geophysical data", Phys. Earth Planet. Interiors 10, 12-48.
- IBM Application Program (1968) "System/360 Scientific Subroutine Package (360A-CM-03X) Version III - Programmer's Manual" (Fourth Edition, File n° H20-0205-3), p. 300.

```

C
2 WRITE (IOUT,6001) LINE
  WRITE (IOUT,6005)
  WRITE (IOUT,6005)
  WRITE (IOUT,6003) DT
  WRITE (IOUT,6005)
  WRITE (IOUT,6005)
  WRITE (IOUT,6008)
  WRITE (IOUT,6009)
  WRITE (IOUT,6005)
  WRITE (IOUT,6005)
  WRITE (IOUT,6001) LINE
  WRITE (IOUT,6005)
  WRITE (IOUT,6005)
  WRITE (IOUT,6005)
  KOUNTL = 13

IC
  CALL FLATG (X,IC,F,1)
  DO 1001 IC = 1,NBC
    WRITE (IOUT,6005)
    KOUNTL = KOUNTL+1
    H = (XC(IC+1)-XC(IC))/DFLOAT(NP(IC))
    I = NP(IC)+1
    DO 1001 J = 1,I
      X = DFLOAT(J-1)*H + XC(IC)
      R = X * RAYON/1.D5
      Z = RAYON/1.D5 - R
      CALL CELAST(X,IC,RHO,CF,CS,BULK,RIG,CLAME,YOUNG,POISS,FHI)

IC
    IRAY = IFIX (SNGL(R)+0.50001)
    IZ = IFIX (SNGL(Z)+0.50001)
    VP = CF/1.D5
    VS = CS/1.D5
    IBU = IFIX (SNGL(BULK/1.D9)+0.50001)
    IRI = IFIX (SNGL(RIG/1.D9)+0.50001)
    ICLA = IFIX (SNGL(CLAME/1.D9)+0.50001)
    IYOU = IFIX (SNGL(YOUNG/1.D9)+0.50001)
    CALL GF (X,IC,G)
    CALL PRESS (X,IC,P)
    CALL MASSE (X,IC,AMAS)
    CALL DENMOY (X,IC,DMOY)
    IND = 3
    IF (IC+J .LT. 3) IND = 2
    CALL FLATG (X,IC,F,IND)
    F = F * 1.D3
    CALL RADAU (X,IC,ETA,ETAP)
    IFRE = IFIX (SNGL(P/1.D9)+0.50001)
    IG = IFIX (SNGL(G)+0.50001)
  2001 KOUNTL = KOUNTL+1

C
  IF (KOUNTL .LT. 61) GOTO 1001
C

```

```

WRITE (IOUT,6004)
WRITE (IOUT,6008)
WRITE (IOUT,6009)
WRITE (IOUT,6005)
WRITE (IOUT,6005)
WRITE (IOUT,6001) LINE
WRITE (IOUT,6005)
WRITE (IOUT,6005)
KOUNTL = 6

```

```

C
1001 WRITE (IOUT,6010) IC,X,IRAY,RHO,VF,VS,IBU,IRI,ICLA,IPRE,IG,AMAS,
1 DMOY,REDIN,ETA,F,IZ

```

```

C
WRITE (IOUT,6005)
WRITE (IOUT,6005)
WRITE (IOUT,6001) LINE
WRITE (IOUT,6000) RHOM,RHOC,RHOS
WRITE (IOUT,6002)
RETURN

```

```

C
C
3 WRITE (IOUT,6030) (LINE(J), J=1,18)
WRITE (IOUT,6001) (DT(J), J=1,18)
WRITE (IOUT,6030) (LINE(J), J=1,18)
WRITE (IOUT,6031)
KOUNTL = 12
XU = XC(NBC+1)
CALL FLATG (XU,0,F,1)
RKM = RAYON/1.D5
XK = 0.D0
DO 3010 IC = 1,NBC
10 DRAD = DRKM(IC)/RKM
IF (DRAD .LT. (XC(IC+1)-XC(IC))) GOTO 11
DRKM(IC) = DRKM(IC) * 0.500
GOTO 10
11 XK = XK + DRAD
JST = IDINT ((XC(IC+1)-XK)/DRAD + 1.D-8) + 1
IF (JST .GT. 0) GOTO 4000
JST = 1
4000 DO 3010 J = 1,JST
IF (J .GT. 1) XK = XK + DRAD
IF (XC(IC) .EQ. XK) GOTO 3001
IF (J .GT. 1) GOTO 3001
IF (J .EQ. 1) X = XC(IC)
GOTO 3002
3001 X = XK
IF (X .GT. XC(IC+1)) X = XC(IC+1)
3002 CALL CELAST (X,IC,RHO,CP,CS,EULK,RIG,CLAME,YOUNG,POISS,PHI)
CALL GF (X,IC,G)
CALL PRESS (X,IC,P)
CALL DENMOY (X,IC,DMOY)
IND = 3
IF (IC+J .LT. 3) IND = 2
CALL FLATG (X,IC,F,IND)

```


C. Denis & A. Ibrahim : Programme M Ø D P Ø L

```

IRAY = IDINT (X*RKM + 0.50000001D0)
VP = CP/1.D5
VS = CS/1.D5
F = F * 1.D3
CALL RADAU (X,IC,ETA,ETAP)
IPRE = IDINT (P/1.D9 + 0.50000001D0)
IG = IDINT (G + 0.50000001D0)
WRITE (IOUT,6032) IRAY,RHO,VP,VS,IPRE,IG,DMOY,REDIN,ETA,F
KOUNTL = KOUNTL + 1
IF (KOUNTL .LT. 61) GOTO 3003
KOUNTL = 12
WRITE (IOUT,6004)
WRITE (IOUT,6030) (LINE(M), M=1,18)
WRITE (IOUT,6001) (DT(M), M=1,18)
WRITE (IOUT,6030) (LINE(M), M=1,18)
WRITE (IOUT,6031)
3003 IF (X .LT. XK) GOTO 3001
IF (X .EQ. XC(IC+1)) GOTO 3010
IF (J .NE. JST) GOTO 3010
X = XC(IC+1)
GOTO 3002
3010 CONTINUE
WRITE (IOUT,6030) (LINE(J), J=1,18)
WRITE (IOUT,6002)
RETURN
C
C
4 CALL MODDAT (JTAB)
RETURN
C
C
END

```

```

SUBROUTINE MODDAT (JTAB)
C SOUS-PROGRAMME A FOURVOIR PAR L'UTILISATEUR, SI NECESSAIRE
RETURN
END

```

SUBROUTINE MODELE

SOUS-PROGRAMME A ENTREES MULTIPLES :
 'MODELE', 'RHO', 'GF', 'MASSE', 'DMOY',
 'CPF', 'CSF', 'PRESS', 'MOMIN', 'GRADRO'

*** VERSION CALCULANT LE PARAMETRE DE RADAU
 *** A L'AIDE DU MOMENT D'INERTIE REDUIT

CE SOUS-PROGRAMME INITIALISE LES COEFFICIENTS DES DISTRIBUTIONS
 POLYNOMIALES DE LA DENSITE, DE LA MASSE, DU MOMENT D'INERTIE,
 DE L'ACCELERATION GRAVIFIQUE, DE LA PRESSION,
 DES VITESSES DES ONDES LONGITUDINALES ET TRANSVERSALES, ET DETERMINE
 LA DENSITE MOYENNE DU MODELE AINSI QUE CERTAINS AUTRES PARAMETRES

INTRODUCTION DU MODELE

LE MODELE EST FOURNI PAR LES COEFFICIENTS POLYNOMIAUX
 DE LA DENSITE (CRHO), DE LA VITESSE DES ONDES P (CVP), ET
 DE LA VITESSE DES ONDES S (CVS) :

$$\begin{aligned} \text{RHO}(X, IC) &= \text{SOMME SUR } J \text{ DE } \text{CRHO}(J, IC) * X^{**}(J-1) \\ \text{VP}(X, IC) &= \text{SOMME SUR } J \text{ DE } \text{CVP}(J, IC) * X^{**}(J-1) \\ \text{VS}(X, IC) &= \text{SOMME SUR } J \text{ DE } \text{CVS}(J, IC) * X^{**}(J-1) \end{aligned}$$

L'ARGUMENT $X=R/\text{RAYON}$ DESIGNE LE POINT A L'INTERIEUR DU MODELE OU
 L'ON EVALUE LES PROPRIETES, L'INDICE IC DENOTE LE NUMERO DE LA
 COUCHE DANS LAQUELLE CE POINT SE TROUVE: IC VARIE DE 1 A NEC.
 L'INDICE MUET J VARIE DE 1 A MRHO(IC) POUR RHO, DE 1 A
 MVP(IC) POUR VP, ET DE 1 A MVS(IC) POUR VS, RESPECTIVEMENT.
 LES COEFFICIENTS CRHO, CVP ET CVS SONT EN DOUBLE PRECISION; ILS SONT
 MESURES DANS DES UNITES C.G.S.

L'INDICE INITMO SERT A INITIALISER LES COEFFICIENTS POLYNOMIAUX
 CRHO, CVP ET CVS :

INITMO=1 ON LIT CES COEFFICIENTS EN MEME TEMPS QUE D'AUTRES
 PARAMETRES DU MODELE A PARTIR DE CARTES EN GENERAL
 PREPAREES PAR L'ORDINATEUR LORS D'UN PASSAGE
 PRECEDENT

INITMO=2 ON UTILISE LE NAMELIST COEF

INITMO=3 ON CALCULE LES COEFFICIENTS D'APRES DES VALEURS
 DU MODELE TABULEES DE MANIERE STANDARD
 SELON LE FORMAT 5301

INITMO=4 ON CALCULE LES COEFFICIENTS D'APRES DES VALEURS
 FOURNIES PAR LE NAMELIST COUCHE

INITMO=5 ON CALCULE DE MANIERE STANDARD LES COEFFICIENTS
 D'APRES DES VALEURS TABULEES DU MODELE
 SELON LE FORMAT 5301

INITMO>5 ON APPELLE LE SOUS-PROGRAMME 'MODEL1'

```
IMPLICIT REAL*8 (A-H,O-Z)
```

```
REAL*4 LINE(33), FLUS
```

```
REAL*4 DT(20), DEUM(10), XIF(10), RVAL, DENS, VP, VS
```

```
REAL*4 DENSIT(250), VITP(250), VITS(250), XR(250)
```

```

1  DIMENSION COA(10,10), DDEUM(10), SOL(10), XRA(50), Densa(50),
2      VITPA(50), VITSA(50), GMR(201), XC(201), CRHO(7,200),
3      CVP(7,200), CVS(7,200), MRHO(200), MVP(200), MVS(200),
4      ICINF(200), ICSUF(200), ICIND(200), NC(200), NO(200),
      GIR(201)
1  DIMENSION F(22), NP(200), DRKM(200)
2  DIMENSION ACOA(10,11), ID(10)
3  DIMENSION RKJ(200,23), PK(2,200)
4  EQUIVALENCE (RKJ(1),COA(1)), (RKJ(101),XRA(1)),
1      (RKJ(151),Densa(1)), (RKJ(201),VITPA(1)), (RKJ(251),VITSA(1)),
2      (RKJ(301),DDEUM(1)), (RKJ(311),SOL(1)), (RKJ(321),DENSIT(1)),
3      (RKJ(446),VITP(1)), (RKJ(571),VITS(1)), (RKJ(696),XR(1)),
4      (RKJ(821),DEUM(1)), (RKJ(826),XIF(1)), (RKJ(831),ACOA(1))

```

```

COMMON /ELLIP/ FSURF,ROTPER,FLAT,MRHO,JEP
COMMON /COFPOL/ CRHO, CVP, CVS, GMR, GIR, MVP, MVS
COMMON /CONST1/ PI, QPI2, FIGRHO, EN, ENNE, RHOC, FC, RHOS, FSURF
COMMON /CONST2/ BIGG, RAYON, RHOM, GSR2, QFIGR, QFIGR2, QTFIGR
COMMON /CONST3/ AMASS, AMASR2, ENROND, HFS3R5
COMMON /JWX/ XC, XM, DRKM, JX, NC, NO, NP, NLTB, NREG, NEC
COMMON /LIN/ DT, LINE, KOUNTL
COMMON /QTP/ QTPIR3, QTPTR5
COMMON /REDMOM/ REDIN, AINERT, DMOYEN, ETAPO
COMMON /ZYX/ XYZ(100)

```

```
NAMELIST /COEF/ CRHO, CVP, CVS
```

```
NAMELIST /COUCHE/ XIF, DEUM, NUMB, NOC
```

```

1  NAMELIST /MODEL/ INITMO, BIGG, RAYON, FC, XC, XM, IPU, IPMOD,
2      NREG, NEC, NC, NP, NO, MRHO, MVP, MVS, FSURF, FSURF, ROTPER,
      DRKM, JX, JEP

```

```

1  DATA F /'INITMO =', 'IPU      =', 'IPMOD   =', 'JEP      =',
2      'JX      =', 'NLTB     =', 'NREG     =', 'NEC      =',
3      'BIGG     =', 'RAYON    =', 'RHOM     =', 'AMASS     =',
4      'AMASR2   =', 'FSURF    =', 'FC       =', 'XM       =',
5      'FIGRHO   =', 'ENROND   =', 'ENNE     =', 'EN       =',
      'ROTPER   =', 'FSURF    ='/

```

```
DATA XCD /'XC      ='/
```

```
DATA FLUS/4H++++/
```

```
DATA NDMAX/7/, IN/5/, IOUT/6/, IFUNCH/7/
```

```

C
C FORMATS
C *****
C
5000 FORMAT(20A4)
5101 FORMAT(20I4)
5102 FORMAT (3D25.16)
5103 FORMAT (4D20.13)
5300 FORMAT (8I10)
5301 FORMAT (4E18.6)
5302 FORMAT (4I10)
6000 FORMAT ('1CARACTERISATION DU MODELE'////)
6001 FORMAT (/33A4//)
6003 FORMAT (T27,20A4//)
6006 FORMAT (1H0)
6007 FORMAT (1H1)
6011 FORMAT (T6,A8,G15.6,T39,A8,G15.6,T72,A8,G15.6,T105,A8,G15.6)
6012 FORMAT (' COUCHE NO.',I4,50X,'MRHO =',I2,10X,'MVP =',I2,10X,
1      'MVS =',I2/)
6013 FORMAT (' CRHO =',1F7D17.6)
6014 FORMAT (' CVP  =',1F7D17.6)
6015 FORMAT (' CVS  =',1F7D17.6)
6016 FORMAT (' GMR  =',1FD17.8, 6X, 'GIR  =',1FD17.8, 6X, 'NP  =',
1      I4, 6X, 'XC  =',1FD17.8, 6X, 'DRKM =',1FD17.8)
6017 FORMAT (' REGION NO.',I4,3X,'COMPRENANT LES COUCHES NOS.',I4,
1      '  A',I4,4X,'(NC=',I3,' )',10X,'NO =',I2,
2      '  (COUCHE FLUIDE SI NO=4 )')
6018 FORMAT (T3,A8)
6019 FORMAT (T22, 5G20.8)
7000 FORMAT (' &MODEL  INITMO=1, BIGG=',D20.13,', RAYON=',D23.16,
1      ',','/' PC=',D23.16,', XM=',D23.16,',','/
2      ' PSURF=',D23.16,', IFMOD=',I2,',','/
3      ' IFU = 0, JX = 0, JEP =',I2,',','/
4      ' FSURF =',D23.16,', ROTPER =',D23.16,',','/
5      ' &END')
C
C
C BIGG ..... CONSTANCE D'ATTRACTION UNIVERSELLE EXPRIMEE EN UNITES
C              C.G.S.: BIGG = 6.6720 D-8 DYN.GR-2.CM2
C RAYON ..... RAYON DU MODELE, EN CM
C              (POUR LA TERRE: RAYON = 6.37108 CM)
C PC ..... PARAMETRE DE NORMALISATION REPRESENTANT UNE PRESSION
C              CARACTERISTIQUE A L'INTERIEUR DU MODELE,
C              P.EX. LA PRESSION CENTRALE
C PSURF ..... PRESSION REGNANT A LA SURFACE EXTERNE, EXPRIMEE EN
C              UNITES CGS (BARYES)
C ROTPER ..... PERIODE DE ROTATION DU MODELE, EXPRIMEE EN SECONDES
C              DE TEMPS
C XM ..... DISTANCE AU CENTRE EN UNITES DU RAYON TOTAL A PARTIR
C              DE LAQUELLE ON ARRETE LE DEVELOPPEMENT EN SERIE,
C              S'IL Y A LIEU
C XC(IC) ..... DISTANCES AU CENTRE DES DIFFERENTS INTERFACES ENTRE
C              COUCHES SUCCESSIVES (IC = 1, ... ,NBC+1)
C              IF JX .NE. 1 , LES DISTANCES SONT NORMALISEES
C              IF JX .EQ. 1 , LES DISTANCES SONT EN KILOMETRES

```

```
C FSURF ..... APLATISSEMENT GEOMETRIQUE EXTERNE
C      (CE PARAMETRE EST REDEFINI DANS 'FLATG' PAR FSURF =
C
C      5/2 * (2*PI/ROTFER)**2 * RAYON / (GS * (ES+2))
C
C      OU GS DESIGN L'ACCELERATION GRAVIFIQUE EN SURFACE
C      ET ES LE PARAMETRE DE RADAU A LA SURFACE DU MODELE;
C      CETTE REDEFINITION N'EST EFFECTUEE QUE SI JEP = 1 )
C IPU ..... PARAMETRE DE PERFORATION DES CARTES-DONNEES A
C      INTRODUIRE AVEC INITMO=1 LORS D'UN PROCHAIN PASSAGE
C      (CETTE PERFORATION A LIEU LORSQUE IPU .GT. 0)
C IFMOD ..... PARAMETRE D'IMPRESSION DE DONNEES CARACTERISANT
C      LE MODELE (CETTE IMPRESSION SE FAIT SI IFMOD .GT. 0)
C NP(IC) ..... NOMBRE DE PAS A CONSIDERER DANS LA COUCHE NO. IC
C      (SOIT POUR LA TABULATION, SOIT POUR L'INTEGRATION
C      SI NP N'EST PAS REDEFINI PAR LE NAMELIST INPUT)
C NO(IR) ..... ORDRE DU SYSTEME DIFFERENTIEL DANS LA REGION NO. IR
C
C
C      PI = 3.141592653589793200
C      QPI2 = PI*PI*4.D0
C      BIGG = 6.6720D-8
C      RAYON = 6.371D8
C      PSURF = 0.D0
C      FSURF = 3.35282D-3
C      ROTFER = 86164.1D0
C      FLAT = 0.D0
C      XM = 1.0D-2
C      PC = 1.0D12
C      CRHO(2,1) = 0.D0
C      DO 11 J = 1,200
C        NP(J) = 4
C 11 DRKM(J) = 1.D2
C    DO 1 J = 1,33
C      1 LINE(J) = PLUS
C      IFMOD = 1
C      IPU = 0
C
C      READ(IN,5000) DT
C      READ (IN,MODEL)
C
C      IF (JX .NE. 1) GOTO 3
C      RKM = RAYON/1.D5
C      I = NBC + 1
C      DO 2 J = 1,I
C        2 XC(J) = XC(J)/RKM
C
C      3 INIT = INITMO
C      IF (INITMO .GT. 6) INIT = 6
C      GOTO (510,520,530,540,550,600), INIT
C
C.1 INITMO=1, ENTRER CRHO EN G/CC, CVP ET CVS EN CM/S
C
C 510 READ(IN,5101) NREG,NBC,(NC(J),J=1,NREG),
C      1 ((MRHO(IC),MVP(IC),MVS(IC)),IC=1,NBC)
```

```

      READ(IN,5101)  (NO(J), J=1,NREG), (NP(J), J=1,NBC)
      DO 511 IC = 1,NBC
      I = MRHO(IC)
      J = MVP(IC)
      K = MVS(IC)
      READ(IN,5102)  (CRHO(IJ,IC),IJ=1,I), (CVP(IJ,IC),IJ=1,J),
1          (CVS (IJ,IC),IJ=1,K)
511 CONTINUE
      K = NBC+1
      READ(IN,5103)  (XC(I),I=1,K)
C      LES XC SONT DONNES ICI COMME FRACTIONS DU RAYON
      GOTO 3001
C
C.2 INITMO=2, ENTRER CRHO EN G/CC, CVP ET CVS EN CM/S
C
      520 READ(IN,COEF)
      GOTO 3001
C
C.3 INITMO=3, ENTRER RVAL, DENS, VP ET VS EN SIMPLE PRECISION
C      RVAL (EN KM) ..... DISTANCE A L'ORIGINE
C      DENS (EN G/CC) ..... MASSE VOLUMIQUE
C      VP (EN KM/S) ..... VITESSE DES ONDES P
C      VS (EN KM/S) ..... VITESSE DES ONDES S
C
C      NLTB ..... NOMBRE DE LIGNES DANS LE TAELEAU REPRESENTANT
C      LE MODELE
C      NBC ..... NOMBRE TOTAL DE COUCHES (AU MAXIMUM: 200)
C      NREG ..... NOMBRE DE REGIONS COMPOSANT LE MODELE
C      (AU MAXIMUM: 200)
C      NC(IR) ..... NOMBRE DE COUCHES DANS LA REGION NO. IR
C      ICINF(IC) ..... NUMERO DE L'INTERFACE INFERIEUR DE LA COUCHE NO. IC
C      ICSUP(IC) ..... NUMERO DE L'INTERFACE SUPERIEUR DE LA COUCHE NO. IC
C      ICIND(IC) ..... INDICE D'AIGUILLAGE POUR LA COUCHE NO. IC
C      ... K=0 ... COUCHE HOMOGENE, VALEURS PRISES SUR L'INTERFACE
C      INFERIEUR
C      ... K=1 ... COUCHE HOMOGENE, VALEURS PRISES SUR L'INTERFACE
C      SUPERIEUR
C      ... K=2 ... COUCHE HOMOGENE, VALEURS MOYENNES DANS LA COUCHE
C      ... K=3 ... AJUSTEMENT POLYNOMIAL DANS LA COUCHE
C
      530 READ (IN,5300)  NLTB,NBC,NREG
      READ (IN,5101)  (NC(J), J=1,NREG)
      READ (IN,5101)  (NO(J), J=1,NREG)
      READ (IN,5302)  ((IC, ICINF(IC), ICSUP(IC), ICIND(IC)), IC=1,NBC)
      READ (IN,5301)  ((XR(J),DENSIT(J),VITP(J),VITS(J)), J=1,NLTB)
C
      531 XC(NBC+1) = DBLE(XR(NLTB))*1.D5/RAYON
      DO 536 IC = 1,NBC
      I = ICINF(IC)
      J = ICSUP(IC)
      K = ICIND(IC)
      IF (K .LT. 0 .OR. K .GT. 3) K = 2
      NVC = J-I+1
      XC(IC) = DBLE(XR(I))*1.D5/RAYON

```

```

      IF (K .GT. 2) GOTO 534
      MRHO(IC) = 1
      MVP(IC) = 1
      MVS(IC) = 1
      IF (K .GT. 0) GOTO 532
      CRHO(1,IC) = DBLE(DENSIT(I))
      CVP(1,IC) = DBLE(VITP(I))*1.D5
      CVS(1,IC) = DBLE(VITS(I))*1.D5
      GOTO 536
532 IF (K .GT. 1) GOTO 533
      CRHO(1,IC) = DBLE(DENSIT(J))
      CVP(1,IC) = DBLE(VITP(J))*1.D5
      CVS(1,IC) = DBLE(VITS(J))*1.D5
      GOTO 536
533 CRHO(1,IC) = DBLE(DENSIT(I)+DENSIT(J))*0.500
      CVP(1,IC) = DBLE(VITP(I)+VITP(J))*0.505
      CVS(1,IC) = DBLE(VITS(I)+VITS(J))*0.505
      GOTO 536
534 DO 535 IJ = 1,NVC
      JJ = IJ+I-1
      XRA(IJ) = DBLE(XR(JJ))*1.D5/RAYON
      DENSA(IJ) = DBLE(DENSIT(JJ))
      VITPA(IJ) = DBLE(VITP(JJ))*1.D5
535 VITSA(IJ) = DBLE(VITS(JJ))*1.D5
C
C  AJUSTEMENT POLYNOMIAL DE LA DENSITE ET DES VITESSES P ET S
C  DANS LA COUCHE IC
C
      CALL AJUPOL(CRHO,XRA,DENSA,NVC,IC,MRHO)
      CALL AJUPOL(CVP,XRA,VITPA,NVC,IC,MVP)
      CALL AJUPOL(CVS,XRA,VITSA,NVC,IC,MVS)
536 CONTINUE
      XM = XC(2)
      GOTO 3001
C
C.4 INITMO=4, LIRE NAMELIST COUCHE (ENTRER VP, VS EN KM/S)
C
540 DO 100 J = 1,10
100 COA(J,1) = 1.D0
      DO 110 JJ = 1,NEC
      K = 0
101 READ (IN,COUCHE)
      IF (NUMB .LT. 8) GOTO 112
      DO 111 J = 2,7
      JEXC = J + NUMB - 7
      XIF(J) = XIF(JEXC)
111 DEUM(J) = DEUM(JEXC)
      NUMB = 7
112 WRITE (IOUT,COUCHE)
      DO 200 J = 1,NUMB
200 DDEUM(J) = DBLE(DEUM(J))
      SOL(1) = DDEUM(1)
      IF (NUMB .LT. 2) GOTO 202
      DO 102 I = 1,NUMB
      COA(I,2) = DBLE(XIF(I))

```

C. Denis & A. Ibrahim : Programme M Ø D P Ø L

```

      IF (NUMB .LT. 3) GOTO 102
      DO 102 J = 3, NUMB
      COA(I,J) = DELE(XIF(I))*COA(I,J-1)
102  CONTINUE
      IF (NUMB .GT. 2) GOTO 201
      SOL(2) = (DDEUM(2)-DDEUM(1))/(DELE(XIF(2))-DELE(XIF(1)))
      SOL(1) = -SOL(2)*DELE(XIF(1))+DDEUM(1)
      GOTO 202
201  CALL ELIMIN (COA, NUMB, DDEUM, SOL, 1.D-7, 10, 11, ACOA, XRA, ID, JELIM)
      IF (JELIM .EQ. 2) STOP 1111
202  K = K+1
      GOTO (104, 106, 108), K
104  MRHO(JJ) = NUMB
      DO 105 I = 1, NUMB
105  CRHO(I, JJ) = SOL(I)
      GOTO 101
106  MVF(JJ) = NUMB
      DO 107 I = 1, NUMB
107  CVP(I, JJ) = SOL(I)*1.D5
      GOTO 101
108  MVS(JJ) = NUMB
      DO 109 I = 1, NUMB
109  CVS(I, JJ) = SOL(I)*1.D5
110  CONTINUE
      GOTO 3001

C
C.5  INITMO=5, ENTRER NLTB SELON LE FORMAT 5300=(I10) ET LA DISTANCE
C      AU CENTRE XR(J) EN KM, LA DENSITE DENSIT(J) EN G/CC,
C      LA VITESSE DES ONDES P, VITP(J), EN KM/S DE MEME QUE
C      LA VITESSE DES ONDES S, VITS(J), POUR CHAQUE VALEUR
C      ENTIERE J COMPRISE ENTRE 1 ET NLTB, SELON LE FORMAT
C      5301=(4E20). TOUS LES AUTRES PARAMETRES TELS QUE NBC,
C      NREG, NC(IR), NO(IR),... SONT DEDUITS AUTOMATIQUEMENT
C
550  READ (IN, 5300) NLTB
      READ (IN, 5301) ((XR(J), DENSIT(J), VITP(J), VITS(J)), J=1, NLTB)
C
      I = 0
      IC = 0
      K = 1
C
      DO 553 J = 2, NLTB
      IF (XR(J)-XR(J-1)) 551, 552, 551
C
551  IC = IC+1
      I = I+1
      ICINF(IC) = J-1
      ICSUP(IC) = J
      ICIND(IC) = 3
      MRHO(IC) = 1
      MVP(IC) = 1
      MVS(IC) = 1
      IF ((DENSIT(J)-DENSIT(J-1)) .NE. 0.) MRHO(IC) = 2
      IF ((VITP(J)-VITP(J-1)) .NE. 0.) MVP(IC) = 2
      IF ((VITS(J)-VITS(J-1)) .NE. 0.) MVS(IC) = 2
      GOTO 553
C

```



```

552 IF ((VITS(J).NE.0.) .AND. (VITS(J-1).NE.0.) .OR.
1      (VITS(J).EQ.0.) .AND. (VITS(J-1).EQ.0.)) GOTO 553
C
NC(K) = I
I = 0
NO(K) = 4
IF (VITS(J-1) .NE. 0.) NO(K) = 6
K = K+1
553 CONTINUE
C
NBC = IC
NREG = K
NC(K) = I
NO(K) = 4
IF(VITS(NLTE) .NE. 0.) NO(K) = 6
C
GOTO 531
C
C.6 INITMO>5, APPELER 'MODEL1'
C
600 CALL MODEL1 (INITMO)
C
C CALCUL DES COEFFICIENTS DE MASSE GMR(K), K=1,2,...,NBC
C CALCUL DES COEFFICIENTS D'INERTIE GIR(K), K=1,2,...,NBC
C
3001 DO 5 IC = 1,NBC
K = MRHO(IC)+1
IF (K .GT. NDMAX) GOTO 5
DO 4 J = K,NDMAX
4 CRHO(J,IC) = 0.D0
5 CONTINUE
GMR(1) = 0.D0
GIR(1) = 0.D0
IF (NBC .LT. 2) GOTO 10
DO 1002 K = 2,NBC
KM1 = K-1
GMR(K) = GMR(KM1)
GIR(K) = GIR(KM1)
I = MAX0(MRHO(KM1),MRHO(K))
DO 9 J = 1,I
JJ = J+2
J4 = J+4
GIR(K) = GIR(K) + (CRHO(J,KM1)-CRHO(J,K))*(XC(K)**J4)/DFLOAT(J4)
9 GMR(K) = GMR(K) + (CRHO(J,KM1)-CRHO(J,K))*(XC(K)**JJ)/DFLOAT(JJ)
1002 CONTINUE
C
C EVALUATION DE LA DENSITE MOYENNE RHOM
C
10 AUX = GMR(NBC)
M = MRHO(NBC)
DO 1003 J = 1,M
1003 AUX = AUX + CRHO(J,NBC)/DFLOAT(J+2)
C
C AUX REPRESENTE LA MASSE TOTALE EN UNITES 4*PI*RAYON**3

```

C

```

RHOM = AUX*3.D0
FIGRHO = PI*BIGG*RHOM
AMASS = 1.333333333333333D0 * PI * RHOM * RAYON ** 3
ENROND = BIGG * AMASS / RAYON
ENNE = 0.75D0 * ENROND
EN = ENNE / RAYON
AMASR2 = AMASS * RAYON * RAYON
ETAP0 = - 1.361111111111111D0 * CRHO(2,1)/CRHO(1,1)
GSR2 = BIGG/RAYON/RAYON
QFIGR = 4.D0*PI*BIGG*RAYON
QFIGR2 = QFIGR*RAYON
QTPIGR = QFIGR/3.D0
QPIR3 = 4.D0*PI*RAYON**3
QTPIR3 = QPIR3/3.D0
HPS3R5 = RAYON**5 * 8.D0*PI/3.D0
QTPIR5 = HPS3R5/2.D0

```

C
C
C
C

CALCUL DES COEFFICIENTS DE PRESSION RKJ(K,J), PK(1,K), PK(2,K)

```

DO 400 IC = 1,NBC
JG = MRHO(IC)*2-1
DO 400 J = 1,JG
RKJ(IC,J) = 0.D0
DO 400 M = 1,J
IF (J-M+1 .LE. MRHO(IC)) AUX1 = CRHO(J-M+1,IC)
IF (J-M+1 .GT. MRHO(IC)) AUX1 = 0.D0
IF (M .LE. MRHO(IC)) AUX2 = CRHO(M,IC)
IF (M .GT. MRHO(IC)) AUX2 = 0.D0
400 RKJ(IC,J) = RKJ(IC,J) + AUX1*AUX2/DFLOAT(M+2)

```

C
C

```

DO 404 IC = 1,NBC
JG = MRHO(IC)*2-1
DO 404 I = 1,2
IF (I .LT. 2) AX = XC(IC)
IF (I .GT. 1) AX = XC(IC+1)
IF (AX) 401, 401, 402

```

C

```

401 PK(I,IC) = 0.D0
GOTO 404

```

C

```

402 PK(I,IC) = -CRHO(1,IC)/AX
IF (MRHO(IC) .GT. 1) PK(I,IC) = PK(I,IC) + DLOG(AX)*CRHO(2,IC)
IF (MRHO(IC) .GT. 2) PK(I,IC) = PK(I,IC) + CRHO(3,IC)*AX
PK(I,IC) = PK(I,IC)*GMR(IC)
DO 403 J = 1,JG
IF (J+3 .LE. MRHO(IC)) AUX1 = CRHO(J+3,IC)
IF (J+3 .GT. MRHO(IC)) AUX1 = 0.D0
403 PK(I,IC) = PK(I,IC)+(GMR(IC)*AUX1+RKJ(IC,J))*AX**(J+1)/DFLOAT(J+1)
404 CONTINUE

```

C

C
C
C

IMPRESSION DE DONNEES CARACTERISANT LE MODELE

```

IF (IPMOD .LT. 1) GOTO 560
WRITE (IOUT,6000)
WRITE (IOUT,6001) LINE
WRITE (IOUT,6003) DT
WRITE (IOUT,6001) LINE
WRITE (IOUT,6006)
WRITE (IOUT,6011) F(1),INITMO,F(2),IFU,F(3),IFMOD,F(4),JEP
WRITE (IOUT,6011) F(5),JX,F(6),NLTE,F(7),NREG,F(8),NEC
WRITE (IOUT,6011) F(9),BIGG,F(10),RAYON,F(11),RHOM,F(12),AMASS
WRITE (IOUT,6011) F(13),AMASR2,F(14),FSURF,F(15),PC,F(16),XM
WRITE (IOUT,6011) F(17),FIGRHO,F(18),ENROND,F(19),ENNE,F(20),EN
WRITE (IOUT,6011) F(21),ROTFER,F(22),FSURF
WRITE (IOUT,6006)
WRITE (IOUT,6018) XCD
K = NEC+1
WRITE (IOUT,6019) (XC(J), J=1,K)
WRITE (IOUT,6006)
WRITE (IOUT,6006)
KOUNTL = 28 + K/5
IF (KOUNTL .LT. 55) GOTO 455
KOUNTL = 0
WRITE (IOUT,6007)
455 DO 555 IC = 1,NEC
WRITE (IOUT,6006)
I = MRHO(IC)
J = MVP(IC)
K = MVS(IC)
WRITE (IOUT,6012) IC, I, J, K
WRITE (IOUT,6013) (CRHO(IJ,IC), IJ=1,I)
WRITE (IOUT,6014) (CVP (IJ,IC), IJ=1,J)
WRITE (IOUT,6015) (CVS (IJ,IC), IJ=1,K)
WRITE (IOUT,6016) GMR(IC), GIR(IC), NP(IC), XC(IC), DRKM(IC)
KOUNTL = KOUNTL + 8
IF (KOUNTL .LT. 55) GOTO 555
KOUNTL = 0
WRITE (IOUT,6007)
555 CONTINUE
WRITE (IOUT,6006)
K = 0
DO 556 IR = 1,NREG
J = K+1
K = K + NC(IR)
WRITE (IOUT,6017) IR, J, K, NC(IR), NO(IR)
KOUNTL = KOUNTL + 1
IF (KOUNTL .LT. 62) GOTO 556
KOUNTL = 0
WRITE (IOUT,6007)
556 CONTINUE
WRITE (IOUT,6006)
WRITE (IOUT,6001) LINE

```

C

C STOCKAGE EVENTUEL SUR CARTES PERFOREES DES COEFFICIENTS CRHO,CVF,CVS

C

```

560 IF (IPU .LT. 1) RETURN
WRITE (IPUNCH,5000) DI
WRITE (IPUNCH,7000) BIGG, RAYON, FC, XM, PSURF, IFMOD
WRITE (IPUNCH,5101) NREG, NEC, (NC(J), J=1,NREG),
1      ((MRHO(IC),MVP(IC),MVS(IC)), IC=1,NEC)
WRITE (IPUNCH,5101) (NO(J), J=1,NREG), (NF(J), J=1,NEC)
DO 1004 IC = 1,NEC
I = MRHO(IC)
J = MVP(IC)
K = MVS(IC)
WRITE (IPUNCH,5102) (CRHO(IJ,IC), IJ=1,I), (CVF(IJ,IC), IJ=1,J),
1      (CVS(IJ,IC), IJ=1,K)
1004 CONTINUE
K = NEC+1
WRITE (IPUNCH,5103) (XC(I), I=1,K)
RETURN

```

C
C
C
C
C

CALCUL DE LA DENSITE RHO AU POINT X SITUE DANS LA COUCHE NO. IC

C

ENTRY RHOF(X,IC,RHO)

```

RHO = CRHO(1,IC)
M = MRHO(IC)
IF (M .LT. 2) RETURN
DO 2001 J = 2,M
2001 RHO = RHO + CRHO(J,IC)*X**(J-1)
RETURN

```

C
C

570 IF (X) 572, 571, 572

C

```

571 G = 0.D0
RETURN

```

C

```

572 G = GMR(IC)
M = MRHO(IC)
DO 2002 J = 1,M
JJ = J+2
2002 G = X**JJ*CRHO(J,IC)/DFLOAT(JJ) + G
G = G*AU
RETURN

```

C
C
C
C
C
C

CALCUL DE L'ACCELERATION GRAVIFIQUE G AU POINT X
SITUE DANS LA COUCHE NO. IC

C

ENTRY GF(X,IC,G)

C

```

IF (X .NE. 0.D0) AU = QPIGR/X/X
GOTO 570

```

C

$$\text{MASSE} = G * X * X / GSR^2$$

```

AU = QFIR3
GOTO 570

```

DENMOY = QTF:IGR * G / X

```

IF (X) 574, 573, 574
573 G = RHOC
RETURN
574 AU = 3.D0/X/X/X
GOTO 570

```

```

CP = CVP(1,IC)
M = MVP(IC)
IF (M.LT. 2) RETURN
DO 2003 J = 2,M
CP = CP + CVP(J,IC)*X**X(J-1)
RETURN

```

```

CS = CVS(1,IC)
M = MVS(IC)
IF (M .LT. 2) RETURN
DO 2004 J = 2,M
2004 CS = CS + CVS(J,IC)*X*(J-1)
RETURN

```

```

C
C CALCUL DE LA PRESSION P AU POINT X SITUE DANS LA COUCHE IC
C
C ENTRY PRESS(X,IC,P)
C
C JG = MRHO(IC)*2-1
C
C IF (X) 580, 580, 581
C
580 P = 0.D0
GOTO 583
C
581 P = - CRHO(1,IC)/X
IF (MRHO(IC) .GT. 1) P = P + DLOG(X)*CRHO(2,IC)
IF (MRHO(IC) .GT. 2) P = P + CRHO(3,IC)*X
P = P*GMR(IC)
DO 582 J = 1,JG
IF (J+3 .LE. MRHO(IC)) AUX1 = CRHO(J+3,IC)
IF (J+3 .GT. MRHO(IC)) AUX1 = 0.D0
582 P = P+(GMR(IC)*AUX1+RKJ(IC,J))*X*(J+1)/DFLOAT(J+1)
C
583 P = (PK(2,IC)-P)*QFIGR2 + PSURF
C
C IF (IC .EQ. NBC) RETURN
JG = IC+1
DO 584 J = JG,NBC
584 P = P + (PK(2,J)-PK(1,J))*QFIGR2
RETURN
C
C
C CALCUL DU MOMENT D'INERTIE AI DE LA SPHERE DE RAYON NORMALISE X
C
C ENTRY MOMIN(X,IC,AI)
C
C AI = GIR(IC)
M = MRHO(IC)
DO 2500 J = 1,M
JJ = J + 4
2500 AI = X**JJ * CRHO(J,IC)/DFLOAT(JJ) + AI
AI = AI * HPS3R5
RETURN
C
C
C CALCUL DU GRADIENT DE DENSITE, EN SUPPOSANT QUE LES COEFFICIENTS
C CRHO SOIENT PHYSIQUEMENT SIGNIFICATIFS
C
C ENTRY GRADRO(X,IC,DERRHO)
C
C M = MRHO(IC) - 1
IF (M .LT. 1) DERRHO = 0.D0

```

CC

SUBROUTINE MODEL1 (INT,TMO)

END

C

C

SUBROUTINE FLATG (X, TC, F, IND)

CCCCC

IMPLICIT REAL*8 (A-H,O-Z)

EXTERNAL FADAM

```

DIMENSION FOK(201),XC(201),NC(200),NO(200),NF(200),MRHO(200)
DIMENSION DRKM(200)

```

```

C ***
COMMON /CONST1/ PI,QPIZ,PTGRHO,EN,ENNE,RHOC,PC,RHOS,PSURF
COMMON /CONST2/ BIGG,RAYON,RHOM,CSRZ,QPIGR,QPIGR2,QTPIGR
COMMON /ELLIP/ FSURF,ROTPER,FLAT,MRHO,JEP
COMMON /FRK/ FOK, F01, XU, FY
COMMON /JWX/ XC, XM, DRKM, JX, NC, NO, NP, NLTB, NREG, NBC

C
GOTO (1000,2000,3000), IND

C
1000 FOK(1) = 0.D0
DO 2 K = 1,NBC
Y = FOK(K)
N = NP(K)
H = (XC(K+1)-XC(K))/DFLOAT(N)
DO 1 J = 1,N
XU = DFLOAT(J)*H + XC(K)
XL = XU - H
CALL DGR4 (XL,XU,K,RADAU,FY)
1 Y = Y + FY
2 FOK(K+1) = Y
F01 = Y
DO 3 K = 1,NBC
3 FOK(K) = FOK(K) - F01
FOK(NBC+1) = 0.D0

C ***
IF (JEP.NE.1) GOTO 4
CALL RADAU (1.D0,NBC,ES,ETAPS)
CALL GF (1.D0,NBC,GSURF)
FSURF = 10.D0*(PI/ROTPER)**2 * RAYON / (ES+2.D0)/GSURF

C ***
4 RETURN

C
2000 XL = XC(IC)
XU = X
CALL DGR4 (XL,XU,IC,RADAU,Y)
Y = FOK(IC) + Y
FY = Y
GOTO 4000

C
3000 XL = XU
XU = X
Y = FY
CALL DGR4 (XL,XU,IC,RADAU,FY)
Y = Y + FY
FY = Y

C
4000 F = DEXP (Y) * FSURF

C
RETURN
END

```


SUBROUTINE RADAU (X,IC,ETA,ETAP)

CE SOUS-PROGRAMME CALCULE LA VALEUR ETA DU PARAMETRE DE RADAU
ET LA VALEUR ETA/X AU POINT X DANS LA COUCHE NO. IC

IMPLICIT REAL*8 (A-H,O-Z)

COMMON /REDMOM/ REDIN, AI, D, ETAP0
COMMON /QTP/ QTPIR3, QTPIR5

IF (X .GE. 1.D-5) GOTO 1
REDIN = 0.4D0
ETA = 0.D0
ETAP = ETAP0
RETURN

1 CALL MOMIN (X,IC,AI)
CALL DENMOY (X,IC,D)
REDIN = AI/(X**5 * QTPIR5*D)
ETA = (2.5D0-REDIN*3.75D0)**2 - 1.D0
ETAP = ETA/X
RETURN
END

SUBROUTINE AJUPOL (C,XR,V,N,IC,M)

AJUSTEMENT POLYNOMIAL PAR MOINDRES CARRES

REFERENCE: R.H. FENNINGTON "INTRODUCTORY COMPUTER METHODS AND
NUMERICAL ANALYSIS", MACMILLAN (1967), PP. 363-374.

IMPLICIT REAL*8 (A-H,O-Z)
DIMENSION C(7,1),XR(1),V(1),M(1)
DIMENSION F(50,7),A(7,7),AA(7,8),B(7),X(7),ID(7)

N DESIGNER ICI LE NOMBRE D'EQUATIONS INDEPENDANTES, I.E. LE NOMBRE DE
COUPLES DE VALEURS (XR,V) QUE L'ON CONSIDERE DANS LA COUCHE DONNEE
MM = M DESIGNER LE NOMBRE DE COEFFICIENTS POLYNOMIAUX A DETERMINER,
C'EST-A-DIRE LE DEGRE DU POLYNOME AJUSTANT PLUS UN

.....	N .GT. M	SOLUTION PAR MOINDRES CARRES
.....	N .EQ. M	SOLUTION UNIQUE
.....	N .LT. M	ON REDUIT M A LA VALEUR N, SINON SOLUTION IMPOSSIBLE

```

C
  1 IF (M(IC) .GT. N) M(IC) = N
    MM = M(IC)
    IF (MM .LT. 1) MM = 1
C
C M EST EGAL A N, DONC SOLUTION UNIQUE
C
  IF (MM .GT. 1) GOTO 1000
C
  C(1,IC) = V(1)
  RETURN
C
1000 DO 101 K = 1,MM
      DO 101 J = 1,N
101  F(J,K) = XR(J)**(K-1)
      IF (MM .LT. N) GOTO 2000
C
      DO 102 K = 1,MM
      DO 102 J = 1,MM
102  A(J,K) = F(J,K)
C SOLUTION DU SYSTEME LINEAIRE (A).X = V PAR LA METHODE D'ELIMINATION
  CALL ELIMIN (A,MM,V,X,1.D-7,7,8,AA,B,ID,JELGS)
  GOTO (103,105), JELGS
103 DO 104 K = 1,MM
104  C(K,IC) = X(K)
  RETURN
C SOLUTION DU SYSTEME LINEAIRE (A).X = V
C PAR LA METHODE DE GAUSS-SEIDEL
105 CALL GAUSID (A,MM,V,X,1.D-7,7,8,AA,JELGS,25)
  GOTO (103,106), JELGS
106 M(IC) = M(IC)-1
  MM = M(IC)
C
C M EST INFERIEUR A N, DONC SOLUTION PAR MOINDRES CARRES
C
2000 DO 202 I = 1,MM
      DO 202 K = 1,I
      A(K,I) = 0.D0
      DO 201 J = 1,N
201  A(K,I) = A(K,I)+F(J,I)*F(J,K)
202  A(I,K) = A(K,I)
      DO 203 K = 1,MM
      B(K) = 0.D0
      DO 203 J = 1,N
203  B(K) = B(K)+V(J)*F(J,K)
C SOLUTION DU SYSTEME LINEAIRE (A).X = B
C PAR LA METHODE DE GAUSS-SEIDEL
  CALL GAUSID (A,MM,B,X,1.D-7,7,8,AA,JELGS,25)
  GOTO (103,204), JELGS
204 M(IC) = M(IC)-1
  GOTO 1
  END

```

SUBROUTINE DGQ4 (XL,XU,IC,RADAU,Y)

4-POINT GAUSS-LEGENDRE QUADRATURE ALGORITHM

IMPLICIT REAL*8 (A-H,O-Z)

A = (XU+XL)*0.5D0

B = XU-XL

C = 0.43056815579702629D0*B

X = A+C

CALL RADAU (X,IC,ETA,ETAP)

X = A-C

CALL RADAU (X,IC,ETA,ETAQ)

Y = (ETAP+ETAQ)*0.17392742256872693D0

C = 0.16999052179242813D0*B

X = A+C

CALL RADAU (X,IC,ETA,ETAP)

X = A-C

CALL RADAU (X,IC,ETA,ETAQ)

Y = ((ETAP+ETAQ)*0.32607257743127307D0 + Y)*B

RETURN

END

SUBROUTINE ELTMIN (AA,N,BB,X,EPS,ND,NDFU,A,Y,ID,JELIM)

CE SOUS-PROGRAMME CALCULE LA SOLUTION X D'UN SYSTEME LINEAIRE
D'ORDRE N

LES COEFFICIENTS SONT REPRESENTES PAR LA MATRICE AA

ET LES CONSTANTES DU MEMBRE DE DROITE PAR LE VECTEUR BB

LA METHODE EMPLOYEE EST CELLE DES ELIMINATIONS SUCCESSIVES

L'ARGUMENT EPS EST LIE AU NOMBRE DE CHIFFRES SIGNIFICATIFS

DONT ON ADMET LA PERTE PAR SOUSTRACTION DE DEUX NOMBRES VOISINS

EX.: SI L'ON ADMET LA PERTE JUSQU'A 4 CHIFFRES,

ON POSE EPS = 1.D-4

AUCUNE DONNEE N'EST DETRUITE

REF.: R.H. FENNINGTON 'INTRODUCTORY COMPUTER METHODS AND

NUMERICAL ANALYSIS', MACMILLAN (1965), PP. 290-295.

IMPLICIT REAL*8 (A-H,O-Z)

DIMENSION AA(ND,ND),A(ND,NDFU),BB(1),Y(1),X(1),ID(1)

1000 FORMAT ('OPAS DE SOLUTION UNIQUE')

IF(N.GT.1) GOTO 100

IF(AA(1,1)) 300,102,300

300 X(1) = BB(1)/AA(1,1)

JELIM = 1

RETURN

```

100 NN = N+1
    DO 200 I = 1,N
        A(I,NN) = BB(I)
    DO 200 J = 1,N
200 A(I,J) = AA(I,J)
    K = 1
    1 CONTINUE
        DO 21 I = 1,N
21 ID(I) = I
    2 CONTINUE
        KK = K+1
        IS = K
        IT = K
        B = DABS(A(K,K))
        DO 3 I = K,N
        DO 3 J = K,N
            IF(DABS(A(I,J))-B) 3,3,31
31 IS = I
        IT = J
        B = DABS(A(I,J))
    3 CONTINUE
        IF(IS-K) 4,4,41
41 DO 42 J = K,NN
        C = A(IS,J)
        A(IS,J) = A(K,J)
42 A(K,J) = C
    4 CONTINUE
        IF(IT-K) 5,5,51
51 IC = ID(K)
        ID(K) = ID(IT)
        ID(IT) = IC
        DO 52 I = 1,N
        C = A(I,IT)
        A(I,IT) = A(I,K)
52 A(I,K) = C
    5 CONTINUE
        IF(A(K,K)) 6,102,6
    6 CONTINUE
        DO 7 J = KK,NN
        A(K,J) = A(K,J)/A(K,K)
        DO 7 I = KK,N
        W = A(I,K)*A(K,J)
        A(I,J) = A(I,J)-W
            IF(DABS(A(I,J))-EPS*DABS(W)) 71,7,7
71 A(I,J) = 0.D0
    7 CONTINUE
        K = KK
        IF(K-N) 2,81,102
81 IF(A(N,N)) 8,102,8
    8 CONTINUE
        Y(N) = A(N,NN)/A(N,N)
        NM = N-1
        DO 9 I = 1,NM
        K = N-I
        KK = K+1
        Y(K) = A(K,NN)
        DO 9 J = KK,N
        Y(K) = Y(K)-A(K,J)*Y(J)
    9 CONTINUE

```

```

      DO 10 I = 1,N
      DO 10 J = 1,N
      IF(ID(J)-I) 10,101,10
101  X(I) = Y(J)
      10 CONTINUE
      JELIM = 1
      RETURN
102  WRITE(6,1000)
      JELIM = 2
      RETURN
      END

```

```

C      SUBROUTINE GAUSID (A,N,B,X,ERR,ND,NDFU,C,JGAUS,NIT)
C      METHODE DE GAUSS-SEIDEL POUR LA DETERMINATION DE LA SOLUTION X
C      D'UN SYSTEME LINEAIRE A X = B DE DIMENSION N
C      REFERENCE - R.A. FENNINGTON 'INTRODUCTORY COMPUTER METHODS AND
C                  NUMERICAL ANALYSIS' (1965), PP. 295-303.
      IMPLICIT REAL*8 (A-H,O-Z)
      DIMENSION A(ND,ND), C(ND,NDFU), B(1), X(1)
6000  FORMAT('0GAUSID NE CONVERGE PAS APRES',I4,' ITERATIONS'////)
      K = 0
      NN = N+1
      DO 11 I = 1,N
      IF (A(I,I)) 12,6,12
12  X(I) = 1.D0
      C(I,NN) = B(I)/A(I,I)
      DO 11 J = 1,N
11  C(I,J) = A(I,J)/A(I,I)
      1 CONTINUE
      E = 0.D0
      DO 3 I = 1,N
      P = C(I,NN)
      DO 2 J = 1,N
      P = P-C(I,J)*X(J)
2  CONTINUE
      X(I) = X(I)+P
      E = E+DABS(P)
3  CONTINUE
      IF (E-ERR) 4,4,5
4  JGAUS = 1
      RETURN
5  K = K+1
      IF(NIT-K) 6,1,1
6  WRITE (6,6000) K
      JGAUS = 2
      RETURN
      END

```

Exemples-témoinsFichiers d'entréeFichier 1 :
.....

PEM-O-HAW EATON-HILL OCEANIC CRUST, LVZ-VS= 4.3345 KM/S

Fichier 2 :
.....

```

&MODEL BIGG=6.672D-8, RAYON=6.371D8, FC=3.6324D12, PSURF=0.D0, XM=0.01D0,
XC= 0.D0, 0.1910375137D0, 0.5471197614D0, 0.8948359755D0,
0.9340762832D0, 0.9654685293D0, 0.9905823262D0, 0.9981164652D0,
0.9989012714D0, 0.9996860775D0, 1.D0, DRKM= 3*2.5D2, 2*1.D2, 5.D1, 4*1.D1,
NF= 3,4,4,2,2,3,2,1,1,1, NC= 1,1,8, MRHO= 3,4,3,2,3*2,3*1,
MVF= 3,3,4,2,2,5*1, MVS= 3,0,4,2,2,5*1, JX=0,
INITMO=2, IPU=0, IPMOD=1, NREG=3, NEC=10, NO=6,4,6, JEP=1, &END

```

Fichier 3,2 :
.....

```

&COEF CRHO=
13.01219, 0., -8.45292, 4*0.,
12.58416, -1.69929, -1.94128, -7.11215, 3*0.,
6.81430, -1.66273, -1.18531, 4*0.,
11.11978, -7.87054, 5*0.,
7.15855, -3.85999, 5*0.,
7.15855, -3.85999, 5*0.,
7.15855, -3.85999, 5*0.,
3.000, 6*0.,
2.800, 6*0.,
2.600, 6*0.,
CVP=
11.24094E5, 0., -4.09689E5, 4*0.,
10.03904E5, 3.75665E5, -13.67046E5, 4*0.,
16.69287E5, -6.38826E5, 4.68676E5, -5.30512E5, 3*0.,
21.05692E5, -12.31433E5, 5*0.,
30.00026E5, -22.53683E5, 5*0.,
7.87320E5, 6*0.,
7.90000E5, 6*0.,
7.00000E5, 6*0.,
5.00000E5, 6*0.,
3.90000E5, 6*0.,
CVS=
3.56454E5, 0., -3.45241E5, 4*0.,
7*0.,
9.20501E5, -6.85512E5, 9.39892E5, -6.25575E5, 3*0.,
15.04371E5, -10.69726E5, 5*0.,
15.87214E5, -11.86483E5, 5*0.,
4.33450E5, 6*0.,
4.55000E5, 6*0.,
4.00000E5, 6*0.,
2.50000E5, 6*0.,
2.00000E5, 6*0., &END

```

```

si IPMOD = 1
.....

```

PEM-O-HAW EATON-HILL OCEANIC CRUST, LVZ-V5= 4.3345 KM/S

INITMO	=	2	IPU	=	0	IPMOD	=	1	JEP	=	1
JX	=	0	NLTS	=	1100546049	NREG	=	3	NEC	=	10
EIGG	=	.667200D-07	RAYON	=	.637100D+09	RHOM	=		AMASS	=	.597982D+28
AMASR2	=	.24719D+46	PSURF	=	.0	FC	=	5.53047	XM	=	.10000D-01
PIGRHO	=	.115713D-05	ENKOND	=	.626233D+12	ENNE	=	.363240D+13	EN	=	.10000D-01
KOTPER	=	86164.1	FSURF	=	.335282D-02		=	.469675D+12		=	737.208

XC	0	19103751	54711976	89483598	93407438
		99058233	99811647	99800127	99968608
		1.0000000			

[illegible]

COUCHE NO.	2	MRHO = 4	MUP = 3	MUS = 0
CRHQ =	1.258416D+01	-1.941260D+00		
CVP =	1.003904D+06	-1.367046D+06		
CVS =	0.0			
GIR =	1.28681160D-03	2.84875441D-05	1.91037514D-01	2.50000000D+02

COUCHE NO. 3	CRHO = 4.814300D+00	-1.662730D+00	-1.185310D+00	MRHO = 3	MVP = 4	MVS = 4
	CVP = 1.662870D+06	-6.388260D+05	4.886760D+05			
	CVS = 9.205010D+05	-6.855120D+05	9.959200D+05			
	CMR = 2.76247698D-01	GIR = 4.77150723D-02	NP = 4	XC =	5.47119761D-01	DRKM = 2.50000000D+02

COUCHE	NO.	4	MRHO = 2	MUP = 2	MUS = 2
CRHO	=	1.11978D+01			
CVP	=	2.10582D+06			
CVR	=	1.504371D+06			
CAS	=	1.06976192D-01			
GIR	=	7.06239940D-03	NP = 2	XC =	0.94835975D-01
					DRKM = 1.00000000D+02

(suite du fichier de sortie correspondant à

IPMØD = 1)

```

.....
COUCHE NO. 5.
CRHO = 7.158550D+00
CVP = 3.000026D+06
CVS = 1.587214D+06
GMR = 4.19822699D-01
-3.859990D+00
-2.253683D+06
-1.186483D+06
GIR = 1.26440967D-01
NP = 2 XC = 9.34076283D-01 DRKM = 1.00000000D+02
MRHO = 2 MVP = 2 MVS = 2
COUCHE NO. 6
CRHO = 7.158550D+00
CVP = 7.873200D+05
CVS = 4.334500D+05
GMR = 4.19822699D-01
-3.859990D+00
GIR = 1.26440967D-01
NP = 3 XC = 9.65468529D-01 DRKM = 5.00000000D+01
MRHO = 2 MVP = 1 MVS = 1
COUCHE NO. 7
CRHO = 7.158550D+00
CVP = 7.900000D+05
CVS = 4.550000D+05
GMR = 4.19822699D-01
-3.859990D+00
GIR = 1.26440967D-01
NP = 2 XC = 9.90582326D-01 DRKM = 1.00000000D+01
MRHO = 1 MVP = 1 MVS = 1
COUCHE NO. 8
CRHO = 3.000000D+00
CVP = 7.000000D+05
CVS = 4.000000D+05
GMR = 8.40440413D-01
GIR = 3.14252254D-01
NP = 1 XC = 9.98116465D-01 DRKM = 1.00000000D+01
MRHO = 1 MVP = 1 MVS = 1
COUCHE NO. 9
CRHO = 2.800000D+00
CVP = 5.000000D+05
CVS = 2.500000D+05
GMR = 9.06887576D-01
GIR = 3.54032991D-01
NP = 1 XC = 9.98901271D-01 DRKM = 1.00000000D+01
MRHO = 1 MVP = 1 MVS = 1
COUCHE NO. 10
CRHO = 2.600000D+00
CVP = 3.900000D+05
CVS = 2.000000D+05
GMR = 9.73491477D-01
GIR = 3.93970246D-01
NP = 1 XC = 9.99686077D-01 DRKM = 1.00000000D+01
MRHO = 1 MVP = 1 MVS = 1
REGION NO. 1 COMPRENANT LES COUCHES NOS. 1 A 1 (NC= 1 ) NO = 6 (COUCHE FLUIDE SI NO=4 )
REGION NO. 2 COMPRENANT LES COUCHES NOS. 2 A 2 (NC= 1 ) NO = 4 (COUCHE FLUIDE SI NO=4 )
REGION NO. 3 COMPRENANT LES COUCHES NOS. 3 A 10 (NC= 8 ) NO = 6 (COUCHE FLUIDE SI NO=4 )
*****

```


Fichier de sortie correspondant à JTAB = 2 :

PEN-O-HAN EATON-HILL OCEANIC CRUST, LVZ-US= 4.3345 KM/S

NL	NORMED RADIUS	RADIUS (KM)	RHO (G/CC)	VP (KM/S)	VS (KM/S)	KAPPA (KB)	MU (KB)	LAMBDA (KB)	P (KB)	G (GAL)	MASSE (G)	DHOY (G/CC)	INRT.MOM. BY MRSQ	ETA	F #1000	DEPTH (KM)
1	0.0	0	13.012	11.24	3.56	14238	1453	13135	3635	0	0.0	13.012	0.400000	0.0	2.41853	6371
1	0.0637	406	12.978	11.22	3.55	14169	1636	13078	3596	147	3.63390+24	12.992	0.399879	0.0009	2.41962	5965
1	0.1274	811	12.875	11.17	3.51	13964	1585	12907	3480	293	2.89330+25	12.930	0.399515	0.0036	2.42292	5560
1	0.1910	1217	12.704	11.09	3.44	13625	1502	12624	3291	436	9.69710+25	12.827	0.398901	0.0083	2.42846	5154
2	0.1910	1217	12.139	10.26	0.0	12773	0	12773	3291	436	9.69710+25	12.827	0.398901	0.0083	2.42846	5154
2	0.2801	1784	11.800	10.02	0.0	11844	0	11844	2936	610	2.91080+26	12.234	0.394453	0.0420	2.45948	4587
2	0.3691	2351	11.335	9.561	0.0	10367	0	10367	2479	779	6.45510+26	11.853	0.393619	0.0469	2.48939	4020
2	0.4581	2919	10.715	8.89	0.0	8470	0	8470	1943	934	1.19280+27	11.454	0.391968	0.0611	2.51800	3452
2	0.5471	3486	9.909	8.00	0.0	6345	0	6345	1355	1070	1.94780+27	10.979	0.388701	0.0865	2.55062	2885
3	0.5471	3486	5.550	13.73	7.24	6582	2912	4641	1355	1070	1.94780+27	10.979	0.388701	0.0865	2.55062	2885
3	0.6340	4040	5.284	13.17	7.04	5676	2520	3929	1044	1015	2.48190+27	8.989	0.352590	0.3872	2.64827	2331
3	0.7210	4593	4.999	12.54	6.80	4770	2314	3227	758	996	3.14890+27	7.757	0.340337	0.4975	2.80654	1778
3	0.8079	5147	4.697	11.79	6.50	3885	1986	2561	491	995	3.94940+27	6.914	0.337589	0.5229	2.97570	1224
3	0.8948	5701	4.377	10.93	6.11	3045	1637	1954	240	1001	4.87850+27	6.286	0.338064	0.5185	3.113869	670
4	0.8948	5701	4.077	10.04	5.47	2480	1220	1667	240	1001	4.87850+27	6.286	0.338064	0.5185	3.113869	670
4	0.9145	5826	3.923	9.80	5.26	2316	1086	1592	190	1000	5.08720+27	6.142	0.337199	0.5265	3.17445	545
4	0.9341	5951	3.768	9.55	5.05	2158	962	1517	142	998	5.29660+27	6.000	0.336213	0.5356	3.21043	420
5	0.9341	5951	3.553	8.95	4.79	1759	815	1215	142	998	5.29660+27	6.000	0.336213	0.5356	3.21043	420
5	0.9498	6051	3.492	8.60	4.60	1594	740	1100	107	994	5.45600+27	5.879	0.334851	0.5483	3.23956	320
5	0.9655	6151	3.432	8.24	4.42	1438	670	992	73	991	5.61790+27	5.763	0.333617	0.5598	3.26912	220
6	0.9655	6151	3.432	7.87	4.33	1248	645	838	73	991	5.61790+27	5.763	0.333617	0.5598	3.26912	220
6	0.9738	6204	3.400	7.87	4.33	1256	639	830	55	989	5.70530+27	5.703	0.333006	0.5656	3.28504	167
6	0.9822	6258	3.367	7.87	4.33	1244	633	822	37	987	5.79330+27	5.644	0.332425	0.5710	3.30106	113
6	0.9906	6311	3.335	7.87	4.33	1232	627	814	19	985	5.88200+27	5.587	0.331870	0.5763	3.31717	60
7	0.9906	6311	3.335	7.90	4.55	1161	690	700	19	985	5.88200+27	5.587	0.331870	0.5763	3.31717	60
7	0.9943	6335	3.320	7.90	4.55	1156	687	697	11	985	5.92220+27	5.561	0.331628	0.5785	3.32445	36
7	0.9981	6359	3.306	7.90	4.55	1151	684	694	3	984	5.96240+27	5.536	0.331391	0.5808	3.33175	12
8	0.9981	6359	3.000	7.00	4.00	830	480	510	3	984	5.96240+27	5.536	0.331391	0.5808	3.33175	12
8	0.9989	6364	3.000	7.00	4.00	830	480	510	2	983	5.97000+27	5.530	0.331299	0.5816	3.33327	7
9	0.9989	6364	2.800	5.00	2.50	467	175	350	2	983	5.97000+27	5.530	0.331299	0.5816	3.33327	7
9	0.9997	6369	2.800	5.00	2.50	467	175	350	1	983	5.97720+27	5.523	0.331179	0.5828	3.33479	2
10	0.9997	6369	2.600	3.90	2.00	257	104	187	1	983	5.97720+27	5.523	0.331179	0.5828	3.33479	2
10	1.0000	6371	2.600	3.90	2.00	257	104	187	0	983	5.97980+27	5.520	0.331120	0.5833	3.33540	0

Fichier de sortie correspondant à JTAB = 3 :

+++++

PEM-O-HAW EATON-HILL OCEANIC CRUST, LVZ-VS= 4.3345 KM/S

+++++

R (KM)	RHO (G/CC)	VP (KM/S)	VS (KM/S)	P (KB)	G (GAL)	DMOY (C/CC)	Z	ETA	F *1000
0	13.012	11.24	3.56	3635	0	13.012	0.4000	0.0	2.43116
250	12.999	11.23	3.56	3620	91	13.004	0.4000	0.0003	2.43158
500	12.960	11.22	3.54	3576	181	12.981	0.3998	0.0014	2.43283
750	12.895	11.18	3.52	3502	271	12.942	0.3996	0.0031	2.43493
1000	12.804	11.14	3.48	3401	360	12.887	0.3993	0.0055	2.43788
1217	12.704	11.09	3.44	3291	436	12.827	0.3989	0.0083	2.44114
1217	12.139	10.26	0.0	3291	436	12.827	0.3989	0.0083	2.44114
1250	12.122	10.25	0.0	3273	446	12.774	0.3980	0.0151	2.44191
1500	11.984	10.17	0.0	3127	523	12.469	0.3950	0.0379	2.45498
1750	11.824	10.04	0.0	2960	600	12.259	0.3945	0.0418	2.47031
2000	11.639	9.87	0.0	2773	675	12.084	0.3943	0.0431	2.48436
2250	11.429	9.66	0.0	2568	750	11.920	0.3940	0.0454	2.49731
2500	11.189	9.41	0.0	2346	821	11.754	0.3935	0.0496	2.50979
2750	10.917	9.11	0.0	2109	890	11.579	0.3927	0.0558	2.52238
3000	10.611	8.78	0.0	1861	955	11.391	0.3916	0.0641	2.53551
3250	10.268	8.40	0.0	1603	1016	11.188	0.3902	0.0745	2.54957
3486	9.909	8.00	0.0	1355	1070	10.979	0.3887	0.0865	2.56394
3486	5.550	13.73	7.24	1355	1070	10.979	0.3887	0.0865	2.56394
3500	5.543	13.72	7.24	1347	1067	10.913	0.3873	0.0978	2.56490
3750	5.425	13.47	7.15	1203	1037	9.898	0.3670	0.2625	2.59772
4000	5.303	13.22	7.06	1065	1017	9.100	0.3541	0.3736	2.65215
4250	5.178	12.94	6.96	932	1005	8.458	0.3462	0.4446	2.71916
4500	5.049	12.65	6.85	805	997	7.930	0.3415	0.4870	2.79281
4750	4.916	12.34	6.73	681	994	7.489	0.3390	0.5101	2.86931
5000	4.779	12.00	6.59	560	994	7.112	0.3378	0.5206	2.94629
5250	4.639	11.64	6.44	443	995	6.785	0.3375	0.5233	3.02235
5500	4.496	11.26	6.27	329	998	6.496	0.3377	0.5215	3.09673
5701	4.377	10.93	6.11	240	1001	6.286	0.3381	0.5185	3.15508
5701	4.077	10.04	5.47	240	1001	6.286	0.3381	0.5185	3.15508
5700	4.078	10.04	5.47	240	1001	6.287	0.3381	0.5184	3.15479
5800	3.955	9.85	5.31	200	1000	6.171	0.3374	0.5247	3.18354
5900	3.831	9.65	5.14	161	999	6.057	0.3366	0.5317	3.21241
5951	3.768	9.55	5.05	142	998	6.000	0.3362	0.5356	3.22720
5951	3.553	8.95	4.79	142	998	6.000	0.3362	0.5356	3.22720
6000	3.523	8.78	4.70	125	996	5.940	0.3355	0.5420	3.24149
6100	3.463	8.42	4.51	90	992	5.822	0.3342	0.5541	3.27099
6151	3.432	8.24	4.42	73	991	5.763	0.3336	0.5598	3.28619
6151	3.432	7.87	4.33	73	991	5.763	0.3336	0.5598	3.28619
6200	3.402	7.87	4.33	56	989	5.708	0.3331	0.5651	3.30089
6250	3.372	7.87	4.33	39	987	5.653	0.3325	0.5703	3.31598
6300	3.342	7.87	4.33	23	986	5.598	0.3320	0.5752	3.33115
6311	3.335	7.87	4.33	19	985	5.587	0.3319	0.5763	3.33450
6311	3.335	7.90	4.55	19	985	5.587	0.3319	0.5763	3.33450
6320	3.329	7.90	4.55	16	985	5.577	0.3318	0.5771	3.33724
6330	3.323	7.90	4.55	13	985	5.566	0.3317	0.5781	3.34029
6340	3.317	7.90	4.55	10	984	5.556	0.3316	0.5790	3.34334
6350	3.311	7.90	4.55	6	984	5.545	0.3315	0.5799	3.34639
6359	3.306	7.90	4.55	3	984	5.536	0.3314	0.5808	3.34914
6359	3.000	7.00	4.00	3	984	5.536	0.3314	0.5808	3.34914

C. Denis & A. Ibrahim : Programme M Ø D P Ø L

(suite du fichier de sortie correspondant à JTAB = 3)

+++++
 PEM-O-HAW EATON-HILL OCEANIC CRUST, LVZ-US= 4.3345 KM/S
 +++++

R	RHO	VP	VS	P	G	DMOY	Z	ETA	F
(KM)	(G/CC)	(KM/S)	(KM/S)	(KB)	(GAL)	(C/CC)			*1000
6360	3.000	7.00	4.00	3	984	5.534	0.3314	0.5809	3.34945
6364	3.000	7.00	4.00	2	983	5.530	0.3313	0.5816	3.35067
6364	2.800	5.00	2.50	2	983	5.530	0.3313	0.5816	3.35067
6365	2.800	5.00	2.50	2	983	5.528	0.3313	0.5819	3.35098
6368	2.800	5.00	2.50	1	983	5.525	0.3312	0.5824	3.35175
6369	2.800	5.00	2.50	1	983	5.523	0.3312	0.5828	3.35221
6369	2.600	3.90	2.00	1	983	5.523	0.3312	0.5828	3.35221
6370	2.600	3.90	2.00	0	983	5.522	0.3311	0.5830	3.35251
6371	2.600	3.90	2.00	0	983	5.520	0.3311	0.5833	3.35282

++ FIN DU PROGRAMME ***

Remerciement

Nous tenons à remercier le Turkish Research Council (TÜBİTAK)
 pour l'aide apportée à l'un de nous (A.İ.).

.....

The coordinates of amphidromic points were determined in figure 7.

ABOUT THE CAUSES OF THE FORMATION OF TIDAL PHENOMENA IN THE EAST SEA.

The complicated tidal picture of the sea might be clarified by different ways.

In my works (Nguyen ngoc Thuy, 1969, 1976) the analysis of the potential and kinetic energies of the main tidal waves, the study of resonance phenomenon, the influence of the Coriolis effect and the depth were made.

From above the following conclusions were drawn :

1. The particular local conditions of the sea were the predominant factors of the formation of the specific tidal picture in this sea.

The resonance phenomenon was the principal cause of the intense increase of tidal amplitude in many areas, specially for the diurnal tide in the whole sea and in the two large gulfs (fig. 6).

This was the same for the semidiurnal wave in Taiwan strait and in Pulo Lakei Bay (Kalimantan).

In fig. 9, the incoming tidal energies of the main waves were calculated for this sea (part A) and for Bacbo gulf (part B). Here, it might be seen that the diurnal wave started like the smaller component at the Bashi Channel (semidiurnal/diurnal = 1,7) and became the predominant component at the entrance of the Bacbo gulf (diurnal/semidiurnal = 10,7). In this gulf, the potential energy of diurnal waves was considerably greater with the ratio : diurnal/semidiurnal = 22,1 !

In general, the direct influence of the depth and the Coriolis effect in this sea were not great. This should be noted specially near the continental shelf in the regions with large tides and strong tidal streams (Taiwan strait, Bacbo gulf).

Inspite of the large area of this sea, the co-oscillation tides caused directly by astronomical tidal forces were estimated to be insignificant. According to Phan Phung (1974), the ratio between these amplitudes and the real tidal amplitudes in the Bacbo gulf and in the gulf of Thailand were about 1/20 and 1/30 respectively.

One of the most important remarks on the complex tidal phenomena in this sea is the appearance of the specific forms of tides in some regions.

For example, we could mention the tides at Hondau (SR Vietnam) and the neighbouring ports with well-known pure diurnal tide, one of the rare phenomenon

in the World Ocean where $H_{O_1} + H_{K_1} / H_{M_2} \geq 25$ (while as a rule 4 was sufficient for the diurnal type). In this area the resonance of the diurnal waves causing the increase of its amplitudes was associated with the nodal of the semidiurnal waves.

The other complicated pictures of the tides could be found in the Taiwan strait, in the gulf of Thailand and in the southern part of the East sea.

CALCULATION OF TIDAL CHARACTERISTICS of the sea with significant diurnal component

The concrete conditions of the East sea needed many perfections in the application of calculation methods of tidal characteristics that were common as yet.

1. METHODS OF TIDAL PREDICTIONS.

The schemes predicting semidiurnal tides, usually efficient in the World Ocean, could not be successfully applied to the conditions of the East sea with large diurnal components. For good results, we might examine in detail the diurnal components and their harmonic shallow-water components with unpaired indices (3, 5, 7 and so on). For example, the amplitudes of the shallow-water components MO_3 , MK_3 could exceed the values of the shallow-water components M_4 , MS_4 , M_6 , ... and even the values of the secondary semidiurnal components as K_2 , N_2 , and so on.

The spectral analysis of the sea level in a port of diurnal type affirmed this important remark.

The 19-year cycle of tides played a marked role in the analysis of tidal data and in the prediction of tides (fig. 10).

In fig. 11, the errors evaluation of tidal prediction for a port of diurnal type was shown. By using the improved Duvanin's method (curve N° 2), we could obtain the best results with analogical data of the 19-year cycle.

The above scheme could also be applied to the prediction of tides in the historical naval battles in Vietnam (13th and 18th centuries) (fig. 12).

2. COMPOSITION OF TIDAL ATLAS OF THE EAST SEA WITH VARIOUS TIDAL TYPES.

Until now, the atlas of tides was made only for the sea with semidiurnal character (the North sea, La Manche, Interior sea of Japan, ...).

The conditions of the East sea were distinctly different. Even in the limited sea basin like the Bacbo gulf and the gulf of Thailand, some types of tides could be observed.

Therefore, the new principles of the composition of tidal atlas might be applied to the sea of various tidal types.

This atlas established for any sea basin was made for a half-month period with mean or extreme astronomical conditions. The tidal characteristics could be determined from the calendar of tropical tides (of diurnal type) or spring tides (of semidiurnal type) that was calculated for the 19-year cycle.

In fig. 13 a fragment of this calendar was taken from the work (Nguyen ngoc Thuy, 1976). The tidal characteristics of any day of every half-month period in the 19-year cycle with determined coefficient of tides (I_1 for the tropical tides and I_2 for the spring tides) at the central day could be calculated without difficulty.

The corresponding formula were shown in fig. 14.

The new principles formed the basis of the composition of the tidal atlas of the Bacbo gulf with various types of tides (Nguyen ngoc Thuy, 1976, 1978).

One of the charts of tidal characteristics taken from the tidal atlas of Bacbo gulf was given in fig. 15.

Specific tidal phenomena in the East sea formed a rare picture in the World Ocean. Hitherto, many works were made, but greater efforts should be devoted to the further development of this research activity.

The scientific researches on the tidal phenomena of the East sea under complex conditions with significant diurnal components, that is the propagation of tidal waves, the method of calculation of tides and tidal streams, the interactions tides-earth tides, tides-flood in the lower river basin, tides-storm surges, and so on, presented one of the most important theoretical and practical problem in the development of oceanography in some next ten years.

HYDRODYNAMIC EQUATIONS FOR
A SINGLE COMPONENT OF THE TIDAL WAVE :

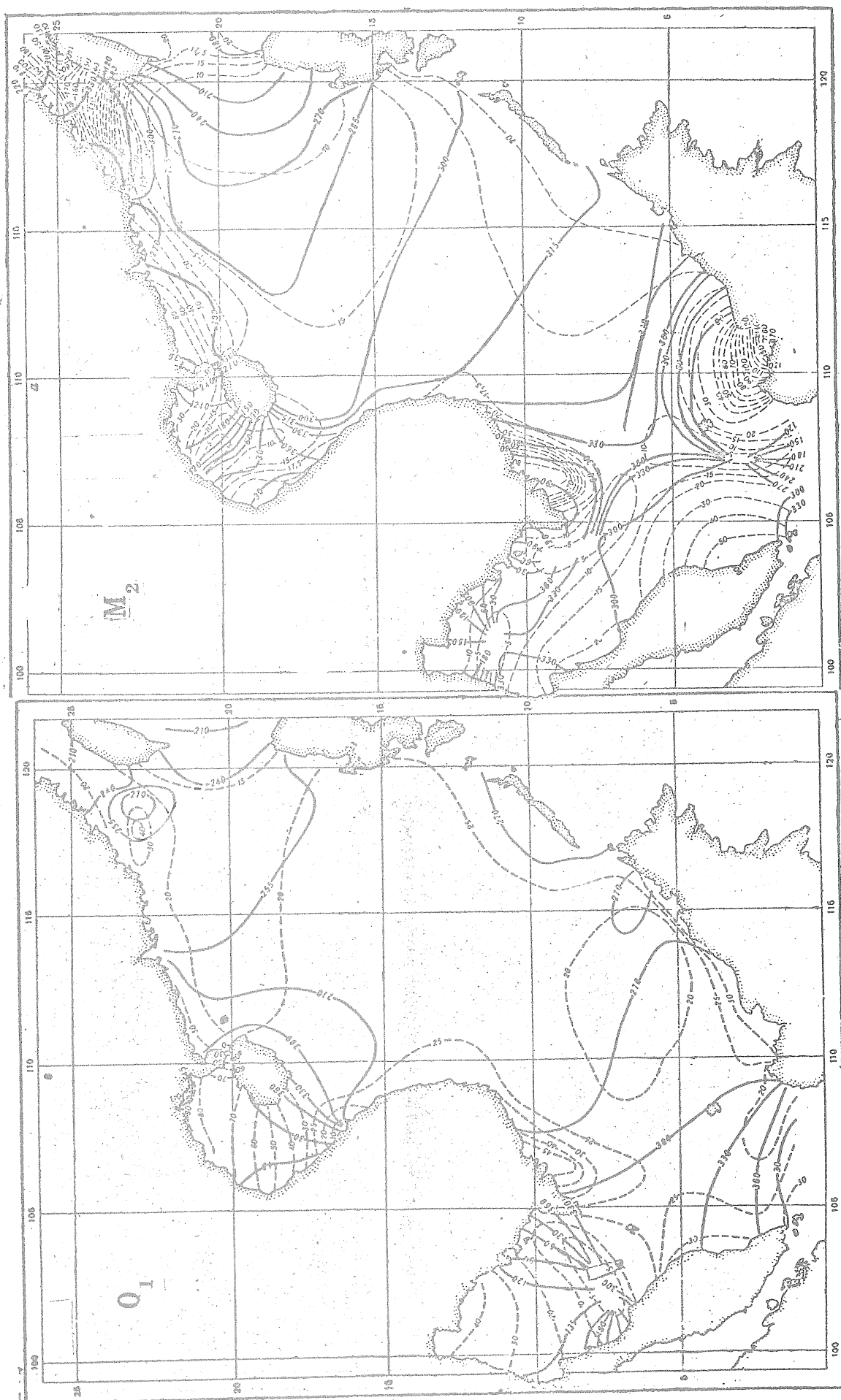
$$\frac{\partial u}{\partial t} - 2 \omega \sin \phi \cdot v + \frac{g}{R \cos \phi} \frac{\partial}{\partial \lambda} (\zeta - \bar{\zeta}) = 0 ,$$

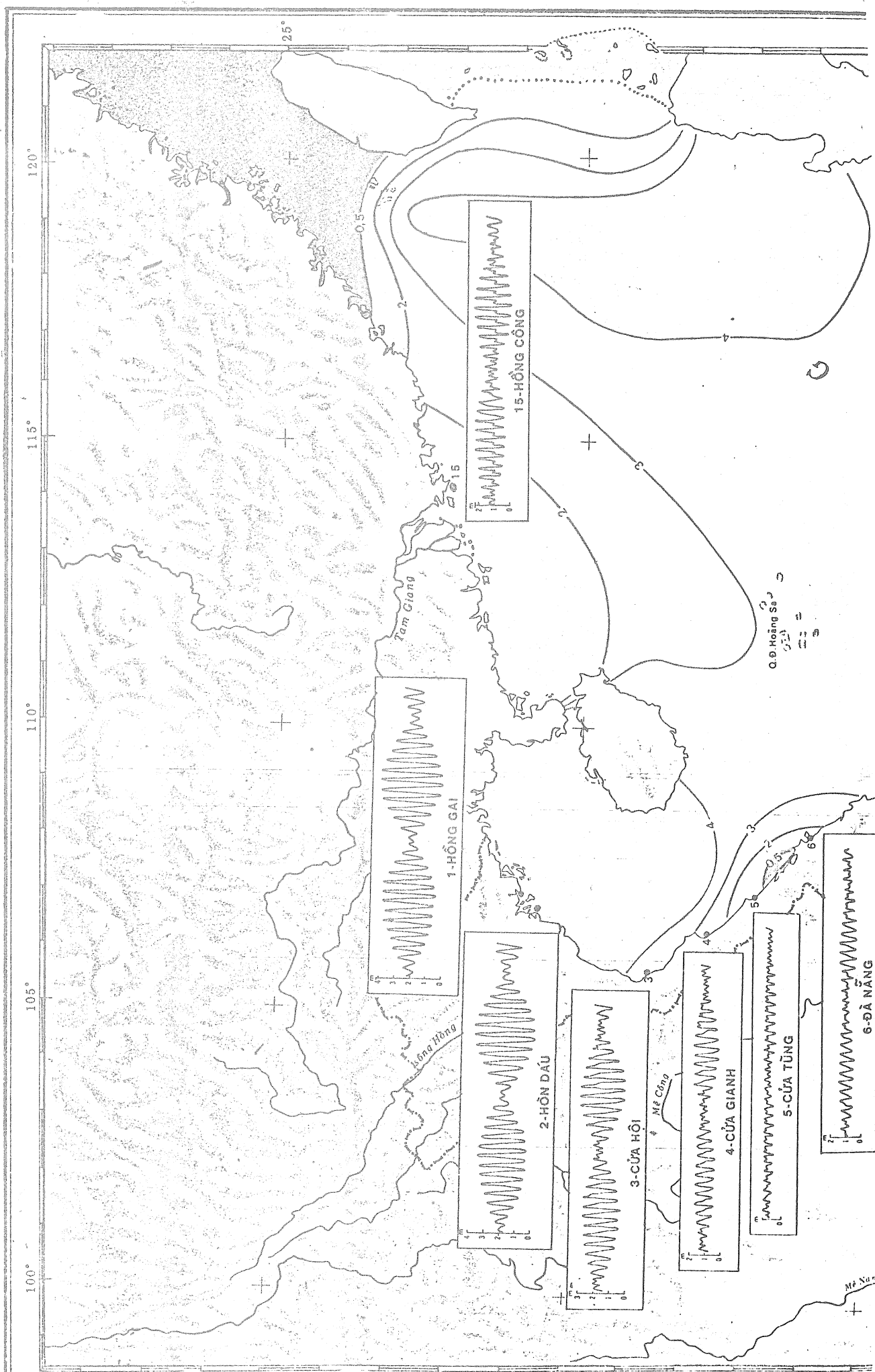
$$\frac{\partial v}{\partial t} + 2 \omega \sin \phi \cdot u + \frac{g}{R} \frac{\partial}{\partial \phi} (\zeta - \bar{\zeta}) = 0 , \quad (1)$$

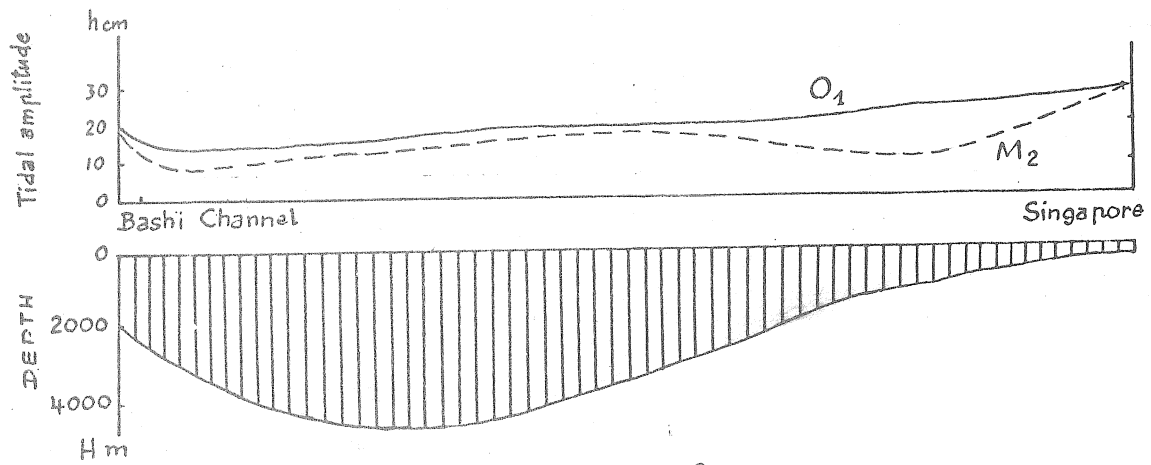
$$\frac{\partial \zeta}{\partial t} + \frac{1}{R \cos \phi} \left\{ \frac{\partial}{\partial \lambda} (hu) + \frac{\partial}{\partial \phi} (hv \cos \phi) \right\} = 0 .$$

Differential equations describing sea level fluctuations :

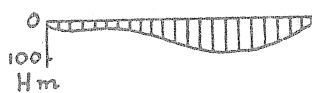
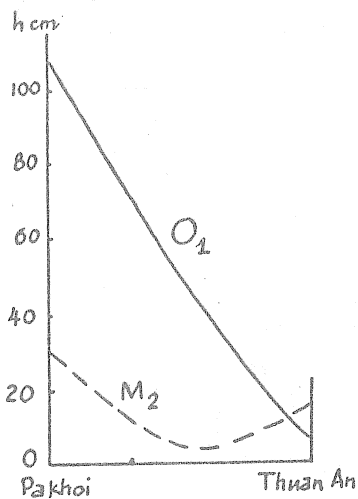
$$\begin{aligned} & \frac{i\delta ab (1 + \alpha^2 \sin^2 \phi)}{gh} \zeta + \frac{\partial^2 (\zeta - \bar{\zeta})}{2} + \frac{1}{\cos^2 \phi} \frac{\partial^2 (\zeta - \bar{\zeta})}{\partial \lambda^2} + \\ & + \frac{\partial (\zeta - \bar{\zeta})}{\partial \phi} \left(\frac{1}{h} \frac{\partial h}{\partial \phi} + \frac{\alpha \operatorname{tg} \phi}{h} \frac{\partial h}{\partial \lambda} - \frac{1 + 2\alpha^2 - \alpha^2 \sin^2 \phi}{1 + \alpha^2 \sin^2 \phi} \operatorname{tg} \phi \right) + \\ & + \frac{\partial (\zeta - \bar{\zeta})}{\partial \lambda} \left(- \frac{\alpha}{h} \frac{\partial h}{\partial \phi} \operatorname{tg} \phi + \frac{1}{h \cos^2 \phi} \frac{\partial h}{\partial \lambda} - \alpha \frac{1 - \alpha^2 \sin^2 \phi}{1 + \alpha^2 \sin^2 \phi} \right) = 0 \quad (2) \end{aligned}$$

ISOAMPLITUDES (Hcm) AND COTIDAL LINES (g°)

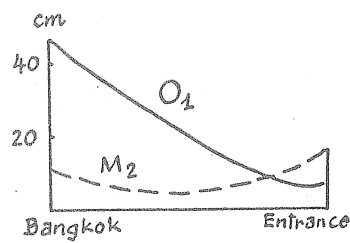




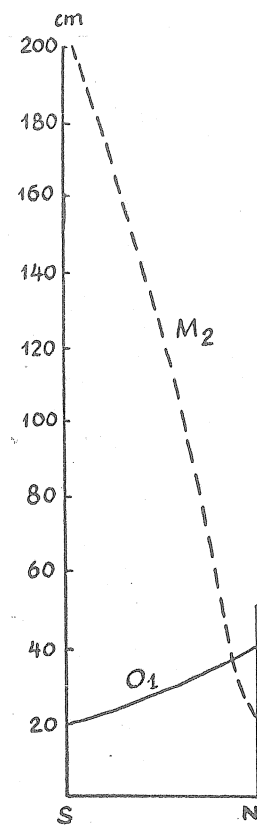
a/- East Viet Nam Sea



b/- Bac Bo Gulf



c/- Gulf of Thailand

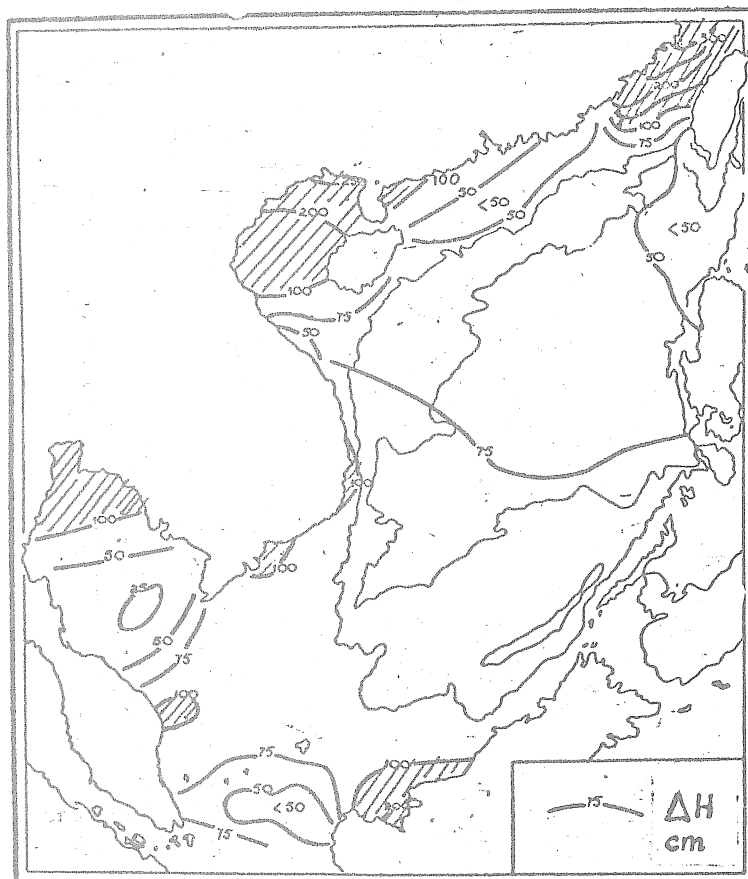


d/- Taiwan Strait

PROFILES OF TIDAL WAVES O_1 AND M_2 ALONG THE MAIN AXES

COORDINATES OF AMPHIDROMIC POINTS

M_2			S_2			O_1			K_1		
симво- лы амфи- дро- мий	с. ш.	в. д.	симво- лы амфи- дро- мий	с. ш.	в. д.	симво- лы амфи- дро- мий	с. ш.	в. д.	симво- лы амфи- дро- мий	с. ш.	в. д.
A_2	11°10'	101°00'	A'_2	11°30'	101°00'	A_1	16°30'	107°40'	A'_1	16°40'	107°40'
B_2	8°30'	104°00'	(B'_2)			B_1	7°45'	102°20'	B'_1	7°50'	102°00'
C_2	2°40'	107°00'									



MAXIMUM AMPLITUDE OF TIDES FOR 19-YEAR CYCLE

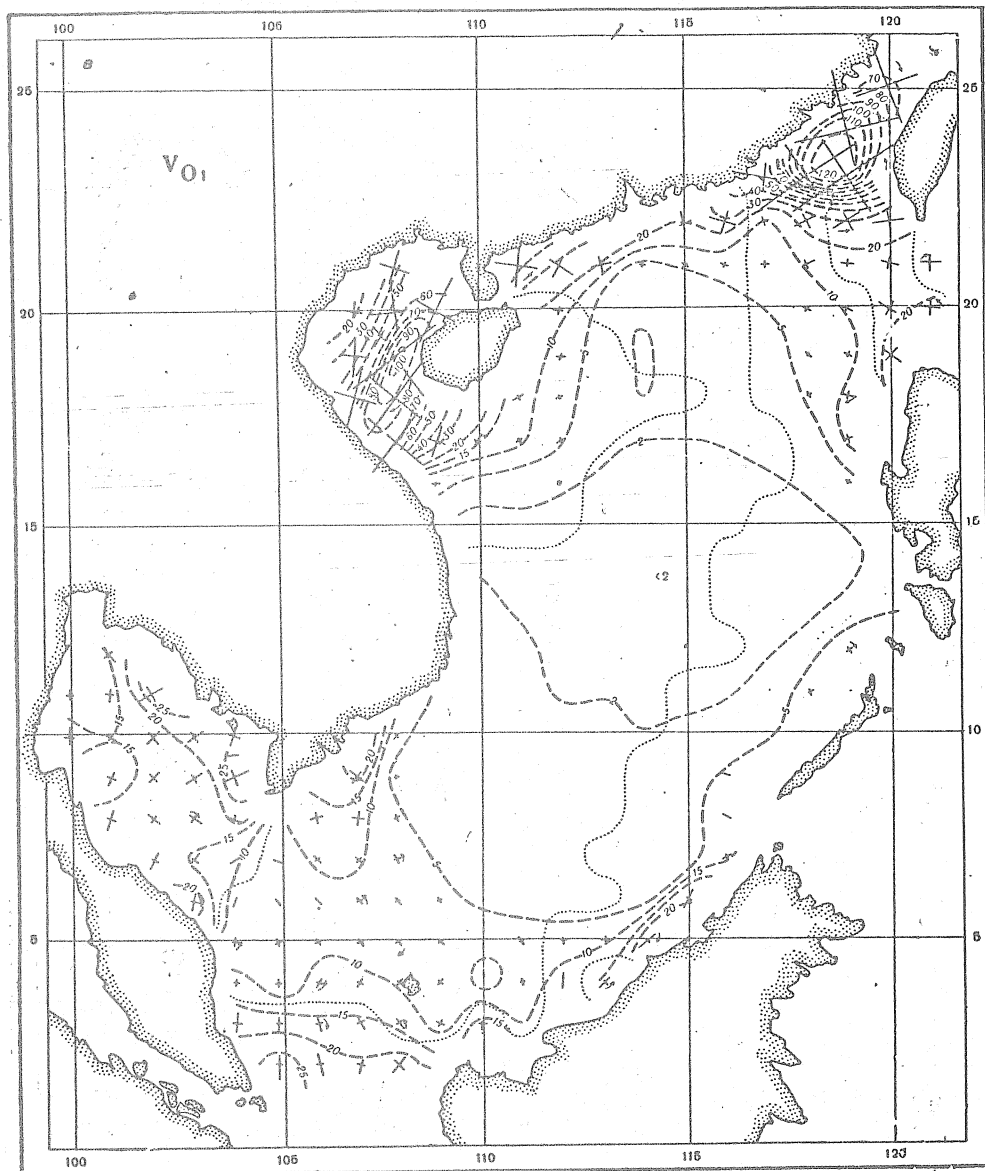


CHART OF ELEMENTS OF THE TIDAL CURRENT ELLIPSE

+ Direction and length of axes, isolines of maximum speed (cm/s)

THE INCOMING TIDAL ENERGIES E FOR THE PRINCIPAL WAVES:

Table A. M_2 , O_1 through Taiwan strait (D), Bashi Channel (B), Palawan strait (P)

	Năng lượng sóng tiến của thủy triều ($E' \cdot 10^{13}$ erg/s)				So sánh giữa các dòng năng lượng triều	
	Σ	Qua eo Đài loan (D)	Qua lạch Bashi (B)	Qua eo Pala Oan (P)	B/D	B/P
Sóng M_2 $\left\{ \begin{array}{l} E' \\ \% \end{array} \right.$	250 100	44 17,6	194 77,6	12 4,8	4,4	16,2
Sóng O_1 $\left\{ \begin{array}{l} E' \\ \% \end{array} \right.$	122 100	6 4,8	113 92,7	3 2,5	18,6	37,8
$\frac{E'_{M_2}}{E'_{O_1}}$	2	7,2	1,7	4	—	—

Table B. O_1 , K_1 , M_2 , S_2 - through the Entrance of Bacbo Gulf (C), Hainan strait (H)

Thành phần sóng triều	Động năng sóng triều truyền qua các cửa (10^6 erg/s)			Thế năng của sóng triều trên toàn vịnh (10^6 erg)
	Cửa vịnh (C)	Eo Hải nam (H)	Cửa eo (C/H)	
O_1	20,0	5,3	3,8	2483
K_1	20,5	5,3	3,8	2266
M_2	3,3	— 0,6*	5,5	190
S_2	0,5	— 0,8	1,7	25
$\frac{O_1 + K_1}{M_2 + S_2}$	10,7	—	—	22,1

$$E' = \frac{1}{2} \rho g H^2 \sqrt{gh} \cdot L; \quad E = \frac{1}{2} \rho g H^2 S$$

$|\Delta f|_{\max}$ and $|\Delta u|_{\max}$ in the 19-year cycle

	PRINCIPAL TIDAL COMPONENTS				
	S_2, P_1	M_2, N_2	O_1, Q_1	K_1	K_2
f_{\max}	0	0,075	0,375	0,231	0,568
u_{\max}	0	4°	20°	17°	35°

ERRORS EVALUATION OF TIDAL PREDICTION in the port of diurnal type

1. Darwin's method (30 components)
2. Duvanin's method by using data from analogical periods in the 19-year cycle (NNT, 1970)
3. Duvanin's method under the good conditions of semi-diurnal type (Tchalysheva, 1959)

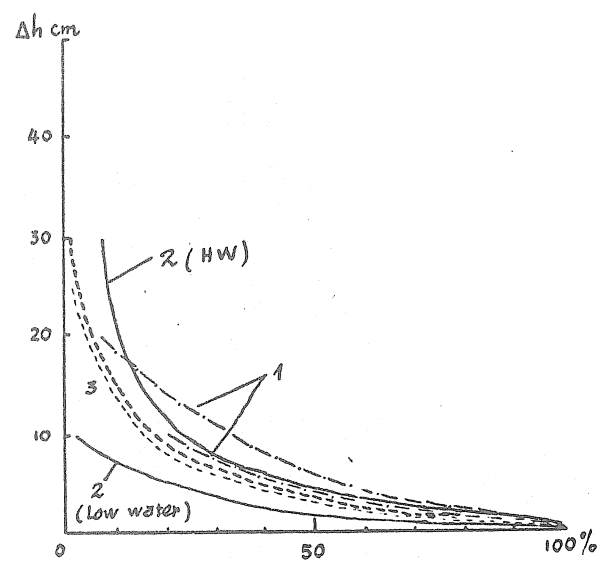
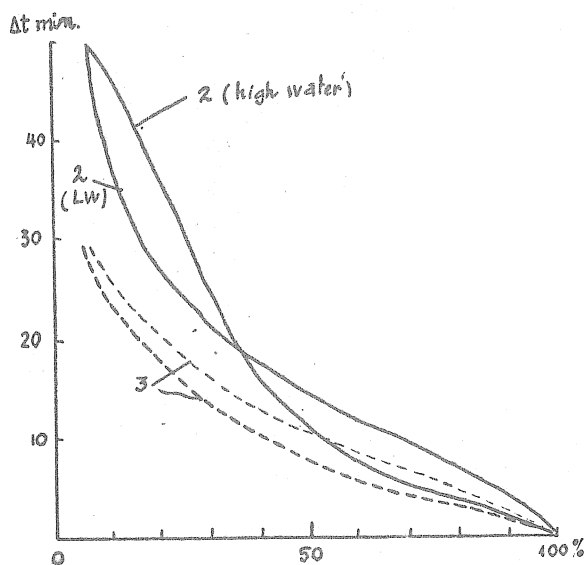


TABLE A. CALENDAR OF THE TROPICAL TIDES WITH DIURNAL TYPE (1970 - 1989)

D_o -date, I_1 -coefficient, b_{K1} -time correction

1970			1971			1972		
D_o	I_1	b_{K1} (gld)	D_o	I_1	b_{K1} (gld)	D_o	I_1	b_{K1} (gld)
7-I	1,42	23,2	10-I	1,22	23,0	14-I	1,16	22,6
20-I	1,10	22,6	24-I	1,31	22,3	28-I	1,23	22,1
3-II	1,28	21,9	7-II	1,06	21,6	10-II	0,99	21,3
17-II	0,94	21,0	21-II	1,12	20,6	25-II	1,04	20,1

TABLE B. CALENDAR OF THE SPRING TIDES WITH SEMI-DIURNAL TYPE (1970-1989)

D_o -date, I_2 -coefficient, b_{S2} -time correction

1970			1971			1972		
D_o	I_2	b_{S2} (gld)	D_o	I_2	b_{S2} (gld)	D_o	I_2	b_{S2} (gld)
7-I	0,99	0,5	11-I	0,89	0,6	1-I	1,00	0,4
22-I	1,86	0,7	26-I	1,08	0,7	15-I	0,95	0,6
6-II	1,10	0,7	10-II	0,95	0,5	30-I	1,03	0,5
21-II	0,97	0,5	25-II	1,16	0,4	14-II	1,14	0,5

FORMULA DETERMINATING THE CHARACTERISTICS OF SPRING TIDES (SEMIDIURNAL TYPE I_2)
OR TROPICAL TIDES (DIURNAL TYPE $-I_1$)

$$D = -\Delta g + b + c = D_o + \Delta D \quad (4)$$

$$I_2 = B_{M2} C_{M2} + 0,318 (B_{S2} - B_{M2} C_{M2}) \quad (5a)$$

$$I_1 = B_{O1} C_{O1} + 0,585 (B_{K1} C_{K1} - B_{O1} C_{O1}) \quad (5b)$$

$$c = 2s - 2h \quad (6)$$

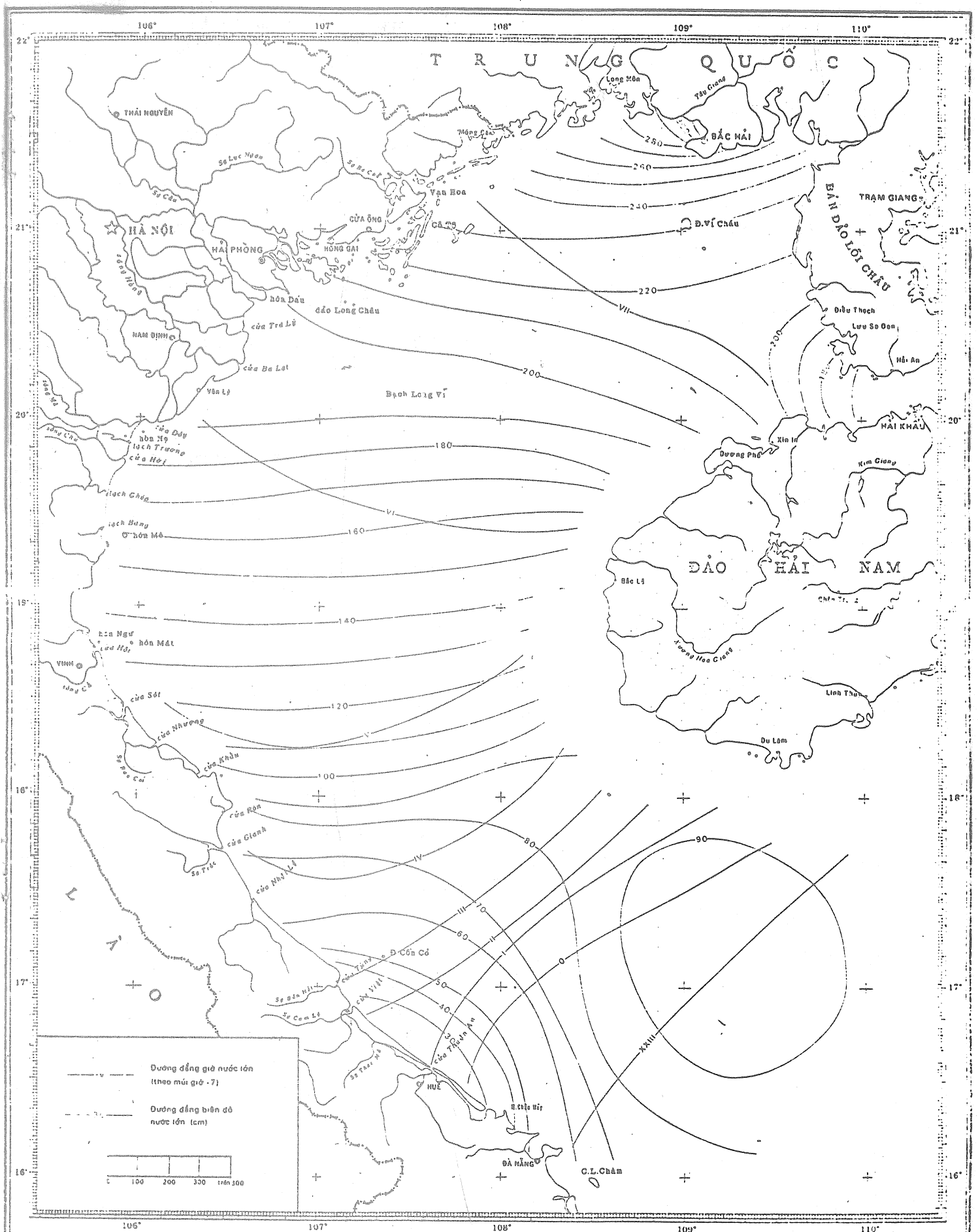
$$C = 1 + 0,165 \cos(s-p) + 0,031 \cos(s-2h+p) + 0,027 \cos(2s-2h) + 0,013 \cos(2s-2p) \quad (7)$$

$$s = 277^\circ 02' + 129^\circ 38' 48'' (Y - 1900) + 13^\circ 17' 64'' (D+1) \quad (8)$$

$$h = 280^\circ 19' - 0^\circ 23' 87'' (Y - 1900) + 0^\circ 98' 57'' (D+1)$$

$$p = 334^\circ 39' + 40^\circ 66' 25'' (Y - 1900) + 0^\circ 11' 14'' (D+1)$$

CHART OF TIDAL CHARACTERISTICS
(from Atlas of Tides-Bac bo Gulf, 1976)



REFERENCES

1 to 4 : in vietnamese ; 5 to 9 in russian.

1. NGUYEN NGOC THUY, 1965. The possibilities of the application of the method of tidal prediction in the sea with large tidal components.
Papers on Meteorology and Geophysics - Hanoi.
2. NGUYEN NGOC THUY, 1967. A coefficient of tidal amplitude and the simple method predicting tides with diurnal type.
Papers on Meteorology and Geophysics - Hanoi.
3. NGUYEN NGOC THUY, 1978. On the method of composition of atlas of tides in the sea with any tidal type.
Papers on Meteorology and Hydrology - Hanoi.
4. NGUYEN NGOC THUY, 1978. On the tidal characteristics of some historical naval battles in Vietnam.
Journal of Hydrometeorology - Hanoi.
5. NGUYEN NGOC THUY, 1968. Calendrier de marée au Vietnam à la lumière des méthodes modernes du calcul des marées.
Vestnik MGY, Geogr. n° 5.
6. NGUYEN NGOC THUY, 1969. Application de la méthode d'analyse spectrale dans les marées précalculées.
Vestnik MGY, Geogr. n° 4.
7. NGUYEN NGOC THUY, 1970. Sur la méthode de précalcul des marées sans application de l'analyse harmonique.
Travaux ГОВИ n° 98, Moscou.
8. 1958 . Tables des marées, Mers étrangères.
Océan Atlantique, Océan Indien et Océan Pacifique.
9. 1960 . Tables des marées, partie Asiatique de l'URSS
et des pays étrangers.

- 1904 - ROLLIN A. HARRIS Manual of tides.
- 1910 - POINCARÉ H. Théorie des marées - Paris.
- 1933 - OGURA S. The tides in the seas adjacent to Japan, Tokyo.
- 1950 - VILLAIN C. Les marées de la Mer de Chine méridionale, du Golfe du Tonkin et du Golfe de Siam, Paris.
- 1961 - DEFANT A. Physical oceanography.
- 1961 - WYRTKI K. Scientific results of marine investigations of the South China sea and the Gulf of Thailand, La Jolla - California.
- 1961 - Climatological and oceanographical atlas for mariners - Washington.
- 1962 - ДИТРИХ Общая океанография . Москва
- 1962 - NGUYEN NGOC THUY Some preliminary remarks on tidal peculiarities along the coast of Vietnam, Hanoi (in vietnamese).
- 1963 - БОГДАНОВ К.Т. Приливы Австрало. Азиатских морей, Тр. ИОАН
- 1964 - СЕРГЕЕВ Д.Н. Применение метода краевых значений для расчета карт гармонических постоянных приливов в Южно Китайском море. Океанология №4
- 1968 - Hydro. Dep. of Thailand The type of tides and currents in the Gulf of Thailand - Bangkok.
- 1969 - НГУЕН НГОК ТВИ Особенности Формирования приливных явлений Южно-Китайского моря, Океанология №2
- 1974 - PHAN PHUNG Tides in the Gulf of North Vietnam and the Gulf of Thailand - Saigon (in vietnamese)
- 1975 - БОГДАНОВ К.Т. Приливы Мирового океана Москва.
- 1976 - NGUYEN NGOC THUY Tides in the Bacbo Gulf (and the atlas of tides) - Hanoi (in vietnamese).

Stresses in the Earth caused by Earth tides and loading influences *

Peter Varga

Hungarian Geophysical Institute Roland Eötvös
H-1145 BUDAPEST, Columbus u. 17-23., Hungary

The investigation of Earth tides is related to questions of forecasting earthquakes in several aspects. Mention should be made first of all about the instruments which are used not only in the seismology but also for recording deformations of the solid Earth caused by lunisolar effects. As a result of processing of horizontal pendulum and extensometer observations having obtained in seismically active belts characteristic anomalies appear on the records. These characteristics depend on the locality and the magnitude of earthquakes are connected always which shallow focus earthquakes and precede the earthquakes by 1 to 2 months /Gerard V.B., 1978/. Wood M.D. and King N.E. /1977/ report that such characteristics manifest themselves in a detectable form only before major magnitude earthquakes. According to Adams R. P. /1977./ similar variations occur also in the gravity with a magnitude of about 0.1 mgal. According to our experiences the detection of anomalies preceding earthquakes is a rather difficult task since they have small amplitude, are very similar to anomalies caused by long period meteorological and hydrological variations.

Another result of Earth tides investigation which may be of even more importance for seismology is that tide parameters undergo changes prior to earthquakes. This phenomenon has been revealed by the harmonic analysis of tide observations

* Paper presented at the Conference on Intra-Continental Earthquakes /September 17-21, 1979, Ohrid, Yugoslavia/ under the auspices of the U.S.-Yugoslav Joint Board on Scientific and Technological Cooperation.

carried out first of all by the aid of extensometers and horizontal pendulums. /Nishimura E., 1950; Beaumont C. and Berger I., 1974; Latinina L.A. and Rizaeva S.D., 1978./ There exists no firmly established uniform opinion on the explanation of this phenomenon, but since changes of amplitudes of 5 to 10 per cent in waves of the lunisolar effect were observed prior to quakes and such changes can be reliably detected on the present level of observation techniques. It is supposed that in future this phenomenon can be used in earthquake forecasts.

Finally, we should like to discuss details of the possible connection between lunisolar effect and outbreak of earthquakes.

Though deformations caused by tidal phenomena are smaller by about three orders of magnitude than those of tectonic origin /Heaton, T. M. 1975./ a number of researchers conclude that the time distribution of earthquakes can not be regarded as random at various parts of the Earth. It is supposed that there must be uniform mechanism triggering the earthquakes. Such conclusion is reached also by Sadeh Dror /1978/, Bloxson D. Jr. /1974/ on the basis of statistical investigation. Brady B. T. /1976/ concluded theoretically in case of that $M \geq 6$ the tidal stress may take the part of the triggering mechanism of earthquakes. According to Heaton /1975/ who bases his opinion not only on his calculations but on statistical analysis of observations as well the lunisolar triggering effect applies first of all to quakes $M \geq 5$ with hypocenter less than 30 kilometers along steeply dipped fractures. Other authors concluded on the contrary that there is no unambiguously detectable relation between Earth tides and earthquake occurrence /Knopoff L. 1964; Schlien S. 1972./.

Since the above works furnish a rather contradictory picture, calculations were made by us on the basis of theory of Molodensky M. S. /1953/ describing deformations of the elastic, radially inhomogeneous Earth which proved useful for Earth tide investigations in order to determine deformations due to the lunisolar effect. The following system of partial differential equations served as a basis for these calculations:

$$\frac{1}{\rho} \operatorname{div} \bar{T} + g \operatorname{grad} (\omega_n + V_i) - \delta g \operatorname{grad} W_0 - g \operatorname{grad} \eta = 0 \quad /1/$$

where

W_0 - potential of gravity

ω_n - lunisolar potential

V_i - potential due to deformation

\bar{u} - vector of displacement

ρ - function of density along the Earth radius

\bar{T} - stress tensor effecting the surface of the elementary volume

δ - elastic dilatation

Unknown in /1/ are the displacement vector and its components, expressed in spherical coordinates $/u_r, u_\varphi, u_\lambda/$. Potential change due to lunisolar effect and the unknown vector components can be given in the following form /Love A.E. 1906/:

$$\omega_n + V_i = R \frac{\omega_n}{r^n}$$

$$u_r = H(r) \cdot \frac{\omega_n}{g}$$

$$u_\varphi = T(r) \cdot \frac{\partial \omega_n}{r \cdot g \cdot \partial \varphi}$$

$$u_\lambda = T(r) \cdot \frac{\partial \omega_n}{r \cdot g \cdot \sin \varphi \partial \lambda}$$

/2/

where $H/r, T/r, R/r$ - auxiliary functions introduced by Love permitting to transform equation /1/ into a system of ordinary differential equations. R is a quantity proportional to the potential, H to radial shift, T to horizontal shift.

By the aid of the introduced auxiliary functions it is possible to determine normal $/N/$ and tangential $/M/$ stresses in the Earth's mantle along radius $/r/$. Since the Earth tide can be described by the order $n=2$ for practical purposes they can be given in the following form:

$$N_R = \left[(\lambda + 2\mu) \frac{dH}{dr} + \lambda \left(\frac{2}{r} H - \frac{6}{r^2} T \right) \right] \cdot \frac{\omega_2}{r^2} = N \cdot \frac{\omega_2}{r^2}$$

$$M_\varphi = \mu \left(\frac{dT}{dr} - \frac{2}{r} T + H \right) \cdot \frac{\partial \omega_2}{r \cdot \partial \varphi} = M \frac{\partial \omega_2}{r \partial \varphi}$$

/3/

$$M_\lambda = \mu \left(\frac{dT}{dr} - \frac{2}{r} T + H \right) \cdot \frac{\partial \omega_2}{r \cdot \sin \varphi \partial \lambda} = M \frac{\partial \omega_2}{r \cdot \sin \varphi \partial \lambda}$$

Our calculations were made by using Gutenberg - Bullen. A model and our results for the functions N and M are presented in Fig.1. It can be established that both normal and tangential components of the stresses increase with depths within the depth range being of interest from the viewpoint of earthquakes. It can be established $N_R, M_\varphi, M_\lambda$ are functions of geographical latitude /3/. Stresses caused by tides increase from the poles toward the equator /Fig.2./. In addition to this significant phase deviation $/\varphi/$ appears as compared to the theoretical tide potential ω_2 for horizontal stress components /Fig.3./. All these indicate that the geographical location of the studied area must be considered when investigating the triggering

effect of lunisolar variations, since the magnitude of stresses varies from one locality to the other and a significant delay in phase can be revealed for horizontal components.

Since we have already determined the stress components N_R , M_φ , M_λ , it is possible to determine the stress components appearing on the elementary plane surface of any orientation. Let us take a plane surface characterized by the dip angle I and azimuth D . Without giving a detailed description of the well known coordinate transformations required for such calculations we present here a qualitative information about our results. In this instance the effect caused by changes in elements D and I is investigated on a point with fixed coordinates R, φ, λ .

1. Normal stresses.

Normal stresses due to lunisolar effect depends on azimuth to a relatively slight extent. Dependence on angle I is more significant; the steeper the plane the higher the value of the appearing normal stress and it achieves the highest value at the vertical plane when the azimuth lies in NS direction.

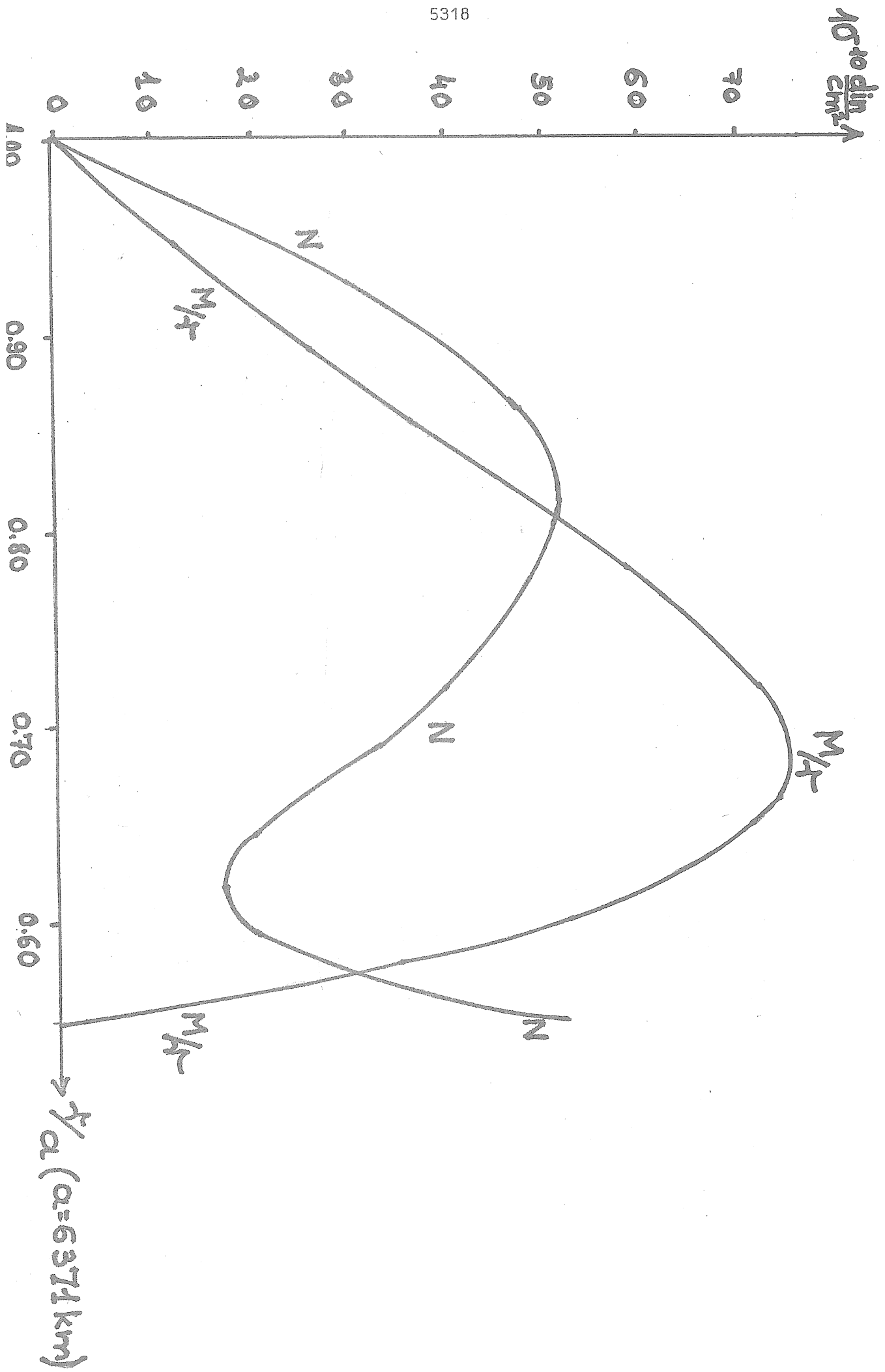
2. Tangential stresses.

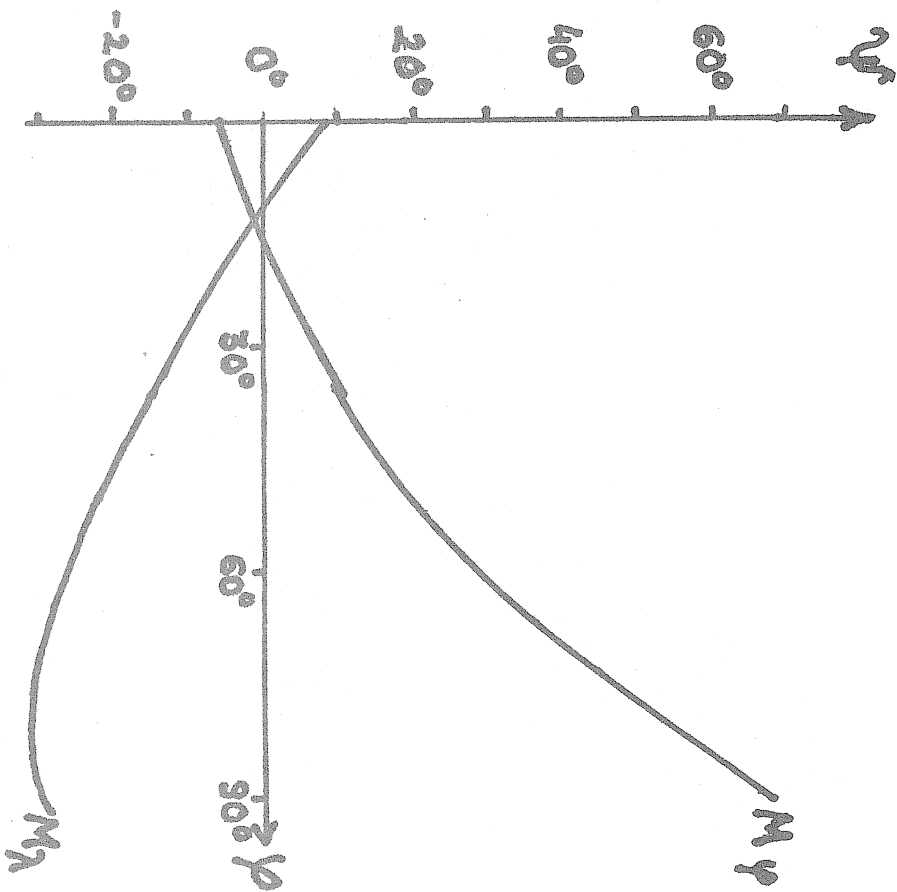
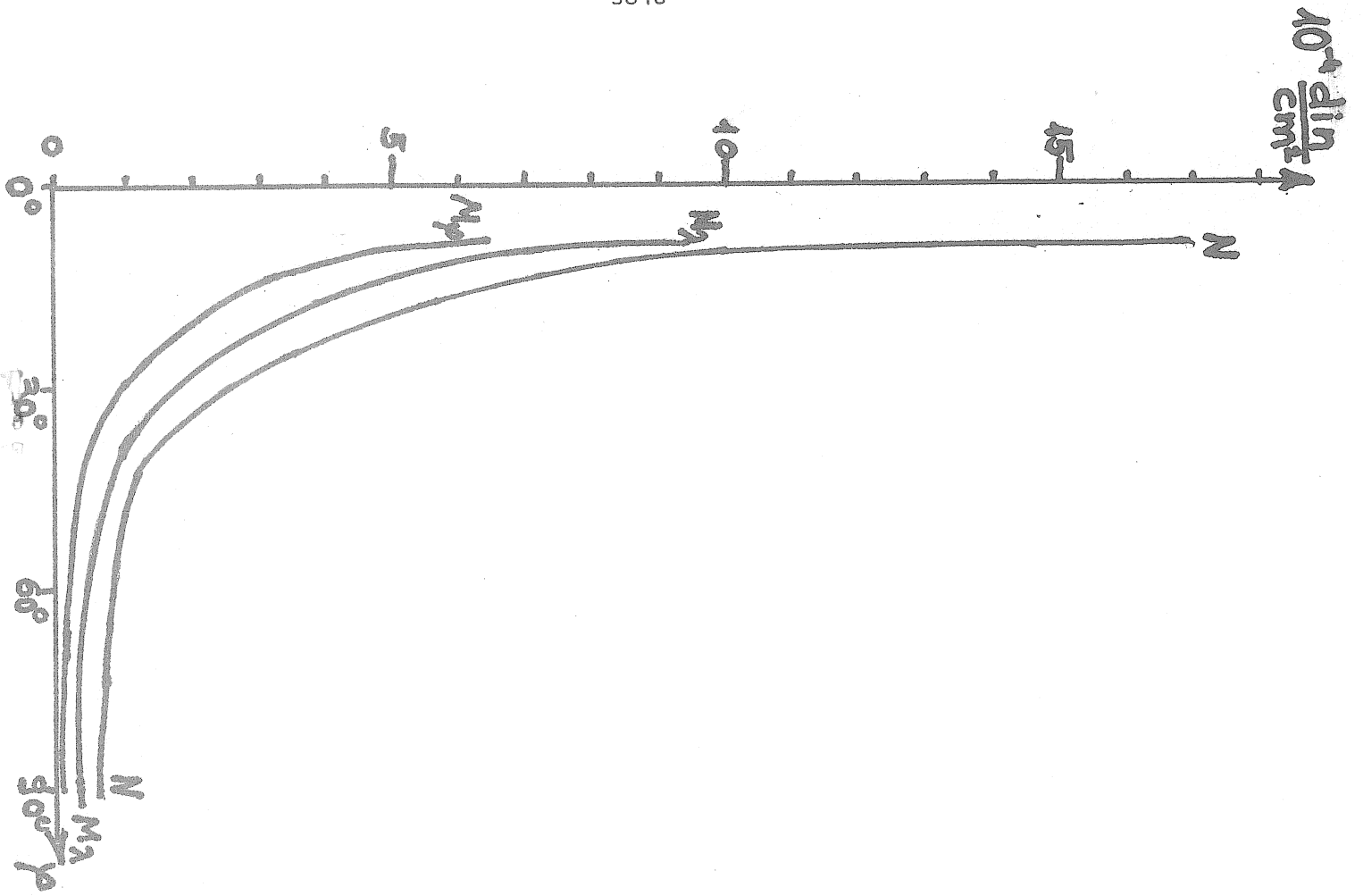
Both amplitude and phase of tangential components due to lunisolar effect depend on the orientation of the investigated plane surface. The effect of azimuth changes is comparatively small also in this case, while the phase shift can be 10 to 12 degrees. For planes taking nearly horizontal position the resulting tangential stresses make up about 0.1 per cent of those occurring along the vertical plane.

As conclusion it can be stated that the lunisolar effect appears first of all on steeply dipping fractures oriented near NS.

This effect may be still enhanced by stresses due to changes in normal loading affecting the surface. Such stresses may take their origin from meteorological, hydrological effects. Among them the loading effect of oceanic tides on shelves or shore belts should be mentioned in the first line. Significant stresses may be caused by fluctuations of the groundwater table. Their amplitude may reach even 1 to 2 meters and the change in loading exercises its influence over an extended area. Even higher loading may be created when water reservoirs are being filled up. Stress conditions of these processes may be adequately studied by the aid of Molodensky's theory. We intend to carry out such a work in the near future.

In summary it can be established that the triggering effect of Earth tides if it affects the release of earthquake energy is probably complex, not exercising the same influence at every place. It depends on geographical location of the studied area and orientation of the tectonic elements as well.





REFERENCES

- 1) ADAMS R.P., 1977., Earthquake prediction
Nature, 269, N° 5623.
- 2) BEAUMONT C., BERGER I., 1974. Earthquake prediction : modification of the
earth tide tilts and strains by dilatancy.
Geophys. J. Roy. Astron. Soc. 39., N° 1.
- 3) BLOXSOM D. Jr., 1974., San Fernando fault earthquakes and earth tides.
Bull. Seismol. Soc. Amer., 64., N° 6.
- 4) BRADY B.T., 1976., Theory of earthquakes IV. General implications for earth-
quake predictions.
Pure and Appl. Geophys. N° 6.
- 5) GERARD V.B., 1978., Earthquake precursors from Earth tilt observations
corrected for rainfall.
Nature, 276, N° 5684.
- 6) HEATON T.H., 1975., Tidal triggering of earthquakes.
Geophys. J. Roy. Astron. Soc., 43., N° 2.
- 7) KNOPOFF L., 1964., Earth tides as a triggering mechanism for earthquakes
Bull. Seismol. Soc. Amer., 54.
- 8) LATININA L.A., RIZAEVA S.D., 1978., Sur les variations des déformations de
marées avant des tremblements de terre.
Marées Terrestres, Bull. Inform. N° 77.
- 9) LOVE A.E., 1906., The yielding of the Earth to disturbing forces,
Proc. Roy. Soc. 82 A.
- 10) MOLODENSKY, M.S., 1953., Uprugije prilivi, svobodnaja nutacija i voprosi
strojenija zemli.
Trudi Geofizitsheskogo Instituta AN SSSR N° 19 (146), Moscow
(in russian)
- 11) NISHIMURA, E., 1950., On earth tides.
Trans Amer. Geophys. Un. 31.
- 12) SADEH D., 1978., Periodic earthquakes in Alaska and Central America.
J. Geophys. Res., N° 3.
- 13) TAMRAZYAN, G.P., 1968., Principal regularities in the distribution of major
earthquakes relative to solar tides and other cosmic sources.
Icarus, 9.
- 14) WOOD M.D., KING N.E., 1977., Relation between earthquakes weather and soil
tilt.
Science, 197, N° 4299.